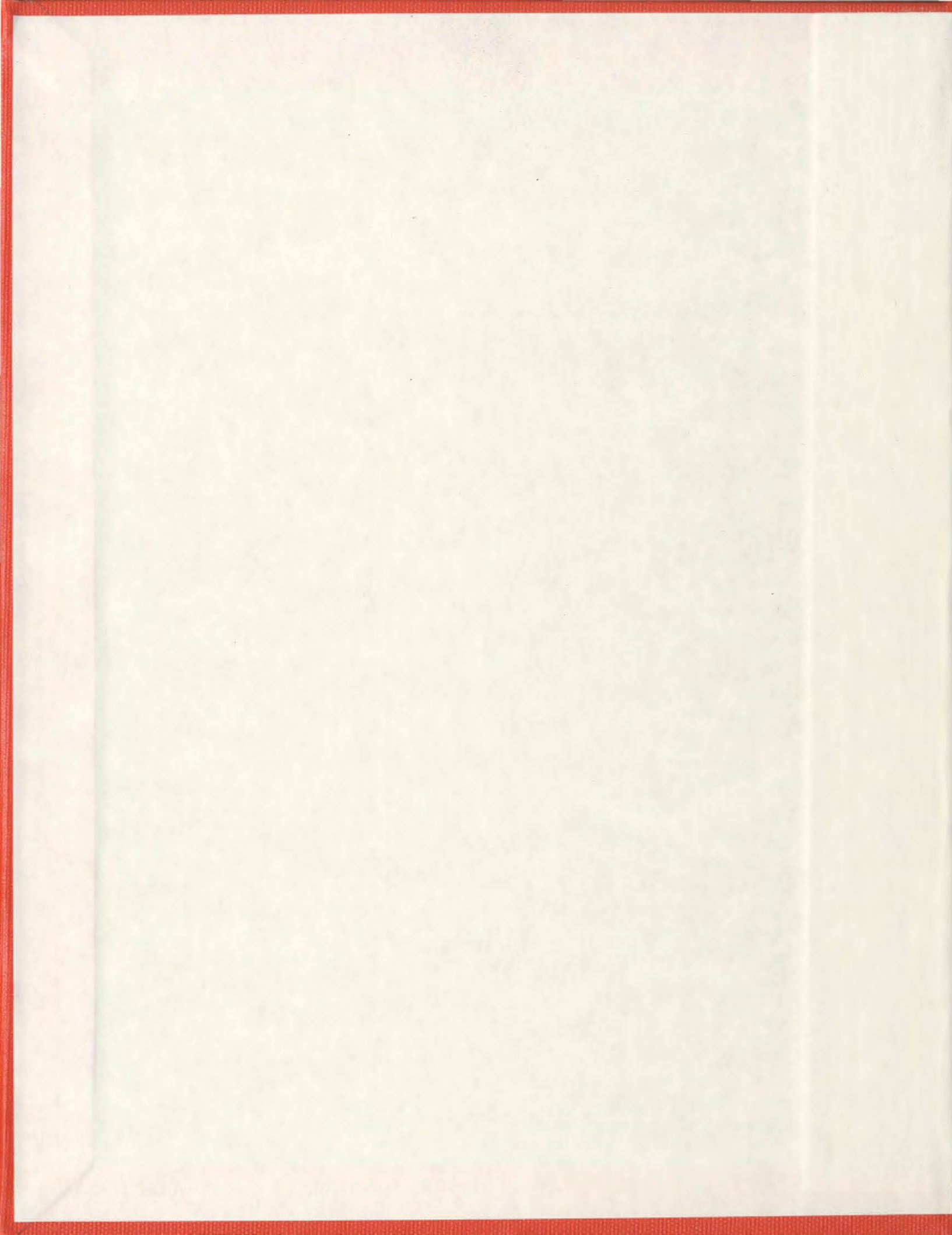


**FINITE ELEMENT MODELING OF STEEL PILES
AND SUCTION CAISSONS IN SAND UNDER
LATERAL AND INCLINED LOAD**

MD IFTEKHARUZZAMAN



**FINITE ELEMENT MODELING OF STEEL PILES AND SUCTION CAISSONS
IN SAND UNDER LATERAL AND INCLINED LOAD**

by

© **MD IFTEKHARUZZAMAN**

A thesis submitted to the

School of Graduate Studies

in partial fulfillment of the requirements for the degree of

Master of Engineering (Civil Engineering)

Faculty of Engineering and Applied Sciences

Memorial University of Newfoundland

April, 2013

St. John's

Newfoundland

ABSTRACT

The behavior of a steel pipe pile in sand subjected to lateral load is examined by three-dimensional finite element (FE) analyses using the commercially available software package ABAQUS/Standard 6.10 EF1. The sand around the pile is modeled using a modified form of Mohr-Coulomb soil model. The modifications involve the nonlinear variation of elastic soil modulus with mean stress and the variation of mobilized angle of internal friction and dilation angle with plastic shear strain, which are implemented in ABAQUS/Standard using a user subroutine. Numerical analyses are also performed by using the LPILE software which is based on the p - y curve approach and widely used in design for estimating lateral load capacity of pile foundations. The FE and LPILE results are compared with the results of two full-scale tests available in the literature. It is shown that the FE model better simulates the response of a pile under lateral load. Comparing the numerical results with the full-scale test results, some limitations of the p - y curve method are highlighted.

In the second part of the study, finite element analyses are performed to estimate the pullout capacity of a suction caisson subjected to oblique loading. Three-dimensional finite element analyses are performed using ABAQUS/Standard 6.10 EF1 finite element software. The effects of two key variables, loading angle and mooring line position, are investigated. The finite element results are compared with centrifuge test results available in the literature. The maximum pullout capacity is obtained when the mooring line is attached at approximately 75% depth of the caisson for the cases analyzed in this study.

ACKNOWLEDGEMENTS

I would like to thank Dr. Bipul Hawlader for his guidance and encouragement in this research work. His suggestions and comments were extremely helpful in the research. It has been a remarkable journey together. I have learned so many things from him.

I would also like to acknowledge the financial support from MITACS, the School of Graduate Studies, and my supervisor's NSERC Discovery Grant to conduct the research presented in this thesis.

I thank my parents and close relatives for their full support, love and affection throughout my life and M.Eng study at Memorial University.

Finally, I thank my friends and colleagues at Memorial University who have directly or indirectly helped me in my research work.

Table of Contents

| | |
|--|------|
| ABSTRACT | ii |
| ACKNOWLEDGEMENTS..... | iii |
| Table of Contents..... | iv |
| List of Tables | viii |
| List of Figures..... | ix |
| List of Symbols..... | xiv |
| 1 INTRODUCTION | 1 |
| 1.1 General..... | 1 |
| 1.2 Scope of the Work | 2 |
| 1.3 Objectives | 3 |
| 1.4 Organization of Thesis..... | 3 |
| 1.5 Contributions..... | 4 |
| 2 LITERATURE REVIEW..... | 5 |
| 2.1 Introduction..... | 5 |
| 2.2 Laterally Loaded Long Piles in Sand..... | 6 |
| 2.2.1 Theoretical Methods | 7 |
| 2.2.2 Physical Modeling | 21 |

| | | |
|-------|--|----|
| 2.2.3 | Continuum Modeling..... | 28 |
| 2.3 | Inclined Loaded Suction Pile..... | 29 |
| 2.3.1 | Field Tests..... | 33 |
| 2.3.2 | Laboratory Tests..... | 35 |
| 2.3.3 | Centrifuge Tests..... | 38 |
| 2.3.4 | Numerical Analysis..... | 41 |
| 2.4 | Summary..... | 44 |
| 3 | NUMERICAL MODELING OF A LATERALLY LOADEDE LONG FLEXIBLE PILE IN SAND..... | 45 |
| 3.1 | General..... | 45 |
| 3.2 | Introduction..... | 46 |
| 3.3 | Finite Element Modeling for Cox et al. (1974)..... | 48 |
| 3.3.1 | Modeling of pile and soil/pile interface..... | 51 |
| 3.3.2 | Modeling of Soil..... | 52 |
| 3.3.3 | LPILE Analysis..... | 56 |
| 3.3.4 | Numerical Results..... | 59 |
| 3.4 | Finite Element Modeling of Rollins et al. (2005) Full-Scale Test..... | 78 |
| 3.4.1 | Modeling of Pile and Soil..... | 80 |
| 3.4.2 | Numerical Results..... | 82 |

| | | |
|-------|--|-----|
| 3.5 | Discussion and Conclusions | 87 |
| 4 | NUMERICAL MODELING OF PULLOUT CAPACITY OF SUCTION CAISSON IN SAND UNDER OBLIQUE LOAD..... | 89 |
| 4.1 | General..... | 89 |
| 4.2 | Introduction..... | 89 |
| 4.3 | Problem Definition..... | 92 |
| 4.4 | Numerical Modeling | 93 |
| 4.4.1 | Modeling of Caisson..... | 95 |
| 4.4.2 | Soil Modeling | 95 |
| 4.4.3 | Mesh Sensitivity Analysis | 97 |
| 4.4.4 | Centrifuge Modeling..... | 97 |
| 4.5 | Numerical Results..... | 98 |
| 4.5.1 | Load-Displacement curves | 99 |
| 4.5.2 | Effects of Depth and Angle of Pulling | 104 |
| 4.5.3 | Plastic Strain and Displacement Vector Diagram | 110 |
| 4.5.4 | Lateral Displacement..... | 113 |
| 4.5.5 | Rotation vs. Mooring Position..... | 115 |
| 4.5.6 | Mobilized Soil Reaction | 116 |
| 4.6 | Conclusion and discussions | 118 |

| | | |
|-----|--|-----|
| 5 | CONCLUSIONS AND FUTURE RECOMMENDATIONS | 120 |
| 5.1 | Conclusions..... | 120 |
| 5.2 | Recommendations for Future Work..... | 122 |
| 6 | Bibliography | 124 |
| 7 | Appendix-A | 141 |

List of Tables

| | |
|---|----|
| Table 2-1: Summary of p - y curves (Revised from Byung et al., 2004) | 15 |
| Table 2-2: Recommended values of k for the of p - y curves method..... | 17 |
| Table 2-3: Summary of pile load test | 27 |
| Table 2-4: Summary of numerical analysis in suction caissons..... | 43 |
| Table 3-1: Geometry and mechanical properties used in finite element analysis for Reese et al. (1974)..... | 57 |
| Table 3-2: Geometry and mechanical properties used in finite element analysis for Rollins et al. (2005) | 81 |
| Table 4-1: Geometry and mechanical properties used in the analysis | 96 |

List of Figures

| | |
|---|----|
| Figure 2-1: Distribution of soil pressure on a pile under lateral load (modified after Reese and Van Impe, 2001) | 6 |
| Figure 2-2: Curves for design of long pile under lateral load in cohesionless soil | 8 |
| Figure 2-3: Subgrade reaction approach..... | 9 |
| Figure 2-4: Set of p - y curves at various depths below soil surface (Reese et al. 1974) | 11 |
| Figure 2-5: Coefficient of initial modulus of subgrade reaction, k (API, 2000) | 13 |
| Figure 2-6: Basic Configuration of SW Model (Ashour and Norris, 2000)..... | 14 |
| Figure 2-7: Comparison of measured and API recommended subgrade reaction (Yan and Byrne, 1992) | 18 |
| Figure 2-8: Empirical coefficients for ultimate resistance, (a) Reese et al. 1974, (b) API code..... | 19 |
| Figure 2-9: Comparison between full-scale test and computed results using p - y curve method (Reese et al. 1974) | 20 |
| Figure 2-10: (a) Typical Geometry of Caissons half (Dilip 2004), (b) Caisson in place (Source: Mercier, 2003)..... | 30 |
| Figure 2-11: Caissons used as foundations for (a) Tension Leg Platform (TLP) and (b) Catenary and taut mooring lines (Dilip 2004) | 31 |
| Figure 2-12: Caisson foundations used in various projects (Byrne 2000) | 32 |
| Figure 2-13: Typical load displacement curve in centrifuge test (Allersma et al. (2000)) | 39 |
| Figure 2-14: Schematics of model suction pile and pulling locations (Bang et al. 2011). | 40 |
| Figure 3-1: Idealized soil and pile load test setup (redrawn from Reese et al. 2001) | 48 |

| | |
|--|----|
| Figure 3-2: Finite element model | 50 |
| Figure 3-3: Mesh sensitivity analysis | 51 |
| Figure 3-4: Mobilized angle of internal friction and dilation angle with plastic strain..... | 55 |
| Figure 3-5: Lateral modulus of subgrade reaction as function of relative density and friction angle (API 2000)..... | 58 |
| Figure 3-6: Comparison of load displacement between numerical predictions and full-scale test result..... | 60 |
| Figure 3-7: Variation of bending moment with depth (Load cases: 33.4 kN, 55.6 kN and 77.8 kN; solid lines for FE analysis, dashed line for LPILE and data points for full-scale test) | 62 |
| Figure 3-8: Variation of bending moment with depth (Load cases: 101.1 kN, 122.3 kN and 144.6 kN; solid lines for FE analysis, dashed line for LPILE and data points for full-scale test) | 63 |
| Figure 3-9: Variation of bending moment with depth (Load cases: 166.8 kN, 189 kN and 211.3 kN; solid lines for FE analysis, dashed line for LPILE and data points for full-scale test) | 64 |
| Figure 3-10: Variation of bending moment with depth (Load cases: 244.6kN and 266.9kN; solid lines for FE analysis, dashed line for LPILE and data points for full-scale test) | 65 |
| Figure 3-11: Comparison of maximum bending moment and lateral load..... | 66 |
| Figure 3-12: Lateral displacement of pile (solid lines: FE analysis; dashed line: LPILE; solid circles: measured at ground line in pile load test) | 67 |

| | |
|---|----|
| Figure 3-13: Soil reaction on pile (solid lines: FE analysis and dashed line: LPILE) | 68 |
| Figure 3-14: Variation of shear force in pile with depth (solid lines: FE analysis, dashed line: LPILE)..... | 69 |
| Figure 3-15: Comparison of p-y curves at four depths (solid lines: FE analysis, dashed line: LPILE, and data points: full-scale test) | 71 |
| Figure 3-16 : Lateral effective stress at various pile depths (dashed lines represent the average effective stress)..... | 73 |
| Figure 3-17: Vertical displacement of soil near the top of the pile at the end of loading (P=266.9 kN) | 74 |
| Figure 3-18: Von-Misses stress distribution at the end of loading (P=266.9 kN)..... | 75 |
| Figure 3-19: Mean effective stress at the end of loading (P=266.9 kN) | 75 |
| Figure 3-20: Magnitude of plastic strain at the end of loading (P=266.9 kN) | 77 |
| Figure 3-21: Soil profile (after Rollins et al. 2005)..... | 78 |
| Figure 3-22: Finite element model | 80 |
| Figure 3-23: Comparison of load displacement between numerical predictions and full-scale test result..... | 83 |
| Figure 3-24: Variation of bending moment with depth (solid lines for FE analysis, and data points for full-scale test) | 84 |
| Figure 3-25: Comparison of maximum Bending moment and Lateral load..... | 85 |
| Figure 3-26: Lateral displacement of pile (solid lines: FE analysis and solid circles: measured at pile top in pile load test)..... | 86 |
| Figure 4-1: Suction piles used in various projects (Byrne 2005b) | 90 |

| | |
|---|-----|
| Figure 4-2: Problem definition | 93 |
| Figure 4-3: Finite element model using in analysis..... | 94 |
| Figure 4-4: Mesh sensitivity analysis | 98 |
| Figure 4-5 : Load-displacement curves for 5% mooring position (right arrows represent the range of centrifuge test results)..... | 100 |
| Figure 4-6 : Load-displacement curves for 25% mooring position..... | 101 |
| Figure 4-7: Load-displacement curves for 50% mooring position..... | 102 |
| Figure 4-8: Load-displacement curves for 75% mooring position..... | 103 |
| Figure 4-9: Load-displacement curves for 95% mooring position..... | 104 |
| Figure 4-10: Lateral load vs. lateral displacement for different mooring positions (Right arrows represent the range of centrifuge results)..... | 106 |
| Figure 4-11: Pullout capacity for different loading angle and mooring position from FE analysis | 107 |
| Figure 4-12: Pullout capacity for different loading angle and mooring position from centrifuge test (Bang et al. 2011)..... | 108 |
| Figure 4-13: Comparison between centrifuge test results and analytical solution (Bang et al. 2011)..... | 109 |
| Figure 4-14: Pullout capacity for different loading angle and mooring position | 110 |
| Figure 4-15: Maximum principle plastic strain and displacement vector diagram for 5% mooring position and 0.5m displacement at 22.5 degree angle..... | 111 |
| Figure 4-16: Maximum principle plastic strain and displacement vector diagram for 75% mooring position and 0.5m displacement at 15 degree angle..... | 111 |

| | |
|---|-----|
| Figure 4-17: Vertical displacement vector for 0.3m displacement at 22.5 degree with horizontal | 112 |
| Figure 4-18: Vertical displacement and failure mechanism observed in centrifuge test (Allersma et al. 2000) | 113 |
| Figure 4-19: Lateral displacement for different loading angle at 5% mooring position . | 114 |
| Figure 4-20: Lateral displacement for different mooring positions | 115 |
| Figure 4-21: Soil reaction for different mooring positions..... | 116 |
| Figure 4-22: Soil reaction for different loading angle at 5% mooring position | 117 |
| Figure 4-23: Soil reaction for different mooring positions..... | 118 |

List of Symbols

| | |
|-----------|--|
| b | width of pile |
| D | diameter of the pile |
| D_r | relative density |
| E_p | modulus of elasticity of the pile |
| ν_p | Poisson's ratio of pile |
| ν_s | Poisson's ratio of soil |
| E | Young's modulus |
| E_{ref} | reference modulus of elasticity |
| γ | submerged unit weight of soil |
| I_p | moment of inertia of the pile section |
| k | coefficient of initial modulus of horizontal subgrade reaction |
| K_h | Horizontal subgrade modulus |
| L | length of the pile |
| μ | pile/soil interaction properties |
| M | bending moment in pile |
| p | soil reaction per unit length of pile |
| p_a | atmospheric pressure |

| | |
|------------|--------------------------------------|
| p' | mean effective stress |
| ϕ' | effective angle of internal friction |
| ϕ'_c | critical state friction angle |
| ϕ'_p | peak friction angle |
| ϕ_μ | pile/soil interface friction angle |
| ψ_m | maximum dilation angle |
| ψ | dilation angle |
| t | thickness of the pipe |
| g | gravitational acceleration |
| x | depth below the ground surface |
| y | lateral deflection of pile |

Chapter 1

INTRODUCTION

1.1 General

Pile foundations have been widely used in onshore and offshore to resist the lateral, axial and inclined load applied to structures. Onshore piles are commonly used in foundations of multistoried buildings, retaining walls, bridge foundations, electric poles and other onshore structures. Offshore piles are used in offshore platforms, Floating Production Storage Offloading vessels (FPSOs) and other offshore structures. Pile foundations are mainly used where shallow foundations are not practical. They are also used in situations where the soil layers near the ground surface do not possess enough strength to bear the load coming from the structure and to transfer the load to a deep stronger soil layer.

The design of offshore piles is different from onshore piles. Onshore pile foundations resist mainly dead loads of the structures and some live loads whereas offshore piles are designed to resist deadweight of the structures, environmental loads induced by waves, wind and current, loads due to earthquake and offshore geohazards like submarine landslides. The consideration of lateral load depends on types of structure and expected loading phenomena. For example, multistoried buildings are usually subjected to high wind load and earthquake load and need to resist a high amount of lateral loading. Fixed offshore platforms are also subjected to lateral load coming from wind and current. Long steel pipe piles are commonly used in both onshore and offshore. In addition to axial

capacity, the lateral load carrying capacity of these piles is equally important in the design. The load on a pile could be inclined upward in some cases. For example, suction caissons (also known as suction pile) are widely used in offshore for anchoring Floating Production Storage Offloading vessels (FPSOs), which have been accepted as a sustainable economic solution for deep water development projects. Suction caissons are preferred to other type piles in floating offshore structures because of the substantial savings from reduced materials and installation times. They are also more environmentally friendly than driven piles as they may be removed by reversing the direction of pumping.

1.2 Scope of the Work

Over the last couple of decades finite element (FE) modeling techniques have been improved significantly in addition to computing facilities. In this study, FE analyses have been performed for modeling the pile foundations. The FE analyses are performed using the commercially available software package ABAQUS/Standard 6.10 EF1. The response of pile foundations in sand under lateral load is studied. Two types of pile foundations are analyzed: (i) a long steel pipe pile subjected to lateral loading, and (ii) a suction pile subjected to lateral and inclined upward loading. For the long steel pile under lateral loading, numerical analyses are also performed using the LPILE software, which is based on the p - y curve method. The FE and LPILE results are compared with the results of two full-scale tests from the literature. For the suction pile, three-dimensional finite element analyses are performed to estimate the pullout capacity of a suction pile subjected to oblique loading.

1.3 Objectives

The main objective of this study is to quantify the load carrying capacity of a single steel pile under lateral load and a suction caisson (pile) under oblique load. The response of the pile is calculated using the fundamental soil properties such as friction angle, dilatancy and stiffness as input parameters in FE analyses. The built-in Mohr-Coulomb model available in ABAQUS can not simulate the post-peak softening behavior of the dense sand. A modified form of Mohr-Coulomb model is implemented into the ABAQUS FE software using user subroutines to show the effects of nonlinearity of elastic modulus with mean effective stress and the variation of mobilized angle of internal friction and dilation angle with plastic shear strain. The FE results are compared with full-scale test results and centrifuge test results and also with the results of LPILE which is widely used software in the industry for calculating lateral load-deflection behavior of pile.

1.4 Organization of Thesis

This thesis consists of a total of five chapters presenting the outcomes of this M.Eng research. It starts with this chapter presenting the objective and background of the study.

Chapter 2 presents the review of previous works related to pile foundations under lateral loading and suction piles under oblique loading. Attention is given to the various modeling techniques including theoretical, numerical and physical modeling. Physical modeling consists of three main categories including small-scale tests, full-scale tests and centrifuge tests.

Chapter 3 presents FE analysis of laterally loaded long steel piles. The performance of FE modeling techniques is shown by comparing the results with two pile load test results and LPILE results.

Chapter 4 presents finite element analysis of a suction pile under oblique loading. A total of 25 cases are analyzed to evaluate the pullout capacity of a suction pile and the results are compared with centrifuge tests.

Finally, Chapter 5 presents the conclusions of the study and some recommendations for further studies in these areas of research.

1.5 Contributions

The present study shows the

- applicability of FE techniques, incorporating a better soil model of sand, for modeling piles in onshore and offshore environments under lateral and inclined loads;
- effects of the nonlinear variation of elastic modulus and post-peak variation of mobilized angle of internal friction and dilation angle of dense sand;
- comparison of finite element and the p - y curve method; and
- effects of loading angle and mooring positions on pullout capacity of a suction pile in sand.

Chapter 2

LITERATURE REVIEW

2.1 Introduction

Pile foundations have been widely used in various civil engineering structures for many years to resist axial, lateral and other forms of loads from structures. They are used where shallow foundations are not practical, especially when the top soil layer does not possess enough strength to carry the load, and pile foundations help to transfer the structure load to a deeper soil layer. Widely used piles are usually made of steel or concrete although timber piles are used in some cases. The shape of the pile could be square, rectangular or circular. Again steel pipe piles could be open-ended or closed ended. Moreover, piles could be installed in sand or in clay either single or in a group. The capacity of a pile depends on all the above factors. A large amount of research was devoted to this subject in the past. In order to conduct the literature review in a systematic way on the focused area of present study, the research available mainly on free-headed single steel pipe pile in sand under lateral load is presented in the following sections. It is also to be noted here that group piles are often used for foundations. The response of group piles depends on interaction between the piles in the group and pile head fixity with pile cap. As the focus of the present study is to model single piles, the research on group piles under lateral load is not discussed in the present literature review.

In offshore, another form of pile known as suction caissons are widely used especially for anchoring Floating Production Storage Offloading vessels (FPSOs). Suction caissons could be installed in sand or in clay seabed. Again in the following sections, the research available on suction caisson in sand is mainly presented in order to avoid any confusion as the response of a suction caisson in clay is different from that of in sand.

2.2 Laterally Loaded Long Piles in Sand

When lateral load is applied on the top of a long pile in sand, the load is transferred to the soil along the length of the pile depending upon the mobilized soil resistances as a function of lateral deflection of the pile at that depth. Figure 2-1 illustrates the distribution of soil stresses on a cylindrical pipe pile before and after pile deflection.

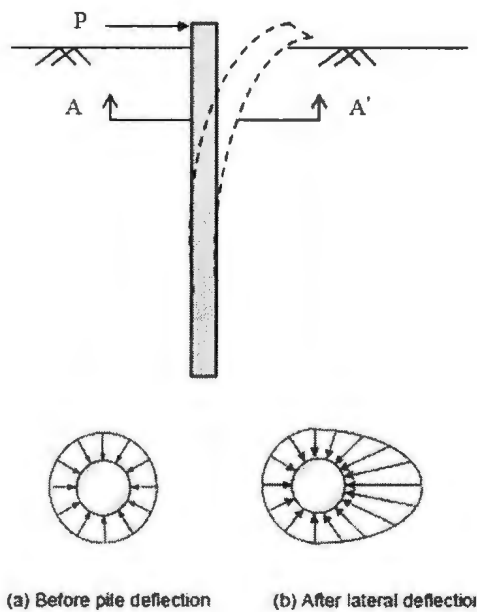


Figure 2-1: Distribution of soil pressure on a pile under lateral load (modified after Reese and Van Impe, 2001)

The response of a pile to an applied lateral load depends on the following factors: i) pile length, ii) pile bending stiffness, the product of the Young's modulus of the pile (E_p) and the moment of inertia (I_p), iii) soil stiffness, and iv) the degree of fixity of the head of the pile (Salgado, 2008). A long pile usually deflects laterally as shown in Fig. 2-1; however, a short pile rotates as a rigid body. The focus of the first part of the present study is the response of a long pile under static lateral load. Several methods have been proposed in the past for modeling this behavior, which is classified into three categories in this study: (i) theoretical method, (ii) physical modeling and (iii) numerical analysis.

2.2.1 Theoretical Methods

The response of a laterally loaded pile is a three-dimensional nonlinear soil-structure interaction problem. The deflection of the pile and the mobilized soil reaction depend on each other. Two approaches are available for modeling lateral resistance and deflection of laterally loaded piles. In the first method the soil mass surrounding the pile is treated and modeled as a homogeneous continuum (Prakash and Sharma 1990) and in the second method the pile is considered to be supported by an array of independent springs (also known as Winkler spring model). The simplest form of analysis of laterally loaded piles is the subgrade reaction method, where the soil stress-strain behavior is assumed to be a set of linear springs. As the soil behavior is nonlinear, the nonlinearity was incorporated in the springs and analyses were performed numerically when an analytical solution is not possible for complex boundary conditions. This method is known as the p - y curve method, which is often used in the current design practice.

2.2.1.1 Limit State Method

The limit state method is based on earth pressure theory. When a pile is subjected to lateral load, the excessive deflection could cause the failure. It could be either due to the failure of the pile or due to failure of the surrounding soil. Hansen (1961) proposed a method for estimating the ultimate lateral resistance of vertical piles based on earth pressure theory. He developed simple limit state methods for short rigid pile for free or fixed head conditions. Both short term (undrained) and long term (drained) conditions were considered. It is applicable to clay or sand and to multilayered soils.

Broms (1964 a, b) proposed methods for calculating the ultimate lateral resistance based on earth pressure theory simplifying the analyses for purely cohesionless and purely cohesive soils for short rigid and long flexible piles. Design charts similar to Fig. 2-2 have been developed for estimating the ultimate lateral resistance of a pile.

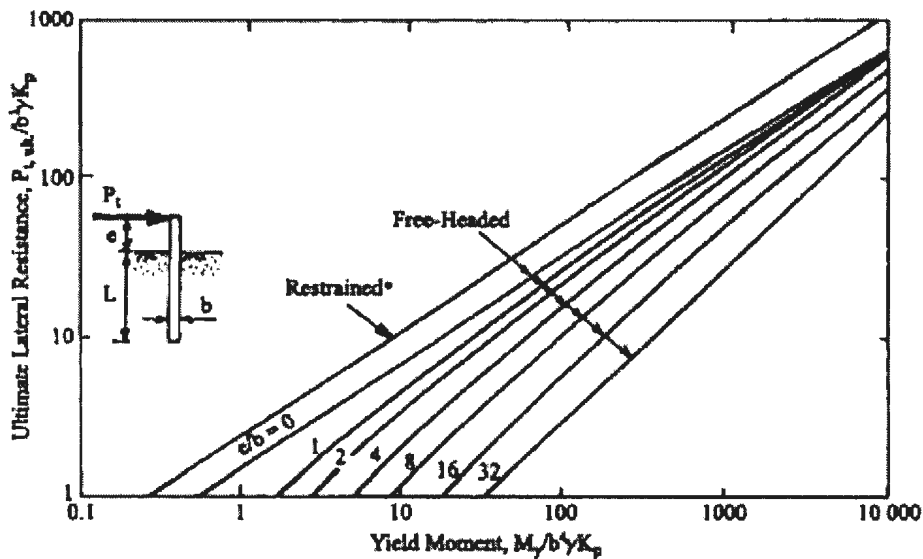


Figure 2-2: Curves for design of long pile under lateral load in cohesionless soil

While the design chart shown above is very useful for estimating the ultimate lateral resistance, it does not provide the load-deflection behavior. In the current design practice based on limit state design method, the deflection of the pile head is required to be estimated to meet the criteria required for the serviceability limit state design.

2.2.1.2 Subgrade Reaction Method

The subgrade reaction method is based on the beam on elastic foundation. In this method, the pile/soil behavior is idealized as a Winkler foundation (1876) in which the soil response is modeled as a series of independent linear elastic springs (Figure 2-3).

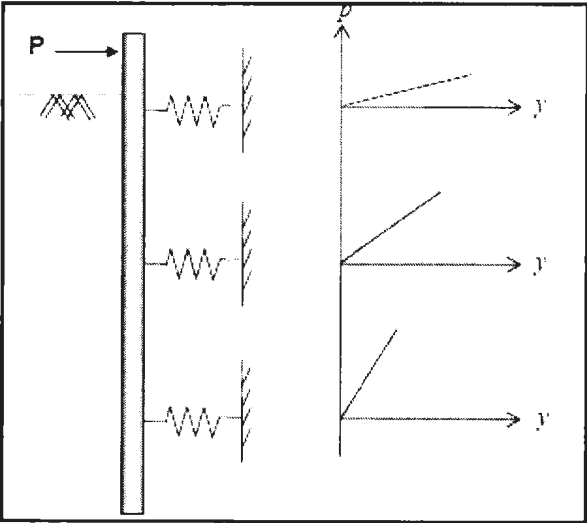


Figure 2-3: Subgrade reaction approach

This method is relatively simple and can incorporate factors such as nonlinearity, variation of subgrade reaction with depth, and layered systems. It is able to calculate deflections, moments, shear force and reactions on the pile. However, this method suffers from the disadvantages that it ignores the continuity of the soil, and the modulus of

subgrade reaction is an empirical parameter that depends on the foundation size and deflection (Reese and Matlock, 1956).

2.2.1.3 p - y Curve Method

The p - y curve method, the most widely used in design due to versatility and simplicity, has been developed to account for non-linearity between soil pressure and pile deflection at any point along a pile, which are capable of calculating lateral capacity of piles beyond the elastic range. Reese et al. (1974) proposed a method to define the p - y curves for static and cyclic loading. A modified version of Reese et al. (1974) is employed by the American Petroleum Institute (API 2000) in its manual for recommended practice. Both of these models have been implemented in the different versions of commercially available software LPILE (e.g. LPILE Plus 5.0, 2005).

Figure 2-4 presents the schematic diagrams of the p - y curve at various depths of the pile based on the Winkler springs model. In the p - y curve method of analysis, the pile is modeled as an elastic member, whereas the soil is modeled as a series of nonlinear springs. The shapes of the load-deflection relationships are described by specific p - y curves representing each independent spring. The p - y curve is a function of soil properties (e.g. stiffness and strength) and pile (pile type and geometry). The p - y curves represent the soil response along the pile length by relating pile deflection and soil reaction.

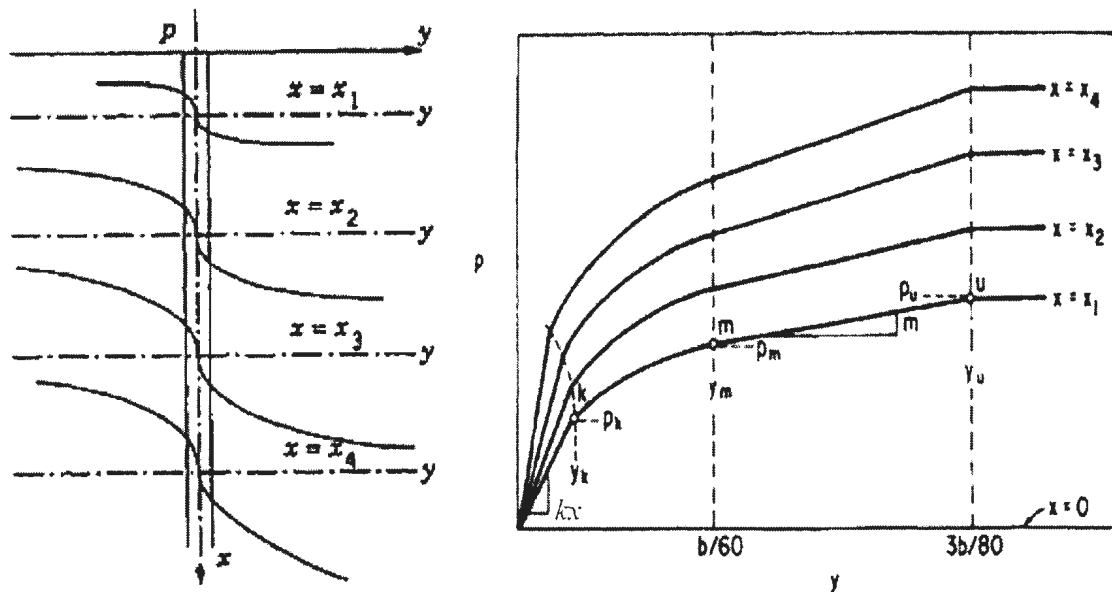


Figure 2-4: Set of p - y curves at various depths below soil surface (Reese et al. 1974)

The p - y curve methods developed by Matlock (1970) and Reese et al. (1974) are semi-empirical models in which soil response is characterized as independent nonlinear springs (Winkler springs) at discrete locations.

Madhav et al. (1971) have employed an elasto-plastic Winkler model, while Kubo (1965) has employed the following nonlinear relationships between pressure p , deflection y , and depth x .

$$p = kx^m y^n \quad (2.1)$$

Where k , m , n are experimentally determined coefficients. The governing differential equation incorporating Eq. 2.1 has been solved using finite difference method.

As mentioned before, the p - y curve developed by Reese et al. (1974) is widely used in the current design practice. For establishing the p - y curve, three portions of the curve should be studied which are the initial stiffness of the curve, the ultimate capacity of the soil and the transition portion between the initial curve and the final soil capacity curve (Fig. 2-4). The p - y curve in Reese et al. (1974) consists of four segments: (i) initial linear segment, which is mainly governed by the coefficient of initial modulus of horizontal subgrade reaction, k . As shown in Fig. 2-4 that the horizontal subgrade modulus (K_h) increases with depth (x) as $K_h=kx$ (ii) parabolic segment between the initial linear segment and lateral displacement of $b/60$, (iii) linear segment between lateral displacements of $b/60$ and $3b/80$, and (iv) constant soil resistance segment after lateral displacement of $3b/80$. Here, b is the width of the pile.

A modified version of Reese et al. (1974) is employed by the American Petroleum Institute (API 2000) in its manual for recommended practice. API (2000) recommended the following hyperbolic function to establish p - y curves for sand.

$$p = Ap_u \tanh\left(\frac{kx}{Ap_u} y\right) \quad (2-2)$$

Where, A is a factor to account for cyclic or static condition, p_u = ultimate bearing capacity (kN/m) and k = coefficient of initial modulus of subgrade reaction (kN/m³). The value of p_u depends of three empirical factors as discussed in the following section. Other parameters have been described previously. For static loading, the value of A depends upon depth and width of the pile as $A=3.0-0.8x/b \geq 0.9$ while for cyclic loading $A=0.9$ is recommended (API 2000).

Figure 2-5 shows the variation of initial modulus of subgrade reaction (k) for sand under and above the ground water table as a function of friction angle of sand as recommended in API (2000).

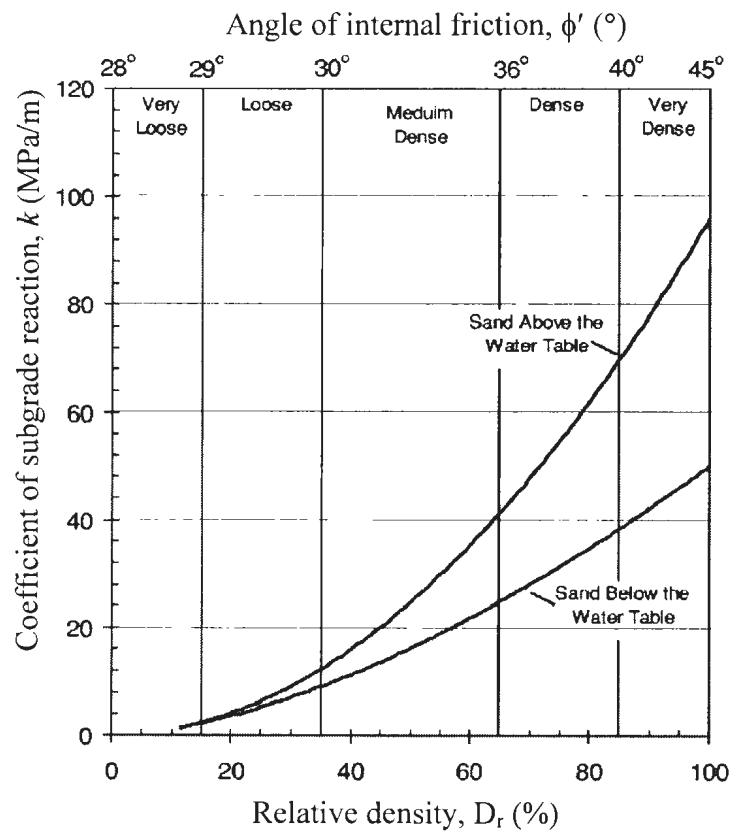


Figure 2-5: Coefficient of initial modulus of subgrade reaction, k (API, 2000)

Norris and his co-workers (e.g. Norris, 1986; Ashour and Norris, 2000) proposed the strain wedge (SW) for modeling lateral soil pile response. The basic configuration is

shown in Figure 2-6. The p - y curves obtained from SW method for a given soil is not unique but depends upon the neighboring soil and pile properties.

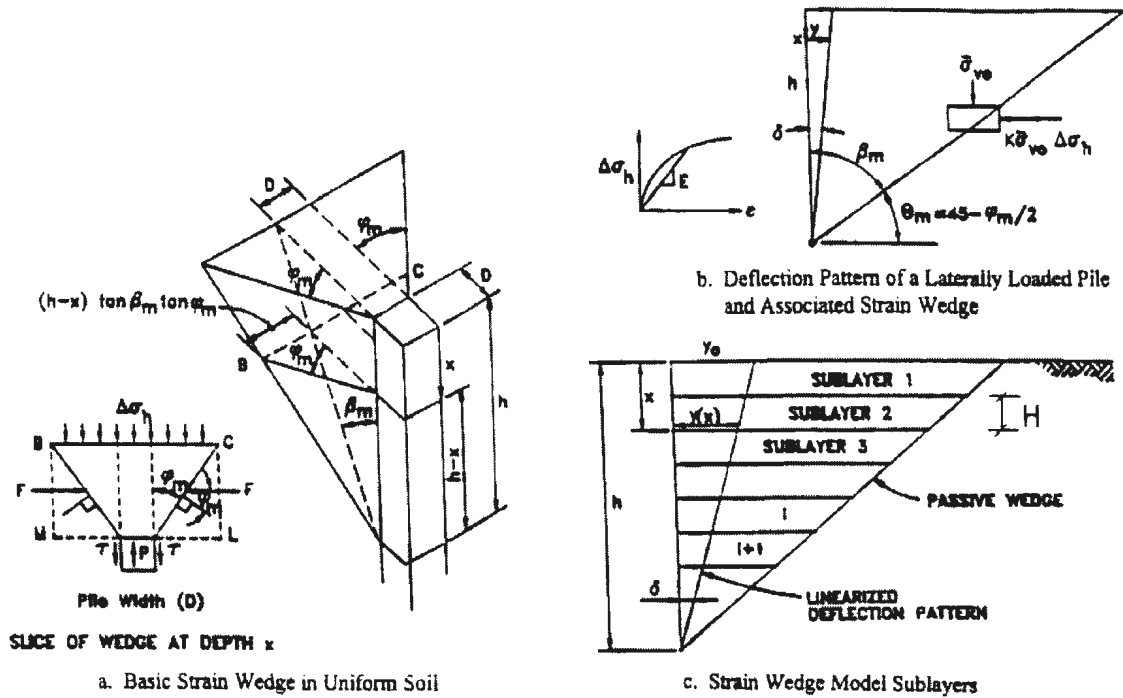


Figure 2-6: Basic Configuration of SW Model (Ashour and Norris, 2000)

In addition, several researchers worked on the development of p - y curves for sands. A brief summary of these works are presented in Table 2.1.

Table 2-1: Summary of p - y curves (Revised from Byung et al., 2004)

| References | Remarks |
|-----------------------------|--|
| Kondner (1963) | Introduced the hyperbolic function from the results of the stress-strain relationship of soil in triaxial compression tests. |
| Kubo (1965) | Developed nonlinear equation of soil pressure, pile deflection and depth. |
| Madhav et al. (1971) | Proposed an elasto-plastic Winkler model. |
| Reese et al. (1974) | Suggested the function from the results of the full-scale tests performed at Mustang Island. The function consists of three segments having two straight lines connecting by a parabola. |
| Scott (1980) | Developed the bilinear function from the results of centrifuge tests. |
| Det Norske Veritas (1980) | Proposed the function of combined hyperbolic and linear from the results of full-scale and model tests. |
| Murchison and O'Neil (1984) | Established the function from back analyses of full-scale instrumented pile load test on sand. |
| Norris (1986) | Developed strain wedge model based on the Wedge theory. |
| Wesselink et al. (1988) | Established the function from the results of the full-scale tests in calcareous sand of the Bass Strait. |
| API (2000) | Proposed hyperbolic relationship based on Reese et al. (1974) |

Comments on selection of soil parameters for the p - y curve method:

Two commonly used p - y curve methods widely used in the design are Reese et al. (1974) and API (2000). As mentioned before that both of them are empirical in nature and developed from experimental observation instead of doing rigorous theoretical formulation or numerical analysis. In these methods the initial and final segments of the p - y curve is established first and then connected them using appropriate curves. The main difference between Reese et al. (1974) (Fig 2-4) and API code is that in the API code, the coefficient of initial modulus of subgrade reaction (k) and ultimate resistance (p_u) of the soil is defined differently. As these two parameters are the key input parameters of the p - y curve method, the selection of these parameters is discussed below.

Coefficient of initial modulus of subgrade reaction (k):

Table 2.2 shows the various recommendations for the values of k for laterally loaded piles in sand. As shown in this table that Terzaghi (1955) recommended a range of value for different density of soil. For example, medium sand in submerged condition the value of k could vary between 2.2 and 7.3 MN/m³. On the other hand, Reese et al. (1974) recommended some values of k which are 2.6 to 4.8 times higher than average values of Terzaghi's recommendation. As mentioned by Reese et al. (1974) that their recommended values of k are simply based on initial straight line portion of the p - y curve measured in the field test. Note that, this recommendation is based on very limited field data. The API code (2000) revised this and recommended the variation of k as a function of ϕ' as shown in Fig. 2-5.

Table 2-2: Recommended values of k for the of p - y curves method

| | | Value of k (MN/m ³) | | |
|---|-------------------|-----------------------------------|-------------|------------|
| | | Loose sand | Medium Sand | Dense sand |
| Terzaghi (1955) | Dry or moist | 0.95-2.8 | 3.5-10.9 | 13.8-27.7 |
| | Submerged | 0.57-1.7 | 2.2-7.3 | 8.7-17.9 |
| Reese et al. (1974) | Above water table | 6.8 | 24.4 | 61.0 |
| LPILE Plus 5.0 | Submerged | 5.4 | 16.3 | 34.0 |
| American Petroleum Institute (API 2000) | Above water table | Fig. 2.5 | | |
| | Submerged | | | |

Both in Reese et al. (1974) and API (2000), the horizontal subgrade modulus K_h increases with depth as $K_h=kx$. Note that, K_h represents the elastic behavior of soil, and therefore the variation of K_h with depth in fact represents the effect of confining pressure on elastic modulus. It has been shown by many researchers that the elastic modulus increases with confining pressure as a power function with an exponent of about 0.5 rather than 1 (linear). Based on model pile load tests, Yan and Byrne (1992) confirmed that the linear variation of K_h with depth does not fit the test data as shown in Fig. 2-7. In the present study (Chapter 4), a power function is used to vary the elastic modulus which better represents the soil behaviour.

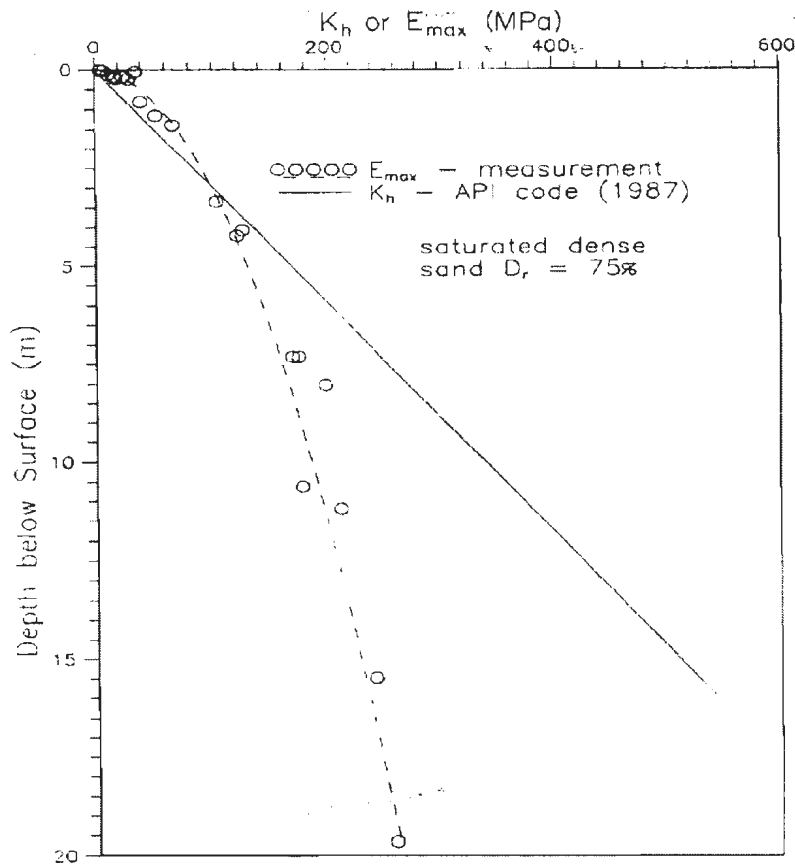


Figure 2-7: Comparison of measured and API recommended subgrade reaction (Yan and Byrne, 1992)

Ultimate soil resistance (p_u):

Reese et al. (1974) also computed the ultimate soil resistance theoretically. The comparison of theoretical and measured values is not satisfactory and therefore, an empirical adjustment factor (A) is recommended. The value of A varies with depth as shown in Fig. 2-8 (a). On the other hand in the API code, three empirical coefficients (C_1 , C_2 and C_3) are required to calculate the value of p_u . The coefficients C_1 , C_2 and C_3 are also function of ϕ' as shown in Fig. 2-8(b).

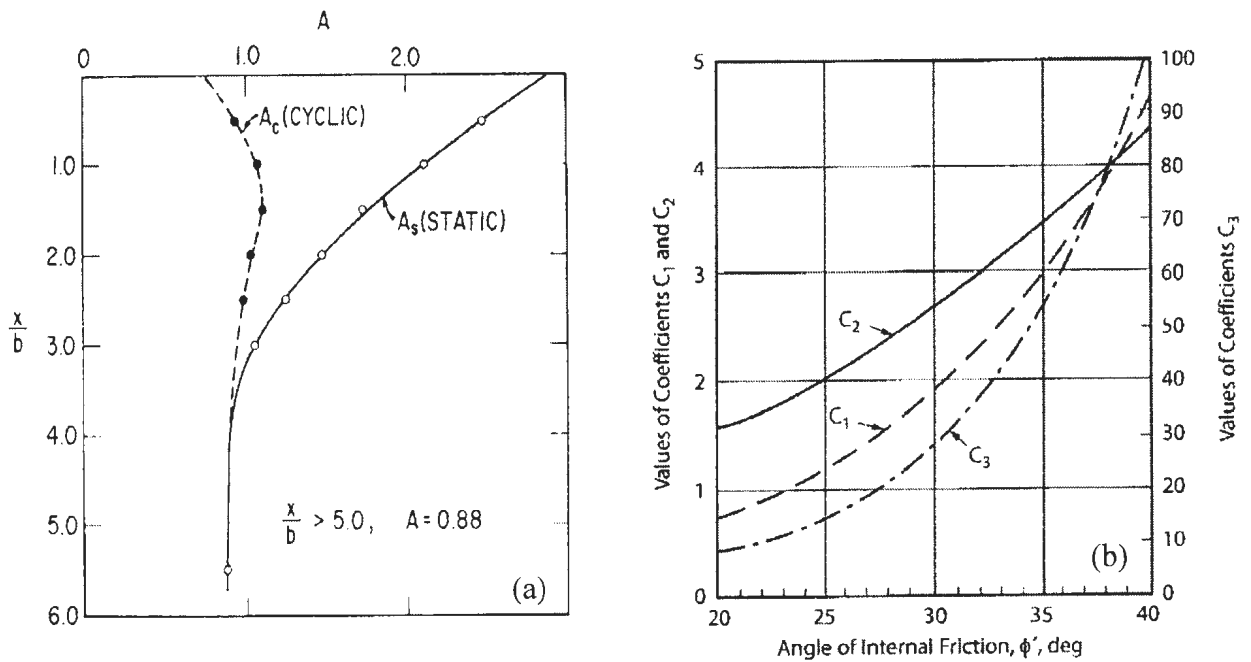


Figure 2-8: Empirical coefficients for ultimate resistance, (a) Reese et al. 1974, (b)

API code

Angle of internal friction (ϕ'):

As shown in Figs. 2-5 and 2-8 that the value of k and coefficients C_1 , C_2 and C_3 are function of ϕ' . Therefore, the selection of appropriate value of ϕ' is very important for successful simulation of lateral response of a pile foundation. However, it is a very difficult task. For example, in dense sand the value of ϕ' decreases from the peak to ultimate with the increase in shear strain. Now the question is which value of ϕ' should be used to find these coefficients (k , C_1 , C_2 and C_3) if the stress-strain behavior of dense sand is given from laboratory tests. The API (2000) recommended a method to calculate a design value of ϕ' if the relative density of sand is known as discussed in Section 3.3.3. However, comparing with full-scale test results several authors (e.g. Rollins et al., 2005)

showed that it significantly underestimates the lateral load for a given lateral displacement if API recommended ϕ' is used. It is to be noted here that selecting appropriate values of k and adjustment factors for p_u , one might match the calculated values and full-scale test results as shown in Fig. 2-9 (e.g. Reese et al., 1974). Further discussion on this comparison is provided in Chapter 3. The aim of the present study is to check whether the response of a laterally loaded pile can be simulated using fundamental soil properties which can be obtained from laboratory and field tests, avoiding above empirical factors.

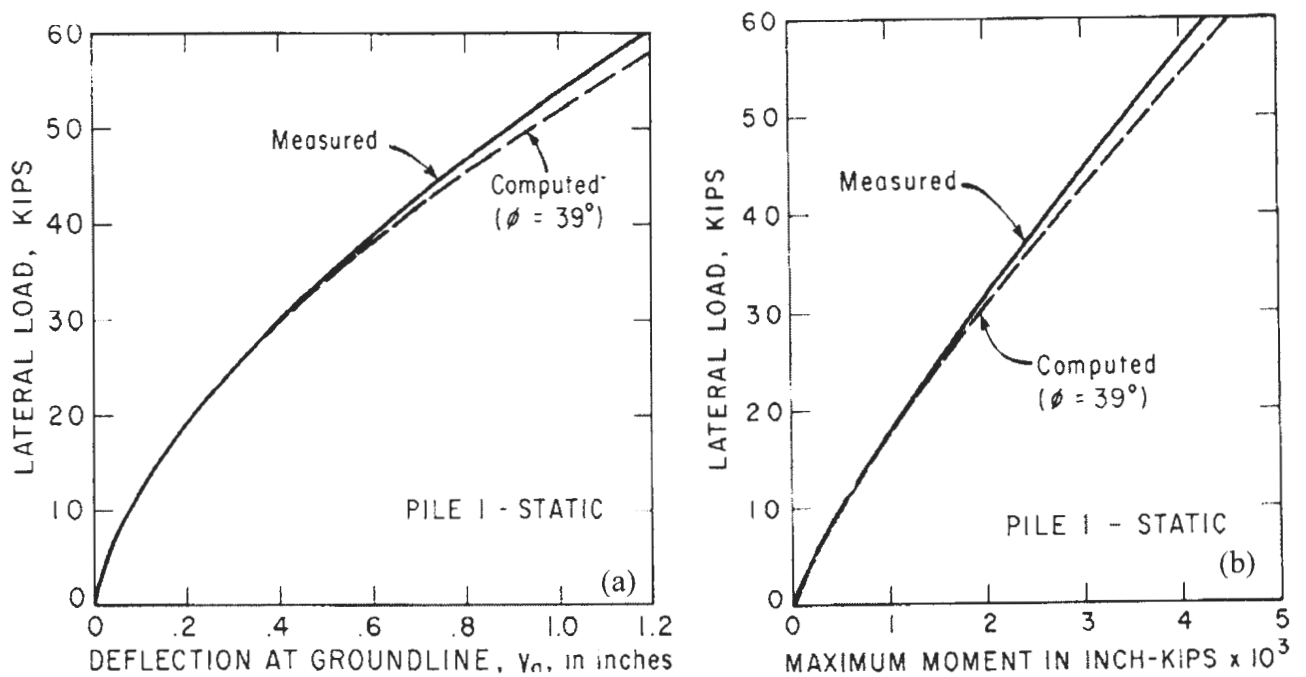


Figure 2-9: Comparison between full-scale test and computed results using p - y curve method (Reese et al. 1974).

2.2.2 Physical Modeling

Over the years researchers also conducted model tests in order to develop the theoretical framework for estimation of lateral load capacity of a pile. To review these works systematically, physical model tests have been classified into three categories: (i) Small-scale test, (ii) Centrifuge test and (iii) Full-scale tests.

2.2.2.1 Small-scale Tests

As full-scale pile load testing is very costly, many researchers conducted small-scale tests. Reese et al. (1981) performed laboratory tests on piles of 25 mm diameter to investigate the behavior of piles under lateral loading in layered cohesionless soils. Experimental results were compared to results from theoretical analysis, and fair to good agreement was obtained.

Meyerhof et al. (1988) carried out lateral load tests on flexible model piles and a small pile groups in loose sand. They suggested that the ultimate lateral resistance of flexible piles can be expressed in terms of an equivalent rigid pile by using an effective embedment depth.

Yan and Byrne (1992) presented a series of model test of single vertical piles in sand. The field stress conditions are simulated using hydraulic gradient similitude method. It was found that the p - y curves are highly nonlinear and stress-level dependent but are insensitive to the Young modulus and pile diameter. The API recommended p - y curves are significantly different from the experimental observed p - y curves. A parabolic

function fits the experiment results well. They also suggested a modification of the API recommended p - y curve that should utilize elastic modulus, a fundamental soil property, rather than subgrade reaction, which is an empirical factor. They also found that API-based p - y curves under predict the pile response at large deflection owing to their unrealistically low ultimate soil resistance.

Mahmoud and Burley (1994) investigated the behavior of unrestrained single model piles in cohesionless seabed sand under static lateral loads. Various parameters which influence the lateral load capacity of single piles including breadth, depth of embedment and cross-sectional shape of the pile were studied.

Poulos et al. (1995) presented a series of laboratory tests on single model piles embedded in calcareous sand subjected to lateral movement to examine the key parameters influencing the maximum bending moment in the pile. Normalized expressions for the maximum bending moment were also derived, which show an agreement with the experimental results and the theoretical predictions based on boundary element program.

Kim et al. (1998) conducted a series of model test on the behavior of single steel pipe pile subjected to lateral load embedded in Nakdong River sand to estimate the effect of non-homogeneity, constraint condition of pile head, loading rate, relative density, embedded length, and flexural stiffness of pile. A new Y parameter equation was developed for the modulus of subgrade reaction proportional to the depth.

Patra and Pise (2001) investigated the response of model single pile and pile groups in dry sand subjected to lateral loads. The load-displacement response, ultimate resistance, and group efficiency with spacing and number of piles in a group have been investigated.

They also proposed analytical methods to predict the lateral capacity of piles and pile groups.

Although small scale laboratory tests are relatively less expensive, it has a number of limitations. One of the major limitations is that the shear strength of sand depends upon effective stress of the soil, which cannot be modeled properly in a small-scale test and therefore, the test does not represent actual field stress conditions. These limitations could be overcome by conducting centrifuge or full-scale tests.

2.2.2.2 Centrifuge Tests

In the late 1970's the first set of tests were conducted in a geotechnical centrifuge to study the behaviour of laterally loaded piles (Scott, 1979a& b). Nunez et al. (1987) performed 17 model pile tests at Cambridge University to investigate lateral load performance of offshore piles in calcareous soil. The test comprised monotonic and cyclic lateral loading on single piles and group piles of diameters in the range 0.3 m to 2.1 m to validate scaling factors and the application of the work. Terashi (1989) conducted a series of centrifuge tests and demonstrated the reliability of centrifuge modeling of laterally loaded piles. He performed 6 similar tests at different accelerations. The results showed good consistency and thus validate centrifuge modeling of laterally loaded piles. Grundhoff et al. (1998) conducted a series of centrifuge tests at an acceleration of 50g to model lateral impact loading. These tests involved long flexible piles constructed from aluminum tubes. The major findings from this report were centered on the investigation of energy dissipation, which occurred as a result of plastic soil deformations.

McVay et al. (1998) conducted a series of centrifuge test on single and group piles. The model pile was constructed from a soil aluminum square bar of 9.525 mm diameter and 304.8 mm length. Tests were conducted using Florida sand mine. The main attempt of this study is to investigate group effects and to validate the p - y multiplier concept. However, the response of the single pile is similar to the presents study.

Dyson and Randolph (2001) conducted centrifuge tests to study the response of piles embedded in calcareous sand under monotonic lateral loading and recommended p - y curves with a magnitude of lateral resistance as a function of cone penetration resistance. A number of features, including method of installation, rate of loading, and pile head restraint have been studied. Modification factors have also been developed to allow for different methods of installation and different rates of loading.

Scott et al. (2005) performed eight dynamic model tests on a 9 m radius centrifuge test to study the behavior of single piles ranging from 0.36 m to 1.45 m diameter and group piles ranging from 0.73 m to 1.17 m diameter in gently sloping nonliquefied crust over liquefiable loose sand over dense sand. Effects of crust strength, pile diameter, pile cap dimensions and soil-pile interaction in liquefiable ground are studied in these experiments. The direction of lateral loads was shown to depend on the direction of the incremental and total relative movements between the soil and piles.

Bouafia and Bouguerra (2006) presented the results of an extensive programme of centrifuge modeling of single piles under lateral loads in the sand to investigate the effect of the proximity of a sandy slope on the response of a single pile. The slope influence

factor on pile deflections was derived for the configuration tested. The large displacements behavior of single piles in sand was also studied.

Duhrkop et al. (2010) conducted centrifuge experiments on laterally loaded piles to observe the pile behaviours and the lateral resistance from the soil.

2.2.2.3 Full-Scale Tests

Full-scale pile load tests are costly and are considered only for large projects. While pile load tests were conducted for many engineering projects for design the test results are not available in the public domain. In the following sections, some pile load tests in the area of present research (long pipe piles in sand) are discussed.

Cox et al. (1974) reported the results of a suit of full-scale lateral load tests in sand at Mustang Island. Tests on a single pile were conducted using a pipe pile of 610 mm diameter and 9.53 mm wall thickness. A 9.75 m length of the test pile near the ground surface was instrumented to obtain the response of the pile under lateral load. Lateral load was applied using a hydraulic jack at 0.3 m above the ground surface. Data was collected for lateral load increments of 11.1 kN up to 66.6 kN and then in increments of 5.56 kN to a maximum lateral load of 266.9kN.

Prakash and Kumar (1996) developed the load-displacement relationship for single piles subjected to lateral load in sands considering the soil nonlinearity using subgrade reaction based on the 14 full-scale lateral pile-load tests. An empirical equation of modulus degradation with strain and depth has also been proposed. This method over predicts the load for a specific displacement compared to the p - y solutions.

Ruesta and Townsend (1997) conducted an isolated single pile and a large-scale test group of 16 prestressed concrete piles subjected to a static lateral loading in sand overlying a partially cemented sand. The p - y curves developed from SPT correlations and PMT results provided reasonable prediction.

Rollins et al. (2005) performed a full-scale lateral load test on single and group piles embedded in medium dense sand to evaluate pile/soil interaction effects. Pile head deflection and bending moment under lateral load are measured using dial gauges and strain gages. Comparing the response of a single pile with group piles the group effects were investigated. Pile load test results are also compared with numerical analyses using LPILE and the SWM method.

Weaver et al. (2005) conducted a full-scale lateral load test on a 0.6 m cast-in-steel (CISS) pile in sand liquefied by controlled blasting. The soil resistance and displacement are presented as the p - y curves and compared to static sand p - y curves resulting from three simplified analysis, which is also compared to the test results. The shape of the back calculated p - y curves for liquefied sand is significantly different from the shape of standard p - y curves.

Bouafia (2007) conducted five full-scale horizontal loading tests of single piles in two sandy soils to define the parameters of p - y curves, namely the initial lateral reaction modulus and the lateral soil resistance to correlate with the pressure meter test parameters.

While the pile load test results only for a steel pipe pile is discussed, tests on concrete or steel H-piles are also available in the literature. A brief summary of some of the tests is given in Table 2-3.

Table 2-3: Summary of pile load test

| Pile material | Diameter or width (mm) | Soil type | Reference |
|----------------------|---------------------------|--|----------------------------|
| Steel pipe | 406 | Dense, medium to fine sand | Alizadeh (1970) |
| Steel H-pile | 370 | Dense, medium to fine sand | Alizadeh (1970) |
| Prestressed concrete | 406 | Dense, medium to fine sand | Alizadeh (1970) |
| Steel pile | 609 | Medium sand | Cox et al. (1974) |
| Timber | 305 & 356 | Loose sand | Wagner (1953) |
| Drilled shafts | 1220 | Dense sand overlaying clay | Long and Reese (1984) |
| Steel pipe | 324 | Loose to medium dense sand underlain by clay | Rollins et al. (2005) |
| Pressed concrete | 760 | Loose fine sand underlain by partially cemented sand | Ruesta and Townsend (1997) |
| Concrete | 300 | Very dense sand with silt | Ismael (2007) |

2.2.3 Continuum Modeling

Continuum modeling of pile foundations under lateral loading has been performed mainly in finite element framework. There are two approaches in the finite element method to handle laterally loaded pile. In the first approach, the laterally loaded pile is modeled using axisymmetric elements that could save the computational time. In the second approach, full three-dimensional analyses are performed using brick elements.

Analyses of laterally loaded piles using the finite element method have been conducted by a number of investigators. Desai and Appel (1976) performed three-dimensional finite element analysis for linear and non-linear soil behavior. They found that the relative movements at the soil-pile interface have a significant influence on pile behavior.

Beguelin et al. (1977) performed two-dimensional finite element analysis of laterally loaded piles using an elastic-perfectly plastic model for the soil with Tresca yield criterion. The influence of the shape of the pile and yield strength of soil has been investigated.

Randolph (1981) developed simple algebraic equations from the results of elastic finite element analysis to compute lateral deflections, rotations and bending moments in the pile. Faruque and Desai (1982) presented results of three-dimensional finite element analysis considering both material and geometric non-linearities. Drucker-Prager criterion was used to model the nonlinear behavior of soil.

Brown and Shie (1991) conducted three-dimensional nonlinear finite element analyses to study the lateral load deflection behavior of piles in undrained loading of saturated clay

or drained loading of sands. They used von Mises and Drucker-Prager criterion to model soil behavior as perfectly elastic-plastic. Their model also allows soil/pile separation at the interface.

Yang and Jermic (2002) present finite element analysis of a single pile in elastic-plastic soils in uniform sand and clay soils as well as cases with sand layer in clay deposit and clay layer in sand deposits. They generated p - y curves from their FE analyses and then compared with commonly used p - y curves.

Trochanis et al. (1991) examined the nonlinearity of soil behavior and separation/slippage between the pile and soil from a series of axisymmetric FE modeling of a free-head flexible pile subjected to lateral load. The nonlinear Drucker-Prager soil model was used in this study.

The advantages of FE method for analyzing a laterally loaded pile are: (i) Various geometry and boundary conditions for soil/pile system can be considered, (ii) Advanced soil model can be incorporated, although for most of the previous studies elastic or elastic-plastic models are used, (iii) Instead of independent springs, the continuity of soil mass and pile-soil interface behavior can be taken into account, and (iv) soil behavior can be defined using fundamental soil properties instead of any empirical relations

2.3 Inclined Loaded Suction Pile

As mentioned in Chapter-1, the second part of this study is devoted to suction piles under oblique upward loading. In the following sections, the literature review on this issue is presented. Suction piles are usually composed of a single or multiple cylinders of large

diameter and relatively shallow penetration depths. It is usually made of steel, one end open and the other end closed that is installed in the ground mainly by suction applied by pumping water out of the caisson interior. These novel foundation systems can be installed within 24 hours and are preferred to piles because of substantial savings from reduced materials and installation times. They are also more environmentally friendly than piles as they may be removed as easily as installed, simply by reversing the direction of pumping. Figure 2-10 shows the different parts of a typical suction pile.

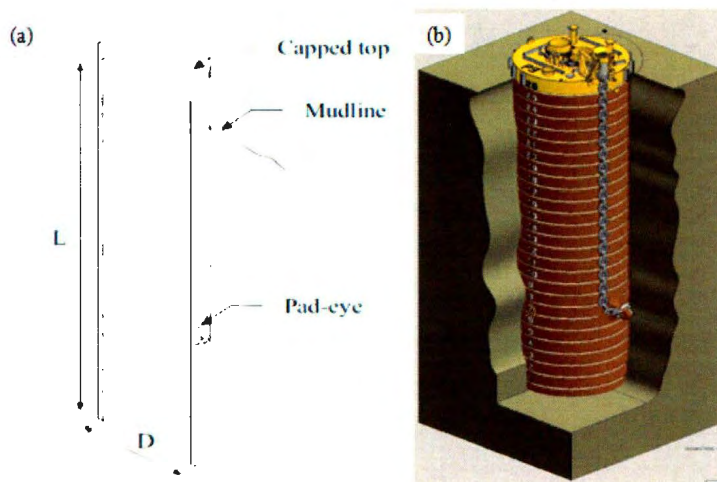


Figure 2-10: (a) Typical Geometry of Caissons half (Dilip 2004), (b) Caisson in place (Source: Mercier, 2003).

Suction caissons have been widely used in offshore industries ranging from anchoring floating facilities to offshore foundations. It is used as a foundation for Tension Leg Platform (TLP) and taut mooring line for FPSO (Floating Production, Storage and Offloading) as shown in Figure 2-11.

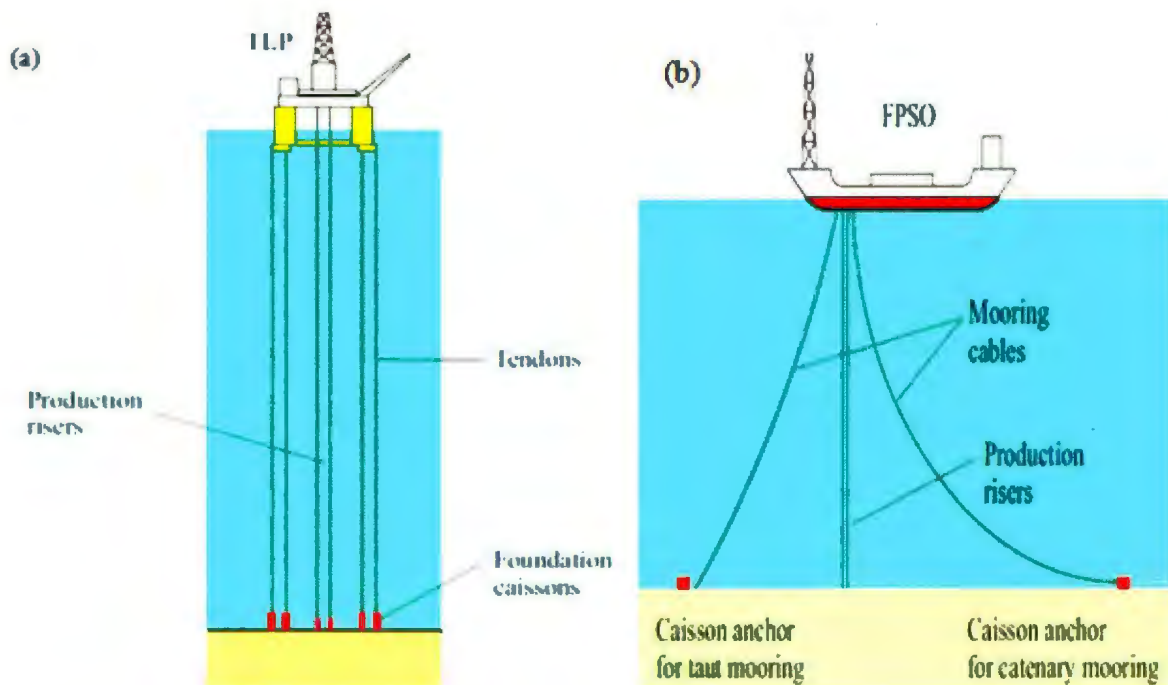


Figure 2-11: Caissons used as foundations for (a) Tension Leg Platform (TLP) and (b) Catenary and taut mooring lines (Dilip 2004)

Suction caissons are an attractive option with regard to provide anchorage for floating structures in deep-water as they offer a number of advantages in that environment. They are easier to install than driven piles and can be used in water depths well beyond where pile driving becomes infeasible. Suction caissons have higher load capacities than drag embedment anchors and can be inserted reliably at preselected locations and depths with minimum disturbance to the seafloor and adjacent facilities. Sparrevik (2001) estimated that there are as many as 300 suction caissons in operation around the world.

Geometrically the suction piles are larger in diameter than typical piles used for foundations.

Figure 2-12 shows examples of suction piles used for various projects in the world. Suction caissons could be installed both in clay and sand seabeds, although the mechanism during installation is different. Houlsby and Byrne (2005a, b) present the design procedure for installation of suction piles in sand, clay and other geomaterials. Not only sand or clay, the installation of suction caisson in sand with silt layers is also investigated (e.g. Watson et al., 2006; Tran et al., 2007).

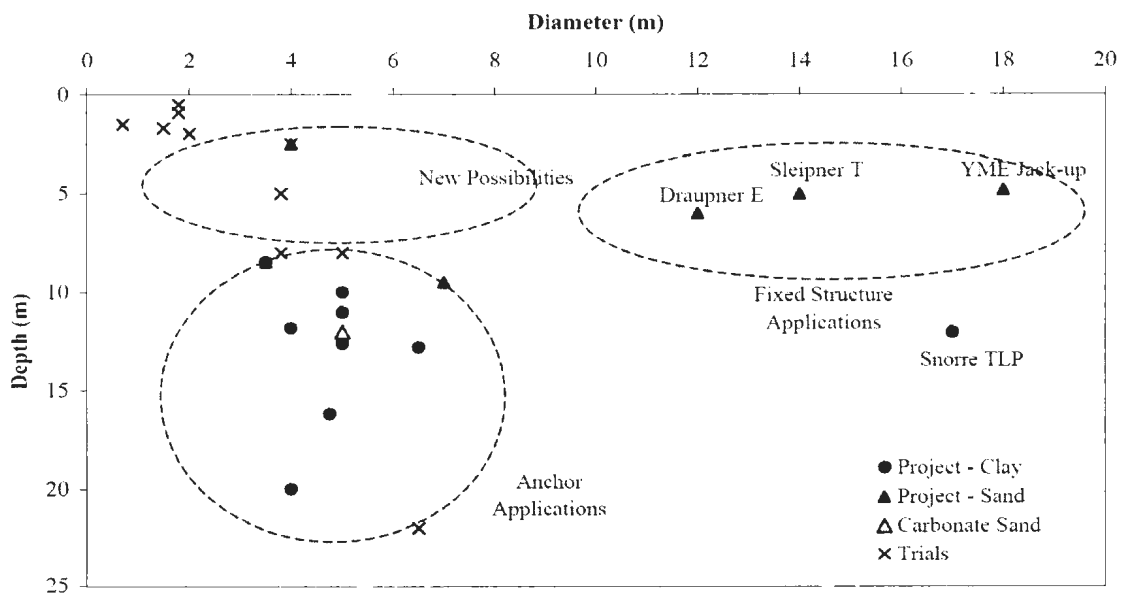


Figure 2-12: Caisson foundations used in various projects (Byrne 2000)

The pull-out capacity is one of main requirements when a suction caisson is used in mooring systems for deep water oil and gas development projects. The caisson is normally pulled by a chain connected to the pad eye on the side of the pile (Figure 2-10). The inclined pull-out capacity of a suction caisson depends on both horizontal and vertical load capacity.

The capacity of suction caissons in holding tensile loads results from the combined effect of the following components (Albert et al., 1987):

1. Passive suction developed under the caisson sealed cap;
2. Self-weight of the caisson, foundation template, and ballast (if any);
3. Shearing or frictional resistance along the caisson-soil interfaces;
4. Submerged weight of the soil plug inside the caisson; and
5. Reverse end bearing capacity.

The very first use of suction caissons was presented by Mackereth (1958) for holding down a piston corer during Lake-bed sampling operations. Later model testing was performed by Goodman et al. (1961) to evaluate the pullout resistance of an inverted cup type anchor subjected to different type of vacuum pressure in various moist soils. In the following sections, literature reviews are presented based on the selected field tests, laboratory tests, centrifuge tests and numerical analysis.

2.3.1 Field Tests

A large number of small-scale field tests and full-scale tests were carried out by several researchers to develop installation procedures and load capacities of suction caissons. The aspect ratio (L/D) of the caissons tested ranged from 1 to 10 and both sandy and clayey soil conditions were examined. During the tests, the caisson behavior was recorded under various loading conditions. In the following paragraphs, a review of selected field tests is presented.

Brown and Nacci (1971) conducted model tests on suction anchoring systems to study the behavior and the flow characteristics of the anchor in granular soil. Five basic elements are examined: anchor housing, penetration skirt, pump, load transmission element, and fixed porous stone mounted inside the skirt to prevent liquefaction of the sand.

Hogervorst (1980) performed three full-scale field tests on suction caisson anchors having 12.5 ft (3.8 m) diameter with length ranging from 16.4 to 32.8 ft (5 to 10m), installed in sandy and clayey soils. The objectives of the tests were to study installation characteristics of the caissons and measure their axial as well as lateral capacities. The successful field tests provided an opportunity for systematic evaluation of the potential of caissons to anchor floating production facilities and proved the feasibility of installing caissons by the application of suction.

Two large-scale field penetration tests were performed by Tjelta et al. (1986) to collect important design information of the CONDEEP Gulfaks C fixed concrete platform consisting of two steel cylinders of 23 m height and 6.5 m diameter connected to each other through a concrete panel. The objectives of the testing program were to observe tip resistance and wall friction and to learn more about the uncertain factors related to installation and operation. The success of the tests proved the feasibility of installing long skirts by suction.

The first major structure installed in dense sand using suction caissons was Statoil's Draupner E riser platform (formerly Europipe 16/11 E) in the North Sea. This was installed successfully during 1994 in 70 m water depth. The caisson foundations were 12

m in diameter and the skirts were 6 m long, and designed to be installed with suction. The design for the installation was based on a combination of field testing, laboratory testing and finite element modeling. Statoil installed a second caisson-founded structure in the North Sea in 1996 (Sleipner T).

Cho et al. (2002) also carried out a series of field tests on steel suction caissons having inside diameter ranging from 0.5 m to 2.5 m and length of 5m installed in silty sand in water depth of about 10m. The objective of the tests was to validate the response of the caissons observed during small-scale (model) laboratory tests (Bang et al., 2000).

Similarly, field tests are also available in clay, which is not discussed in detail in this thesis as the focus of this study is to model caissons in sand. Dyvik et al. (1993) conducted field tests on four small-scale suction anchors consisting of four cylinders with 0.87 m diameter and 0.82 m length installed in soft clays at the Snorre oil and gas field in the North Sea. Keaveny et al. (1994) investigated five large-scale field model tests on a suction anchor installed in saturated clay, which was subjected to static and cyclic horizontal loads.

2.3.2 Laboratory Tests

Laboratory model tests on suction caissons were performed by several researchers to investigate the performance of caissons under various conditions. Laboratory tests can be divided into vacuum anchors and caisson anchors categories.

Tests on Vacuum Anchors:

Brown and Nacci (1971) carried out a series of laboratory test consisting of 14 tests in loose sand and 15 tests in dense sand on vacuum anchors having 254 mm diameter and 44 mm embedded length to study their behaviour and water flow characteristics. The test results show a linear relationship between pullout capacity and applied suction.

The vacuum anchors are shallow surface foundations generally used for providing temporary anchorage and require that the water be pumped out during their application to generate the required capacity (Wang et al., 1975). The aspect ratio of the anchors tested ranged from 0.1 to 2.1 and different soil types were considered. Linear increase in pullout capacity was observed with increasing suction, supporting earlier findings by Brown and Nacci (1971). Later, Wang et al. (1977) developed equations to estimate the pullout capacity of vacuum anchors based on observed failure mechanisms and adopting Mohr-Coulomb failure criteria. Wang et al. (1978) presented sample design examples to demonstrate practical applications of the anchors.

Helfrich et al. (1976) conducted a series of 12 laboratory tests on vacuum anchors having a diameter of 496mm and a length of 254mm installed in the sand to generate additional test data for design purposes.

Tests on Caisson Anchors:

Helfrich et al. (1976) examined the failure modes of suction anchors tested in medium to fine grained sand. The degree of dependence of anchor performance on the flow rate of water through the anchor chamber was also observed. A 400 mm diameter and 250 mm

in depth pile was modeled to determine the pullout force in submerged sand. The weight of the sand plug retained by the anchor was found to be related to the flow rate. Failure of the sand occurred in the vicinity of the cutting edge of the suction anchor and consisted of many small shear failures that appeared as a horizontal bumpy surface.

Larsen (1989) conducted 15 laboratory tests on model suction caissons with diameters equal to 100 mm, 200 mm and 300 mm and a length 381 mm. The model suction caissons were installed in sandy and clayey soils to observe the mechanical behaviour of the soil and caisson during installation and determine the lateral load capacity under static and cyclic loads.

Steensen-Bach (1992) performed 77 laboratory tests on suction caissons with an aspect ratio ranging from 1.67 to 3.33 and a diameter ranging from 48 mm to 80 mm installed in sandy and clayey soils. The goals of the study were to identify the contribution of suction generated during pullout to the capacity and obtain additional test data to develop design procedures.

Byrne and Houlsby (2000 and 2002a) conducted an experimental investigation on suction caissons subjected to a variety of cyclic loads, installed in oil-saturated sandy soil. The authors did not observe any degradation of caisson capacity under cyclic loading but did observe some effect of the rate of load application on the caisson response.

Laboratory tests in clay are also available in the literature, which is not again discussed in detail in this thesis. Cauble (1996) reported 14 laboratory tests on a model suction caisson installed in K_0 -normally consolidated clay samples. Coffman (2003) carried out nine laboratory tests on a model suction caisson in normally consolidated kaolin subjected to

horizontal load applied at various points along the lower half of the caisson to improve analytical methods for design of such caissons.

2.3.3 Centrifuge Tests

To estimate the pullout capacity of suction piles, a large number of centrifuge tests have been conducted in the past. Again the tests mainly in the sand are discussed in detail and some tests in clay are also briefly highlighted.

Allersma et al. (2000) conducted a series of centrifuge tests to estimate the horizontal bearing capacity of suction piles in sand and clay. The effects of several parameters were investigated including the height/diameter ratio, the attachment point of the cable and loading angle. Figure 2-13 shows the typical load-displacement curve for the tests in sand. The initial 20 mm displacement is mainly because of cable stretching. As the exact displacement of the caisson is not known, the formulation of the load-displacement curve for the caisson is difficult. However, there is a clear peak value that represents the bearing capacity of the caisson. The measured bearing capacity was compared with the API standard and also with FE analysis. The horizontal bearing capacity based on API recommendations is conservative while the FE results show a very good agreement with the test results. Comparison between numerical and measured load-displacement response was not preformed.

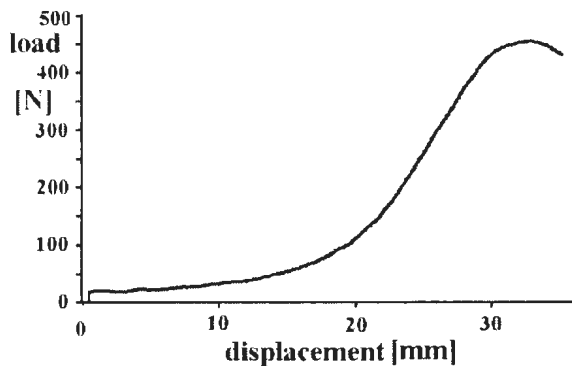


Figure 2-13: Typical load displacement curve in centrifuge test (Allersma et al. (2000))

Lee et al. (2003) conducted a series of centrifuge test on suction anchors to determine the horizontal and inclined load capacity. They also investigated the effects of depth, the location and direction of loading. The maximum pullout capacity in sand is obtained when the padeye is located at approximately 85% of the length of the caisson from the top.

Kim et al. (2005) conducted a series of centrifuge tests to determine the capacity of an embedded suction anchors in sand. In addition to the loading point and load inclination angle, the effects of flanges on pullout capacity are investigated. They also found that the pullout capacity increases if the padeye location is moved downward and the maximum value was obtained when the padeye is located at approximately 67% of the caisson height from the top. Kim et al. (2010) further presented a series of centrifuge test results on pullout capacity of suction caisson. They showed the similar response for mooring position and load inclination angle as discussed before.

Bang et al. (2011) reported a series of centrifuge tests on a model suction pile in medium dense sand to determine its inclined pull-out capacities. The tests were conducted by the Daewoo Institute of Construction Technology between 2007 and 2008. The main variables of the study were the load inclination angle and the point of mooring line attachment which varies from the top to bottom of the suction pile and maximum pullout capacity. Further details about these tests and comparison with the present FE analyses are shown in Chapter 4.

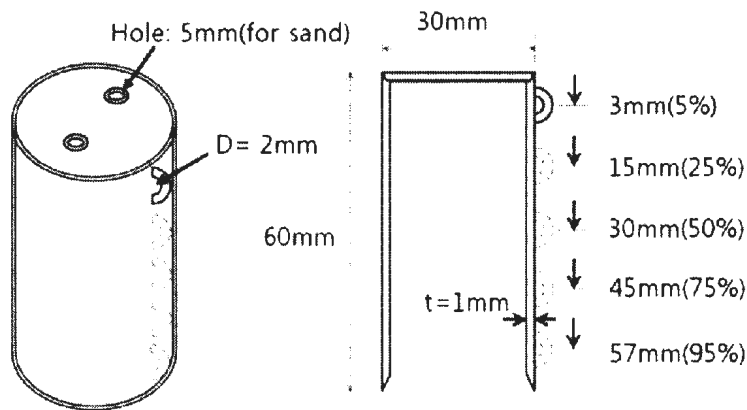


Figure 2-14: Schematics of model suction pile and pulling locations (Bang et al. 2011)

A large number of centrifuge tests were also conducted for suction caissons in clay. Clukey and Morrison (1993) reported a series of centrifuge tests to investigate the response of steel suction caisson foundations under axial pullout load in soil conditions typically encountered in the Gulf of Mexico. Randolph et al. (1998) performed centrifuge tests on suction caissons subjected to quasi-horizontal loads applied through a catenary mooring system and compared the test results with the theoretical predictions using a three-dimensional upper bound solution. House (2000) presented results from a series of

geotechnical centrifuge tests conducted to study installation and response of a scaled prototype caisson in clay. Cao et al. (2001 and 2002a) presented results of eight centrifuge tests in clay conducted at C-CORE's centrifuge center.

2.3.4 Numerical Analysis

The upper bound and FE methods verified with the results of laboratory and centrifuge tests are the most popular methods to predict the pullout capacity of suction anchors. However, several issues and uncertainties related to capacity estimation and failure mechanisms are still unresolved. Most of the FE analyses available in the literature are for suction caissons in clay.

Erbrich (1994) conducted a series of finite element analysis using the ABAQUS FE software to estimate the capacity of suction caisson foundations of fixed offshore platforms. The comparison between FE predictions and the results of a number of model tests conducted by Wang et al. (1978) shows the applicability of FE analyses to estimate foundation capacity. Drucker-Prager and Drucker-Prager with cap plasticity models were adopted to model the nonlinear behavior of dense sand.

Bang and Cho (1999) carried out three-dimensional FE analyses using ABAQUS FE software to evaluate vertical, horizontal and inclined load capacity. The sand was modeled as elastic-perfectly plastic material using the Drucker-Prager plasticity model.

Deng and Carter (2000) presented finite element analyses of a suction caisson in sand assuming axisymmetric loading conditions. Analyses were performed using the finite element software package AFENA and Mohr-Coulomb soil model. The effects of various

parameters were investigated including embedment, load application point, load inclination angle, friction angle of the soil, dilatancy and the initial stress state.

As the focus of the present study is to model suction caissons in the sand, the FE modeling of suction caissons in clay is not discussed in detail here. However, a list of FE analysis of suction caisson in clay is shown in Table 2-4.

Table 2-4: Summary of numerical analysis in suction caissons

| References | FE Modeling & Constitutive model | Notes |
|----------------------------------|---|---|
| <u>Suction pile in sand</u> | | |
| Erbrich (1994) | ABAQUS FE, Drucker-Prager and Drucker-Prager cap | Estimated the capacity of the suction caissons for fixed offshore platform. |
| Bang and Cho (1999) | ABAQUS FE, Drucker-Prager | Studied vertical, inclined and lateral load capacity. |
| Deng and Carter (2000) | AFENA, Mohr-Coulomb | Estimated inclined pull-out capacity in drained condition. |
| <u>Suction pile in clay</u> | | |
| Sukumaran et al. (1999) | ABAQUS FE, von Mises yield criterion | Calculated lateral load capacity; conducted two- and three-dimensional FE analyses. |
| Handayanu et al. (1999 and 2000) | ABAQUS FE, modified Cam clay | Studied vertical uplift and inclined load and compared with model test results. |
| Zdravkovic et al. (2001) | FE, modified Cam clay, MIT-E3 | Studied the effects of load inclination, skirt length, caisson aspect ratio and soil anisotropy on behaviour of suction piles. |
| Cao et al. (2002b& 2003) | ABAQUS FE, modified Cam clay | Studied vertical pullout capacity, compared with centrifuge test results |
| Aubeny et al. (2003a,b) | FE & Simplified upper bound solution, von Mises yield criterion | Proposed procedure to estimate load capacity of suction caisson anchors as a function of the load attachment point location and load inclination angle. |

2.4 Summary

In this chapter, a comprehensive literature review is presented on the two focused areas of the present research, namely lateral load capacity of a flexible pile and pullout capacity of suction caisson in sand. Experimental, numerical and theoretical studies were performed in the past.

In the current design practice, uncoupled nonlinear p - y curves are widely used to calculate the lateral load deflection behaviour. The formulation of p - y curves is somehow empirical. The FE analyses performed in the past did not consider the effects of post-peak softening behavior of dense sand including the reduction of dilation angle and friction angle with accumulated plastic strain.

Limited number of research is available in the literature on FE modeling to estimate the pullout capacity of suction caissons in sand. Three-dimensional FE modeling using an appropriate soil constitutive model verified with the physical model test results might give further confidence in estimated pullout capacity.

Chapter 3

NUMERICAL MODELING OF A LATERALLY LOADEDE LONG FLEXIBLE PILE IN SAND

3.1 General

In this chapter, the behavior of a steel pipe pile in sand subjected to a lateral load is examined by finite element (FE) analysis. Three-dimensional finite element analyses are performed for pure lateral load applied above the ground surface. The FE analyses are performed using the commercially available software package ABAQUS/Standard. The sand around the pile is modeled using a modified form of Mohr-Coulomb soil model. The modification involves the variation of mobilized angle of internal friction and dilation angle with plastic shear strain. The nonlinear variation of elastic modulus with mean effective stress is also considered in the present FE analyses. These important features of a soil constitutive model have been implemented in ABAQUS/Standard using a user subroutine. Numerical analyses are also performed using the LPILE software, which is based on the p - y curve method. The FE and LPILE results are compared with the results of two full-scale tests. It is shown that the FE model can successfully simulate the response of a pile under lateral load. By comparing the numerical results with the full-scale test results, some limitations of the p - y curve method are highlighted.

3.2 Introduction

The lateral resistance of pile foundations is one of the key design considerations in many civil engineering structures both in onshore and offshore applications. Wind, wave, earthquake and ground movement might create significant lateral load on pile foundations. The response of a pile under lateral load is governed by complex three-dimensional soil/pile interaction behaviour. Various approaches have been proposed in the past for analysis of a laterally loaded pile. Hansen (1961) proposed a method for estimating the ultimate lateral load resistance of vertical piles based on earth pressure theory. Broms (1964 a, b) also proposed methods for calculating the ultimate lateral resistance based on earth pressure theory simplifying the analyses for cohesionless and cohesive soils for short rigid and long flexible piles. Meyerhof et al. (1981, 1988) also proposed methods to estimate the ultimate lateral resistance and groundline displacement at the working load for rigid and flexible piles.

The lateral deflection of the pile head is one of the main requirements in the current design practice, especially in limit state design. Mainly two approaches are currently used for modeling the lateral load deflection behaviour of piles. In the first approach, the response of soil under lateral load is modeled using nonlinear independent springs in the form of p - y curves, where p is the soil-pile reaction (i.e. the force per unit length of the pile) and y is the lateral deflection of the pile. Then using the concept of a beam-on-elastic foundation the problem is solved numerically. The p - y curve method is very similar to the subgrade reaction method except that in the p - y curve method, the soil resistance is nonlinear while in the subgrade reaction method, it is linear with

displacement. Reese et al. (1974) proposed a method to define the p - y curves for static and cyclic loading. A modified version of Reese et al. (1974) is employed by the American Petroleum Institute (API 2000) in its manual for recommended practice. Both of these models have been implemented in the commercially available software LPILE Plus 5.0 (2005). Ashour and Norris (2000) showed that the “Strain Wedge” model is capable of evaluating some additional effects such as bending stiffness of the pile, pile shape, pile head fixity and depth of embedment on the p - y curves. The second approach of modeling laterally loaded piles is based on continuum modeling. Poulos (1971) presented finite element analysis of a single pile situated in an ideal elastic soil mass. Finite element analyses of single piles under lateral load have also been conducted by other researchers (Brown and Shie 1991, Kimura et al. 1995, Wakai et al. 1999, Yang and Jeremic 2002). Brown and Shie (1991) performed three-dimensional finite element analysis modeling the soil using von Mises and extended Drucker-Prager constitutive model. Trochanis et al. (1991) examined the effects of nonlinearity in soil stress-strain behaviour and separation or slippage between the soil and the pile surfaces. In addition, there are some full-scale test results (e.g. Cox et al. 1974, Long and Reese 1985, Brown 1985, Rollins et al. 2005, Ruesta and Townsend 1997) and centrifuge test results (e.g. Nunez et al. 1987, McVay et al. 1998, Grundhoff et al. 1997, Dyson and Randolph 2001) are available in the literatures which were used in the previous studies for model verification.

The purpose of this chapter is to present a series of three-dimensional finite element analysis of a long steel pipe pile in sand subjected to lateral load. The finite element

results are compared with LPILE analysis, and also with the results of two full-scale tests. The limitations of the p - y curve method are discussed based on lateral response of the pile.

3.3 Finite Element Modeling for Cox et al. (1974)

The numerical analyses presented in this study are carried out using the finite element software ABAQUS/Standard 6.10-EF-1. The finite element results are verified using the full-scale test results reported by Cox et al. (1974). The full-scale test site was located at the Shell Oil Company tank battery on Mustang Island, near Port Aransas, Texas. The test setup is shown in Figure 3-1. An excavation of 1.68 m (5.5 ft) was carried out first to remove the soil near the ground surface and to reach the groundwater table.

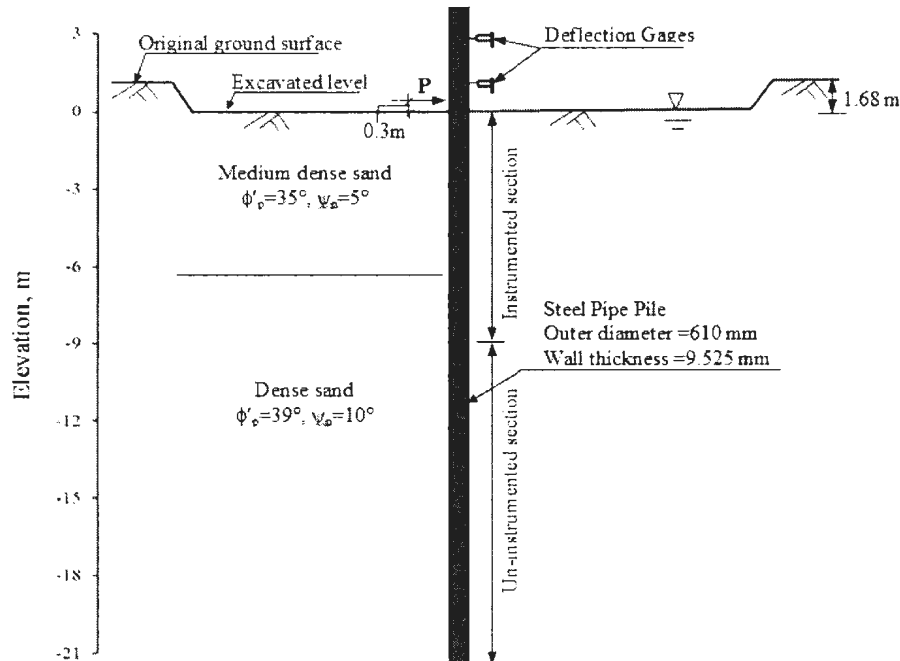


Figure 3-1: Idealized soil and pile load test setup (redrawn from Reese et al. 2001)

There was a clay layer of 0.76 m (2.5 ft) near the groundwater table. This clay layer was also removed and filled with clean sand similar to in-situ condition. Pile load tests were conducted for static and cyclic loading. In this paper, comparison is performed only with the test results of a single pile under static load. Lateral load tests were conducted for a steel pipe pile of 610 mm diameter and 9.53 mm wall thickness. As shown in Figure 3-1, the top 9.75 m length of the test pile was instrumented to obtain the response of the pile under lateral load. A total of 40 strain gauges were placed in the instrumented section of the pile. Lateral load was applied at 0.3 m above the ground surface using a hydraulic jack, and the load was measured using a universal load cell. The lateral deflection under a given lateral load was measured at two points above the load using two deflection gauges. The data was analyzed and the response was reported for lateral load increments of 11.1 kN up to 66.6 kN and then in an increment of 5.56 kN to the maximum lateral load of 266.9kN.

The finite element modeling in this study is carried out in Lagrangian framework. Considering geometry of the problem and loading conditions, the advantage of symmetry is used and only half of the model under lateral load is analyzed. A soil domain of 20 m diameter and 30 m height as shown in Figure 3-2is modeled. The pile is located at the center of the soil domain. The size of the soil domain is sufficiently large and therefore, boundary effects are not expected on predicted lateral load, displacement and deformation mechanisms. The bottom of the soil domain is restrained from any vertical movement while the curved vertical face is restrained from any lateral movement using roller supports. The symmetric vertical xz plane is restrained from any movement in the

y -direction. No displacement boundary condition is applied on the top, and therefore the soil can move freely.

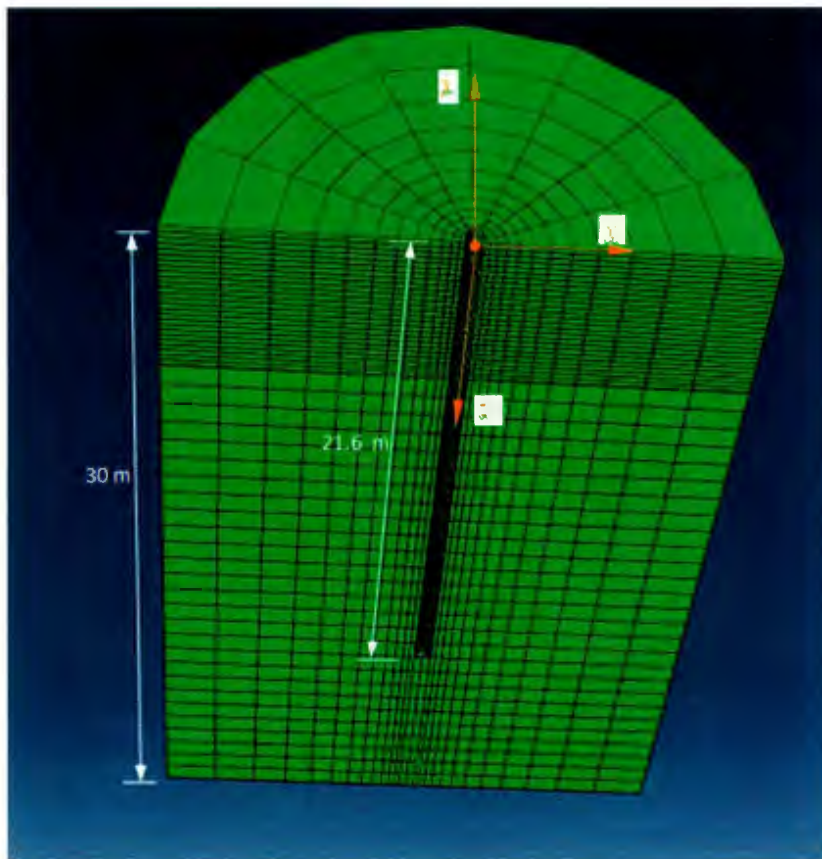


Figure 3-2: Finite element model

Both soil and pile are modeled using the solid homogeneous C3D8R elements, which are 8-noded linear brick elements with reduced integration and hourglass control. The size of the mesh has a significant effect on finite element modeling. Often, finer mesh yields more accurate results but computational time is higher. For successful FE modeling, finer mesh is used in the critical sections. The top five to ten pile diameters depth is critical for modeling piles under lateral load. Therefore, finer mesh is used for the upper 6.0 m of soil and a medium mesh is used for 6.0 to 21.0 m depth. For the soil layer below the pile

(>21m depth) coarse mesh is used, as it does not have a significant effect on load-displacement behaviour of the pile. Based on mesh sensitivity analyses (Figure 3-3) with different mesh sizes and distribution the optimum mesh consists of 18,027 C3D8R elements, shown in Figure 3-2 is selected for the present FE analysis.

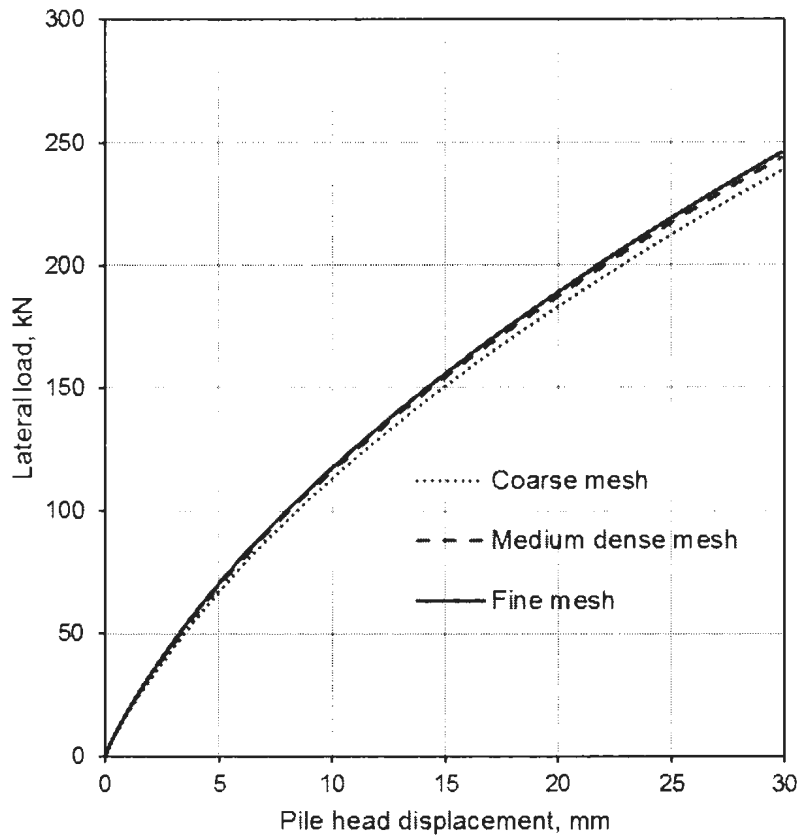


Figure 3-3: Mesh sensitivity analysis

3.3.1 Modeling of pile and soil/pile interface

A free-head steel pipe pile of 610 mm (24") outer diameter with 9.53 mm (3/8") wall thickness is modeled in this study. The embedded length of the pile is 21m. Lateral

displacement is applied at 0.3 m above the ground surface. Summing the nodal force component in the x -direction at the point of loading, the lateral force is calculated. The pile is modeled as linear elastic material with a modulus of elasticity (E_p) of 208×10^6 kN/m² and Poisson's ratio (ν_p) of 0.3. As shown later, the stress in the pile remains below the elastic limit even at the maximum displacement applied and therefore, the modeling of the pile as elastic material is valid.

The Coulomb friction model is used for the frictional interface between the outer surfaces of the pile and sand. In this method, the friction coefficient (μ) is defined as $\mu = \tan(\phi_\mu)$, where ϕ_μ is the pile/soil interface friction angle. The value of ϕ_μ depends on surface roughness of the pile and effective angle of internal friction, ϕ' . Kulhawy (1991) recommended the value of ϕ_μ for steel pipe piles in the range of $0.5\phi'$ to $0.9\phi'$, where the lower values are for smooth steel piles. The value of $\mu=0.4$ is used in this study.

3.3.2 Modeling of Soil

Two boreholes were drilled at the Mustang Island pile load test site. Field tests and laboratory experiments on collected soil samples from these boreholes were conducted for geotechnical characterization (Cox et al. 1974). It was shown that the soil at the pile load test site is mainly sand with varying fine contents and relative density. A thin clay layer at 12.5 m depth was encountered. In the present study, this clay layer is neglected as it does not have a significant effect on lateral behaviour of the pile. The top 0–6m is a medium dense sand layer followed by a dense sand layer (Reese and Van Impe, 2001). Based on borehole logs, the soil profile is idealized as two sand layers for numerical

analyses as shown in Figure 3-1. The geotechnical parameters used in the numerical analyses are shown in Table 3-1. These parameters are estimated from the information provided in borehole logs and the soil investigation.

When a dense sand specimen is sheared in drained condition, the shear stress increases with shear displacement as shown in the inset of Figure 3-4. The peak shear stress is reached at a relatively small strain and then strain softening is occurred. The strain at which the peak shear stress is developed depends upon the density of soil and applied normal/confining stress. At large displacement, the shear stress remains constant which is considered as the critical state. The volume of a dense sand specimen is increased with shear displacement, which is normally characterized by dilation angle (ψ). At the critical state, shearing is occurring at constant volume. Most of the numerical analyses conducted in the past for modeling laterally loaded piles used a constant value of ϕ' and ψ . An appropriate value between the peak and ultimate condition is needed for this type of analyses.

In the present FE analysis, the strain softening behavior is modeled by varying the mobilized friction angle (ϕ') and dilation angle (ψ) with plastic shear strain

($PEMAG = \sqrt{\frac{2}{3} \varepsilon^{Pl} : \varepsilon^{Pl}}$). The variation of ϕ' and ψ for medium and dense sand used in the

analysis are shown in Fig. 3-4. The critical state friction angle (ϕ'_c) of 31° is used. Based on a large number of experimental data, Bolton (1986) showed that the angle of internal friction is related to the angle of dilation as $\phi' = \phi'_c + 0.8\psi$, which is used to calculate the mobilized dilation angle shown in Figure 3-4. It is to be noted here that some researchers

(e.g. Nobahar et al., 2000) successfully used this type of variation of ϕ' and ψ for modeling pipe/soil behavior.

The selection of appropriate values of elastic properties is equally important as the response of a pile depends on these parameters. In this study, isotropic elastic properties are used. Experimental studies (e.g. Janbu, 1963; Hardin and Black, 1966) show that the elastic modulus of granular materials increases with the increase in mean effective stress (p'). It has been also shown by previous researchers that the elastic modulus depends on void ratio. Various expressions have been proposed in the past in order to account for the effects of void ratio and mean effective stress on elastic modulus. Yimsiri (2001) compiled the available expressions in the literature. Based on these studies, the modulus of elasticity (E) is varied with mean effective stress (p') as

$$E = E_0 \left(p' / p_a \right)^n \quad (3-1)$$

Where, p_a is the atmospheric pressure (100 kPa) and n is a constant. The reference modulus of elasticity (E_0) represents the value of E at $p'=100$ kPa. Experimental results show that the value of n is approximately equal to 0.5 for sands (Yimsiri 2001). The above equation gives the variation of E with depth similar to the model pile load test results presented by Yan and Byrne (1992) as shown in Fig. 2.7. Note that, the p - y curve method (Reese et al., 1974; API 2000) linear increase of E (in the form of subgrade modulus) with depth is recommended which is significantly different from the measured values at greater confining pressure as shown in Fig. 2-7. The value of E is updated in the present FE analysis during the progress of calculation based on current mean stress (p')

for each integration point. This is one of the advantages of the present study which is different from the p - y curve methods.

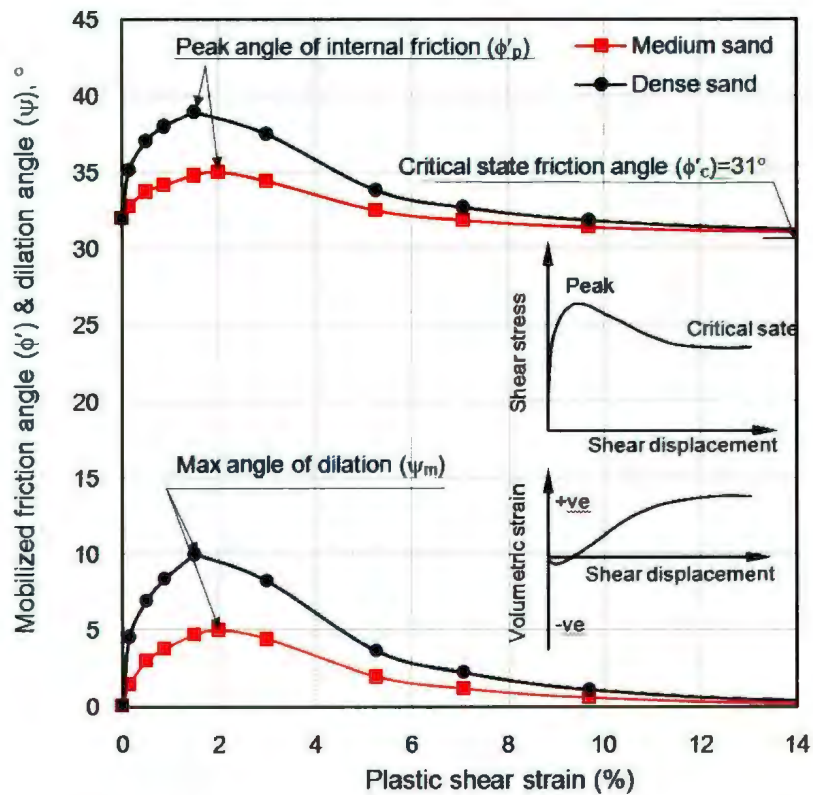


Figure 3-4: Mobilized angle of internal friction and dilation angle with plastic strain

The Mohr-Coulomb soil model is already implemented in ABAQUS/STANDARD 6.10 EF1. It is a simple linear elastic-perfectly plastic model that uses a smooth flow potential of elliptic shape in the deviatoric stress plane and hyperbolic shape in the meridional stress plane. The yield surface is defined by Mohr-Coulomb failure criterion. Finite element modeling using this built-in model is also performed and is shown in Appendix-A (Iftekharruzaman and Hawlader, 2012).

The built-in Mohr-Coulomb model in ABAQUS/Standard is incapable of simulating the varying modulus of elasticity as a function of mean effective stress and the post-peak strain softening behaviour of sand. Therefore, in this study they are incorporated in ABAQUS/Standard using a user subroutine called USDFLD written in FORTRAN. The mean effective stress and plastic shear strain are called at each time increment and two field variables are defined using these values. The model parameters E , ϕ' and ψ are updated based on these field variables.

The top layer of soil (0–6 m) is medium dense sand which is modeled using the following soil parameters: angle of internal friction at the peak, $\phi_p'=35^\circ$; maximum dilation angle, $\psi_m = 5^\circ$; reference modulus of elasticity, $E_0 = 120,000$ kPa; and Poisson's ratio, $\nu=0.3$. The soil layer below 6 m is dense sand. The soil properties used for this layer are: $\phi_p'=39^\circ$, $\psi_m = 10^\circ$, $E_0 = 140,000$ kPa, and $\nu=0.3$. The location of the groundwater table is at the ground surface. Submerged unit weight of 10.4 kN/m³ is used for both soil layers. Other properties in the FE analyses are listed in Table 3-1.

3.3.3 LPILE Analysis

Analysis of pile under lateral static load is also conducted using LPILE Plus 5.0 (2005) software. LPILE is a finite difference software where the pile is modeled as a beam having lateral stiffness equal to the product of elastic modulus and moment of inertia of the pile. The nonlinear p - y curves are defined using the method proposed by Reese et al. (1974). In this method, the ultimate soil resistance per unit length of the pile is calculated using the angle of internal friction of the soil. The initial straight-line portion of the p - y

curve is defined using the initial modulus of subgrade reaction (k). The variation of k with ϕ' and relative density is shown in Figure 3-5 as recommended by the American Petroleum Institute (API, 2000).

Table 3-1: Geometry and mechanical properties used in finite element analysis for Reese et al. (1974)

| | |
|---|----------------------------------|
| Pile: | |
| Length of the pile (L) | 21.6 m |
| Diameter of the pile (D) | 610 mm (24") |
| Thickness of the pile (t) | 9.53 mm (3/8") |
| Modulus of elasticity of pile (E_p) | $208 \times 10^6 \text{ kN/m}^2$ |
| Poisson's ratio (ν_p) | 0.3 |
| Soil (sand): | |
| Poisson's ratio, ν_s | 0.3 |
| Submerged unit weight of soil, γ' | 10.4 kN/m^3 |
| Upper medium sand (0 to 6m depth) | |
| Reference modulus of elasticity, E_{ref} | $120,000 \text{ kN/m}^2$ |
| Angle of internal friction, ϕ'_p | 35° |
| Maximum dilation angle, ψ_m | 5° |
| Initial modulus of subgrade reaction (k) | $21,000 \text{ MPa/m}$ |
| Lower dense sand (6 to 30m depth) | |
| Reference modulus of elasticity, E_{ref} | $140,000 \text{ kN/m}^2$ |
| Angle of internal friction, ϕ'_p | 39° |
| Maximum dilation angle, ψ_m | 9° |
| Initial modulus of subgrade reaction (k) | $36,000 \text{ MPa/m}$ |

It is to be noted here that Reese et al. (1974) also compared these test results based on the p - y curves method as shown in Fig. 2-9. In their simulation they used constant value of $\phi'=39^\circ$. Later the author (Reese and Van Impe, 2001) presented the geotechnical data, which clearly shows that the density of the upper 6 m soil is less than the density of lower soil layer as used in the present study. It is to be noted here that some other researchers (e.g. Fan and Long 2005) also recognized this and used medium sand for the upper 6 m and dense sand below 6 m in their finite element model to simulate the response of this full-scale test.

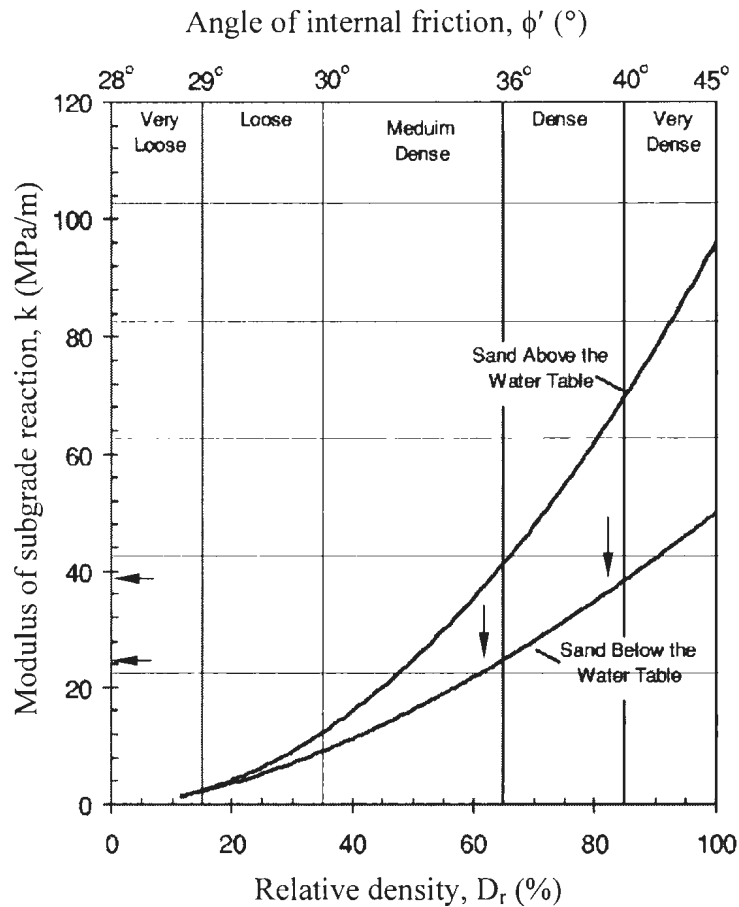


Figure 3-5: Lateral modulus of subgrade reaction as function of relative density and friction angle (API 2000)

this software. The angle of internal friction ϕ' in the horizontal axis at the top of Figure 3-5 is related to relative density as $\phi' = 16D_r^2 + 0.17D_r + 28.4$, where ϕ' is in degrees, and D_r is the relative density (API 1987). Using the value of ϕ' calculated from this equation, Rollins et al. (2005) showed that it underestimates the friction angle and predicts significantly higher lateral displacement and bending moment compared to pile load test results. Therefore, in the present LPILE analyses $\phi' = 35^\circ$ for medium and $\phi' = 39^\circ$ for dense sand is used, which is consistent with Reese et al. (1974).

3.3.4 Numerical Results

The finite element analysis consists of mainly two major steps: gravity step and loading step. In gravity step the soil domain is reached to the in-situ stress condition. In loading step the lateral displacement in the x -direction is applied on the nodes of the pile at 0.3 m above the ground surface.

3.3.4.1 Load-deflection curves

Figure 3-6 shows the variation of lateral load with lateral displacement of the pile at the ground surface obtained from finite element analysis and LPILE analysis. The results of full-scale test (Cox et al. 1974) are also shown in this figure.

In finite element analysis, the lateral displacement is applied at 0.3 m above the ground surface. The lateral load is calculated by adding the horizontal (x) component of nodal force at this level. The lateral displacement at the ground level is calculated by averaging the lateral displacement of all the nodes of the pile at ground level.

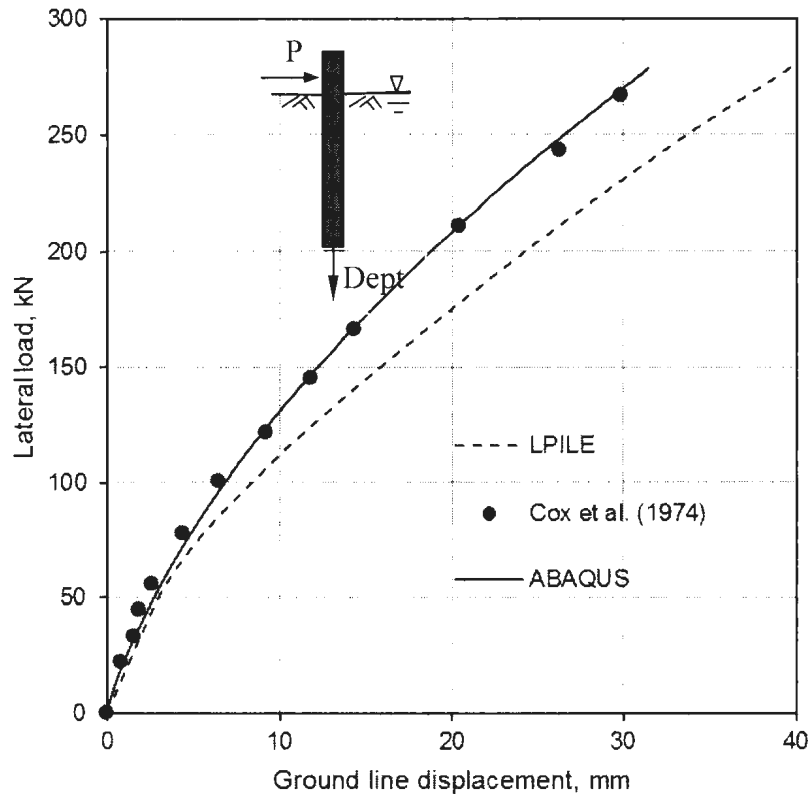


Figure 3-6: Comparison of load displacement between numerical predictions and full-scale test result

In LPILE, the lateral load is applied in 11 increments. The pile is divided into 100 small divisions. The lateral displacement at the ground surface is obtained from the displacement of the element at this level.

Figure 3-6 shows a very good agreement between the full-scale test results and present finite element analysis. LPILE computed displacement for a given lateral load is higher than the measured displacement. The calculated lateral load for a given displacement using LPILE is slightly lower than Reese et al. (1974) because of two reasons: (i) Reese et al. (1974) used constant value of $\phi'=39^\circ$ for the whole soil layer although Reese and

Van Impe (2001) showed that the top 6 m soil is medium sand, and (ii) their k value is different from the value used here. In the present study, the input parameters required for LPILE analyses are obtained following the API (2000) recommendations as discussed above.

3.3.4.2 Bending Moment with Depth

Figure 3-7 to Figure 3-10 show the variation of bending moment with depth for the upper 6 m length of the pile. In these figures, the depth in the vertical axis represents the distance from the point at which the lateral load is applied on the pile. Although the pile is 21 m in length, the variation of bending moment only for the upper 6 m is shown because the maximum bending moment and its variation mainly occur in this zone. Comparison between computed and measured values for 11 lateral load cases (33.4 kN, 55.6 kN, 77.8 kN, 77.8 kN, 101.1 kN, 122.3 kN, 144.6 kN, 166.8 kN, 189 kN, 211.3 kN, 211.3 kN, 244.6 kN, and 266.9 kN) are presented in these figures. In the finite element analyses, the bending moment is obtained from the axial stresses in the pile. In LPILE, it can be easily obtained as the pile is modeled as a beam. The computed bending moment in the present finite element analysis compares exceptionally well with the measured data. However, LPILE computes higher bending moments than measured in the full-scale test.

The depth at which the maximum bending moment occurred in the finite element analysis is slightly less than that of the LPILE analysis. For example, the maximum bending moment for 266.9 kN is obtained at 2.5 m if FE analysis while it is at 3.0 m in LPILE analysis (Fig. 3-10).

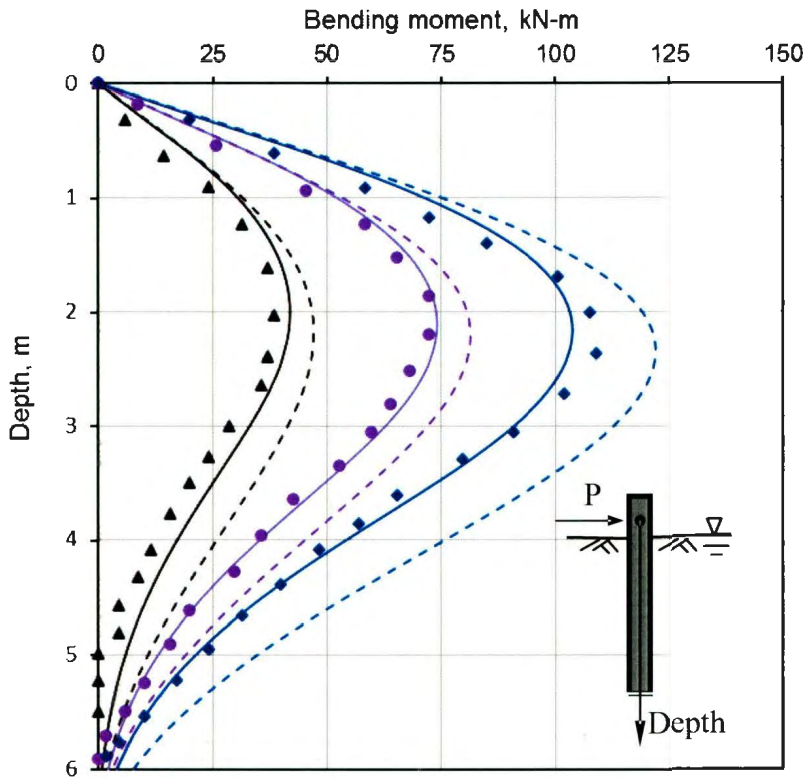


Figure 3-7: Variation of bending moment with depth (Load cases: 33.4 kN, 55.6 kN and 77.8 kN; solid lines for FE analysis, dashed line for LPILE and data points for full-scale test)

It is to be noted here that the pile is in elastic condition even at the maximum lateral load applied. For the maximum lateral load of 266.9 kN, the computed maximum bending moment is 550 kN-m. This gives the maximum tensile/compressive stress of 175MPa, which is less than the yield strength of steel. That means the analyses conducted in this study using elastic behaviour of the pile is valid even for the highest lateral load.

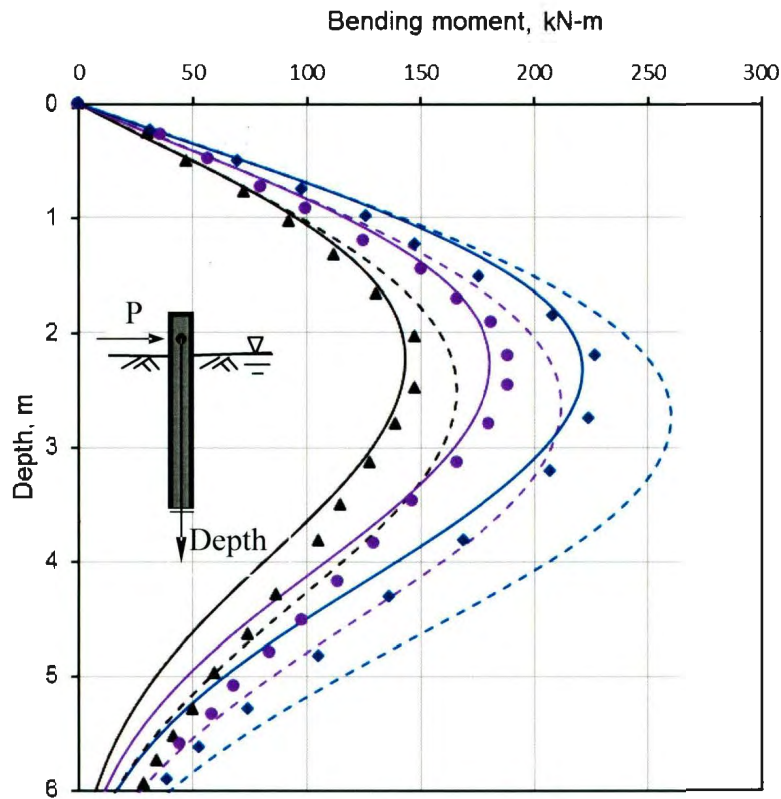


Figure 3-8: Variation of bending moment with depth (Load cases: 101.1 kN, 122.3 kN and 144.6 kN; solid lines for FE analysis, dashed line for LPILE and data points for full-scale test)

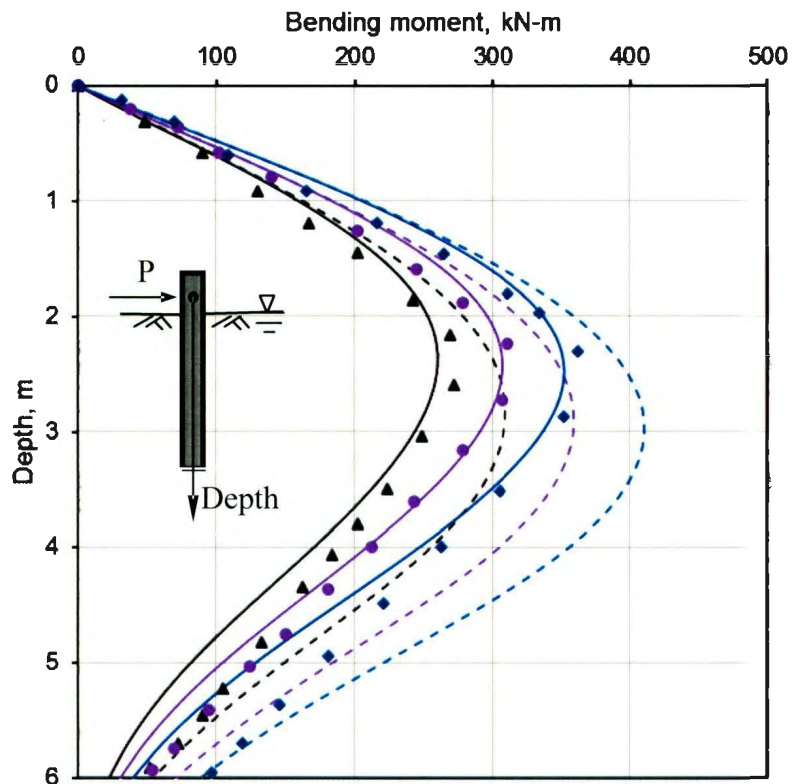


Figure 3-9: Variation of bending moment with depth (Load cases: 166.8 kN, 189 kN and 211.3 kN; solid lines for FE analysis, dashed line for LPILE and data points for full-scale test)

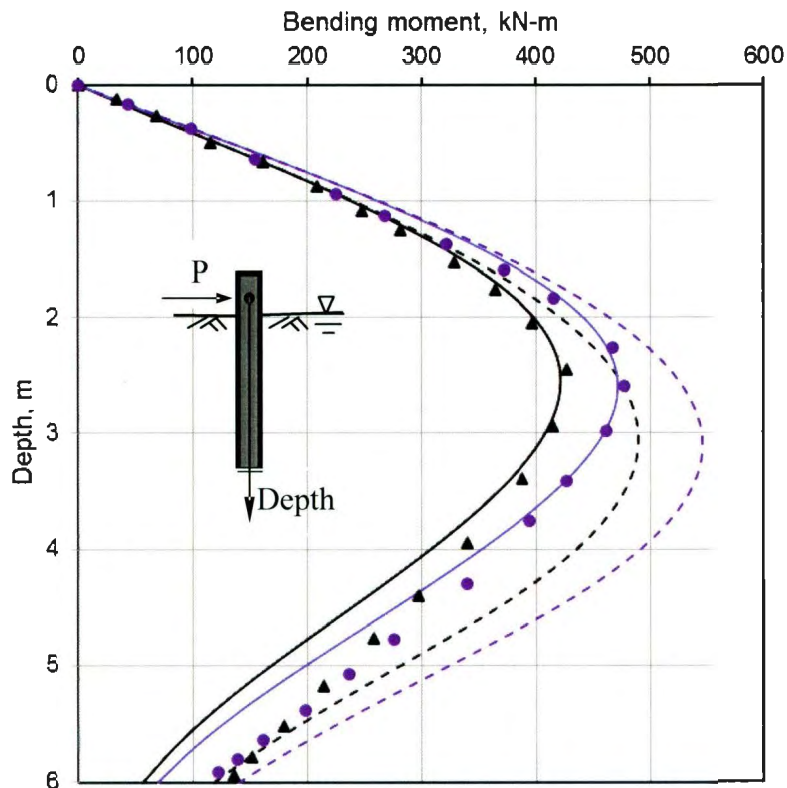


Figure 3-10: Variation of bending moment with depth (Load cases: 244.6kN and 266.9kN; solid lines for FE analysis, dashed line for LPILE and data points for full-scale test)

3.3.4.3 Maximum bending moment

Figure 3-11 shows the variation of the maximum bending moment with lateral load. The maximum bending moment increases with the increase in lateral load. At low values of lateral load, both finite element and LPILE compare well with full-scale test data. However, at larger loads the computed maximum bending moment using LPILE is higher than the values obtained from the present finite element analysis and full-scale test.

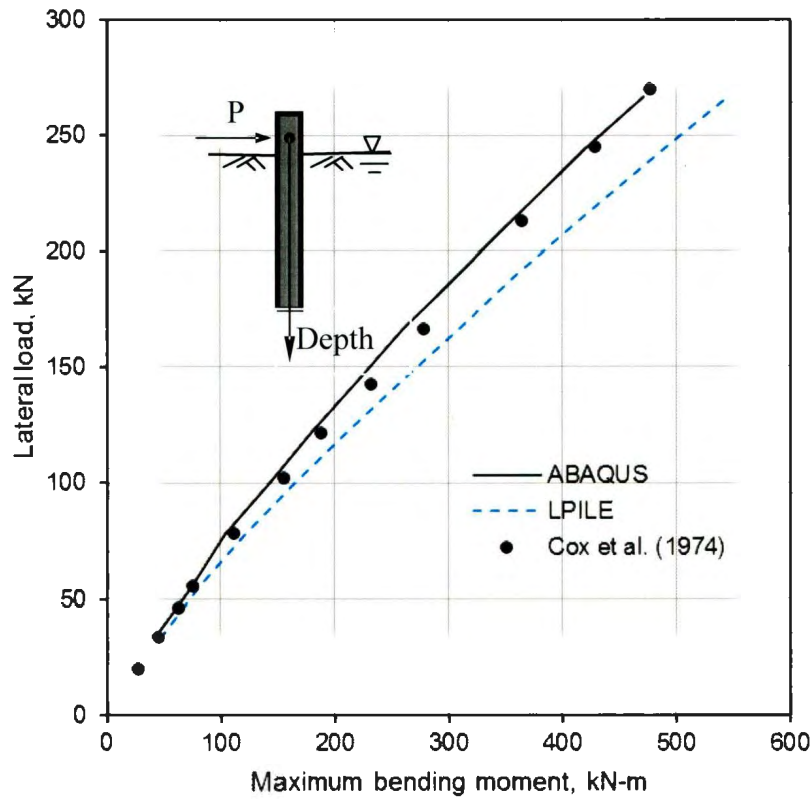


Figure 3-11: Comparison of maximum bending moment and lateral load

3.3.4.4 Lateral displacement

Figure 3-12 shows the computed lateral displacement of the pile with depth for 11 load cases for FE and LPILE analyses. As shown in this figure, LPILE predicts higher lateral displacement than the present FE simulation.

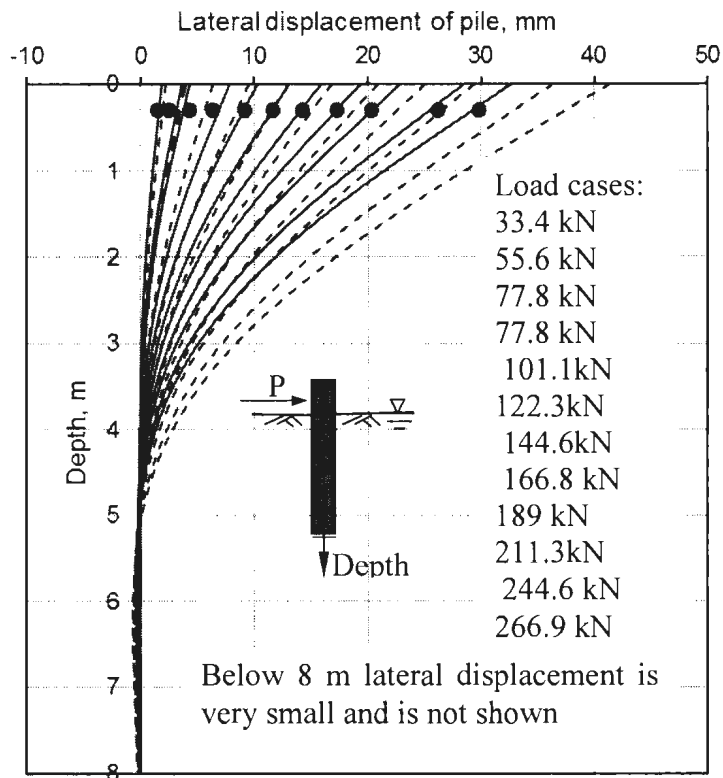


Figure 3-12: Lateral displacement of pile (solid lines: FE analysis; dashed line: LPILE; solid circles: measured at ground line in pile load test)

For comparison with field data, the displacement at the ground surface obtained in the full-scale test is also shown in this figure by solid circles, which match very well with the present FE analysis.

3.3.4.5 Soil reaction

Lateral soil reaction (force per meter length of the pile) is plotted in Figure 3-13. For clarity, the calculated results for 5 load cases are shown in this figure. In finite element analysis, the x-component (lateral) of nodal force is calculated first for all the nodes at a

given depth. Dividing the sum of the nodal force in the x -direction by the vertical distance between two sets of nodes in the pile, the lateral soil reaction is obtained. In the LPILE analysis, the soil reaction can be easily obtained from the output file as the pile is modeled as a beam supported by discrete springs. As shown in this figure, the calculated soil reaction from both LPILE and FE is very similar up to 1.2 m depth. However, below 1.2 m the soil reaction obtained from the FE analysis is higher than the reaction obtained from LPILE. Moreover, after reaching the maximum value of soil reaction, it decreases quickly with depth in the finite element analysis. The maximum soil pressure is developed at greater depth for larger values of lateral load.

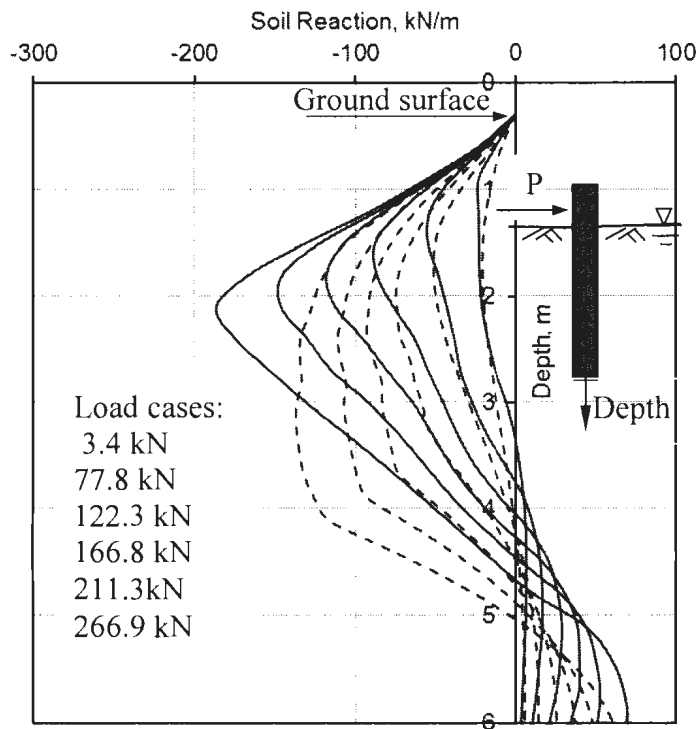


Figure 3-13: Soil reaction on pile (solid lines: FE analysis and dashed line: LPILE)

3.3.4.6 Shear force in pile

Figure 3-14 shows the variation of shear force in the pile with depth for five lateral loads. In the finite element analysis, the shear force is obtained by subtracting the sum of the x-component of nodal force above the point of interest from the lateral load applied at the pile head. As shown in Figure 3-13, the calculated soil reaction in the finite element analysis is higher near the ground surface. Therefore, the shear force is decreased quickly in the finite element analysis near the ground surface as shown in Figure 3-14.

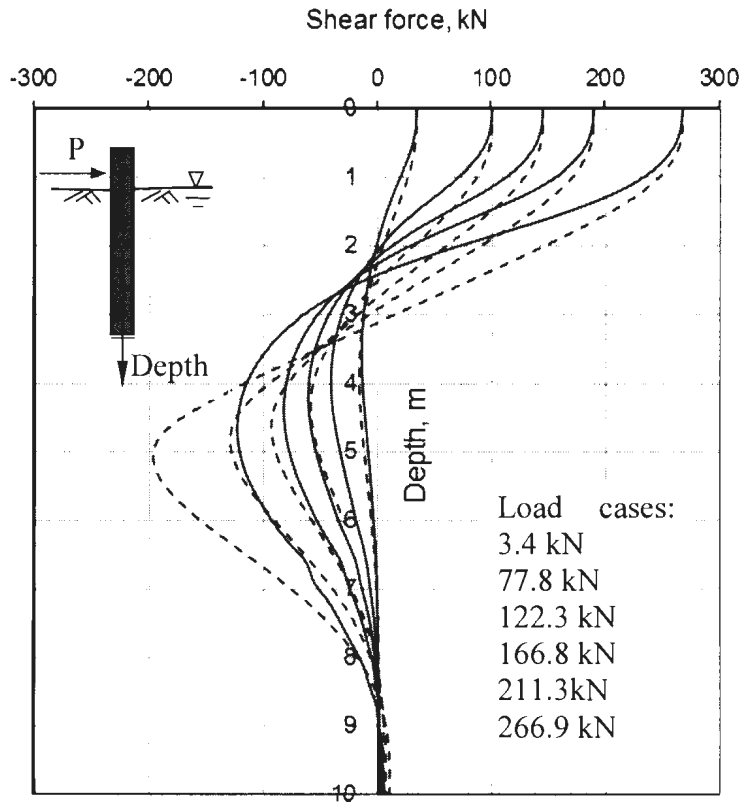


Figure 3-14: Variation of shear force in pile with depth (solid lines: FE analysis, dashed line: LPILE)

The maximum negative shear force from the LPILE analysis is higher than that obtained from the finite element analysis. Below the depth of 9 m the shear force is negligible.

3.3.4.7 p - y curves

In the current engineering practice, the modeling of a laterally loaded pile is generally performed as a beam on elastic foundation, where soil is modeled by discrete springs. The load deformation behaviour of the soil spring is defined using nonlinear p - y curves. The p - y curves for four depths are shown in Figure 3-15.

In LPILE, the p - y curve for a given depth can be easily obtained from the output file. In the finite element analysis, the soil is modeled as a continuum, not as discrete springs. The values of p and lateral displacement are calculated from nodal forces and displacement, respectively. In this study, the model proposed by Reese et al. (1974) for static lateral loading is used in LPILE analysis. The p - y curve in Reese et al. (1974) consists of four segments (Figure 3-15): (i) initial linear segment, which is mainly governed by k value, (ii) parabolic segment between the initial linear segment and lateral displacement of $D/60$, (iii) linear segment between lateral displacements of $D/60$ and $3D/80$, and (iv) constant soil resistance segment after lateral displacement of $3D/80$. The p - y curves obtained from the finite element and LPILE analyses are also compared with full-scale test data (Cox et al. 1974). As shown in Fig. 3-15, the p - y curves obtained from the finite element analysis match better with the measured values.

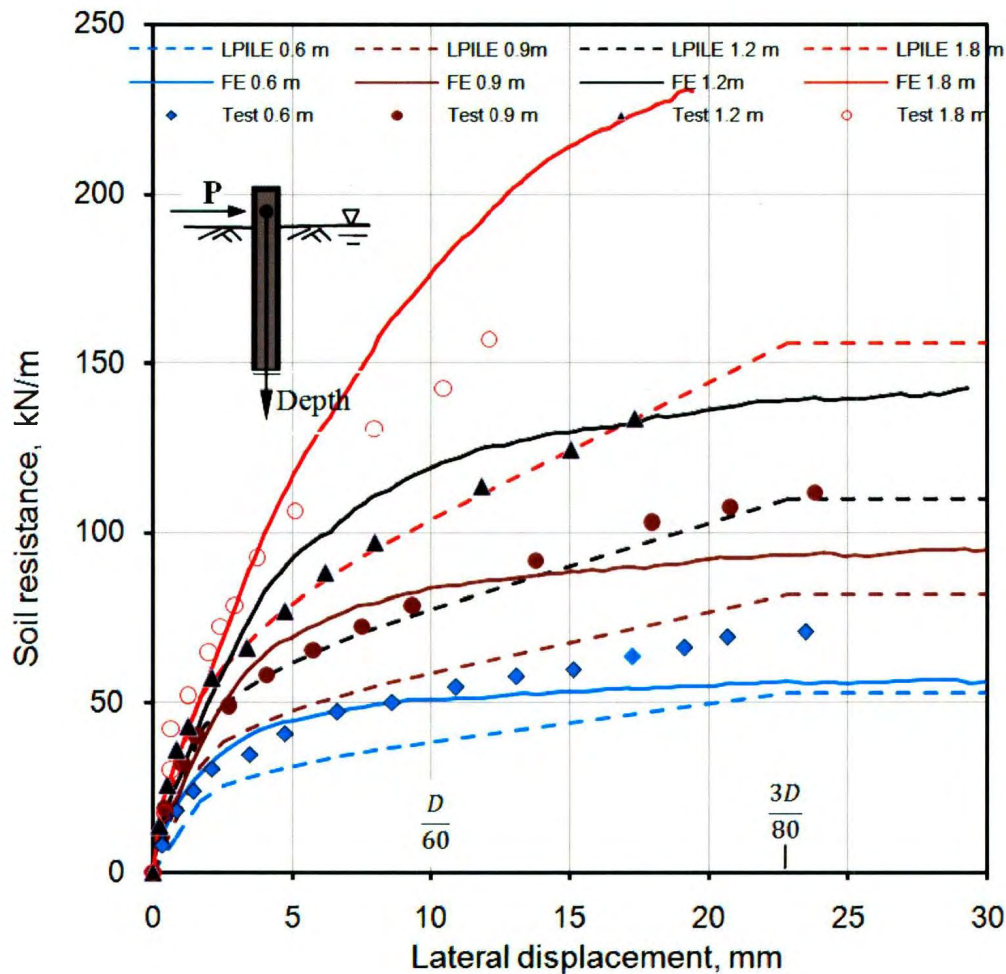
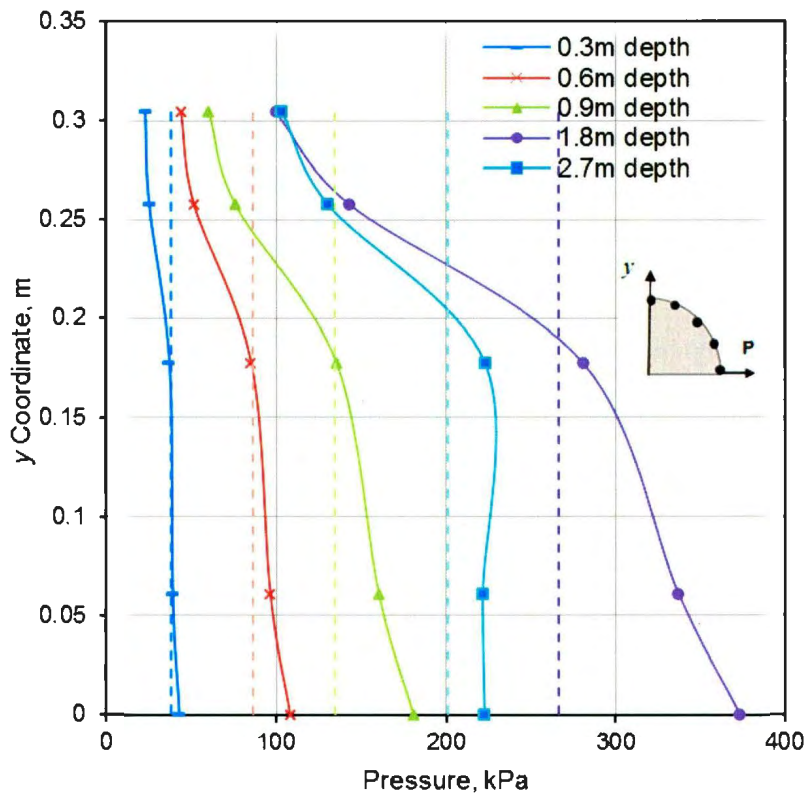


Figure 3-15: Comparison of p - y curves at four depths (solid lines: FE analysis, dashed line: LPILE, and data points: full-scale test)

3.3.4.8 Lateral pressure

In simplified method, such as in the p - y curve method, the lateral pressure on the face of the pile is assumed to be uniform. However, in reality it could be significantly different especially in circular pile. Figure 3-16 shows the pressure (x -direction) distribution at depths of 0.3 m, 0.6 m, 0.9 m, 1.8 m and 2.7 m under 266.9 kN lateral load. The lateral pressure can be calculated from normal stress and shear stress on the pile. In the front

face of the pile, the normal stress and at the side the shear stress contribution is higher on average lateral pressure. To calculate the lateral pressure, first normal and shear force in the nodes of interest are obtained from FE analysis. The sum of the x -component of these forces is divided by the projected area gives the average lateral pressure around that node. As shown in Fig. 3-16, the average lateral pressure at the middle of the pile ($y=0$) is higher, which is mainly from the normal pressure component. At the side of the pile ($y=D/2=0.305$ m) the contribution is mainly from the soil/pile interface shear resistance, which is significantly less than the normal pressure component at $y=0$ especially for larger depths (e.g. 1.8 m depth). The uniform pressure (average value) for each depth is shown by dashed line in Fig. 3-16. As shown in this figure 3-16 at shallow depths (e.g. 0.3 m), the uniform pressure somehow represents the actual pressure distribution which does not vary significantly with y . However, larger depth pressure distributions are far from uniform. Lateral pressure depends on not only the location but also the displacement of the pile. The maximum pressure is developed in this case at 1.8 m. Note that, the pressure at 2.7 m is less than the pressure at 1.8 m as the lateral deflection is less at 2.7 as shown in Fig. 3.16. It is noted that the soil reaction presented in Fig. 3.16 can be obtained by multiplying the uniform pressure by the diameter of the pile.



1

Figure 3-16 : Lateral effective stress at various pile depths (dashed lines represent the average effective stress)

3.3.4.9 Vertical Displacement of Soil

Figure 3-17 shows the vertical displacement of soil at 266.9 kN lateral load. In this figure, the vertical displacement is scaled by 15 times of actual displacement. It is observed that a soil berm is formed in front of the pile and soil settlement is occurred on the back of the pile due to the application of the lateral loads. The vertical displacement is mainly occurred within the 2 m depth of soil below the ground surface.

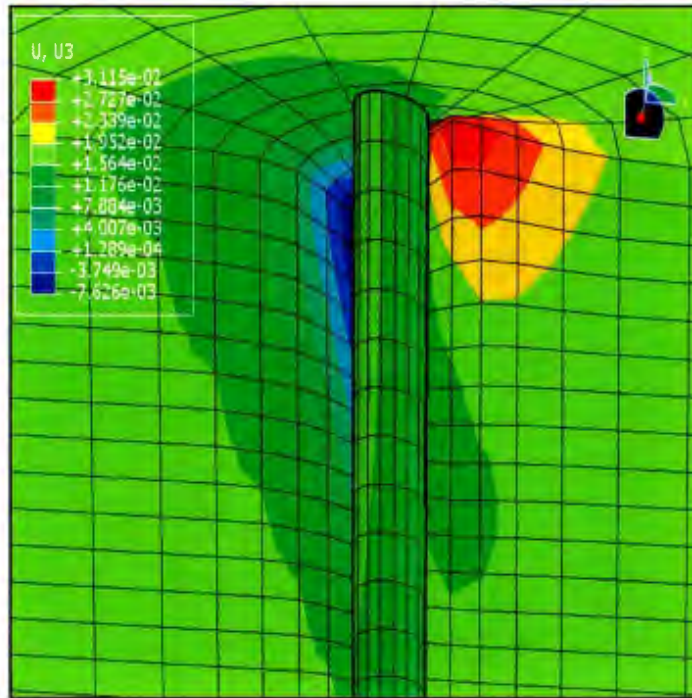


Figure 3-17: Vertical displacement of soil near the top of the pile at the end of loading ($P=266.9$ kN)

3.3.4.10 Von Mises and Mean Effective Stress distributions

Figure 3-18 shows the contours of von-Mises stress and Figure 3-19 shows the contours of mean effective stress on $x-z$ plane for 266.9 kN lateral load. The shear stress and mean stress are mainly developed in front of the pile and concentrated within a depth of 4 m or 7 pile diameter below the ground surface. Figure 3-19 shows that the mean effective stress in front of the pile is reached to a maximum value of 250 kPa, which is almost 6-9 times higher than the in-situ mean stress at this depth before application of lateral load. The increase in mean effective stress to 250 kPa also increased the modulus of elasticity according to Eq. 3-1, which is almost three times of the modulus of elastic at the in-situ

stress condition. This has a significant effect on the calculation as the lateral response of the pile depends upon the behavior of the soil in this zone.

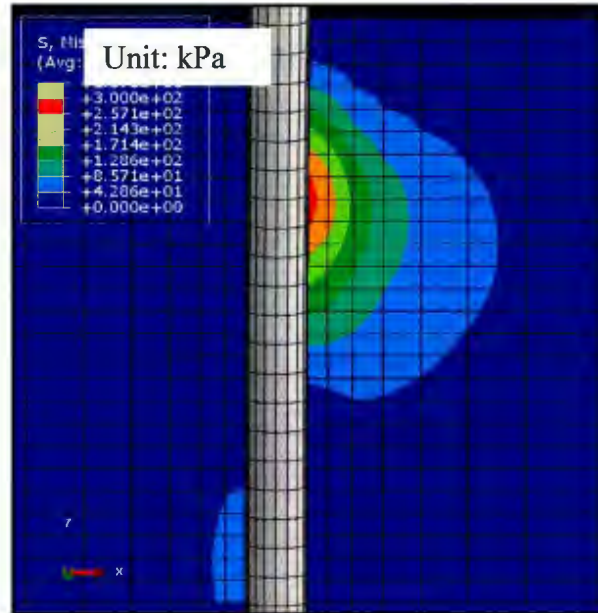


Figure 3-18: Von-Mises stress distribution at the end of loading (P=266.9 kN)

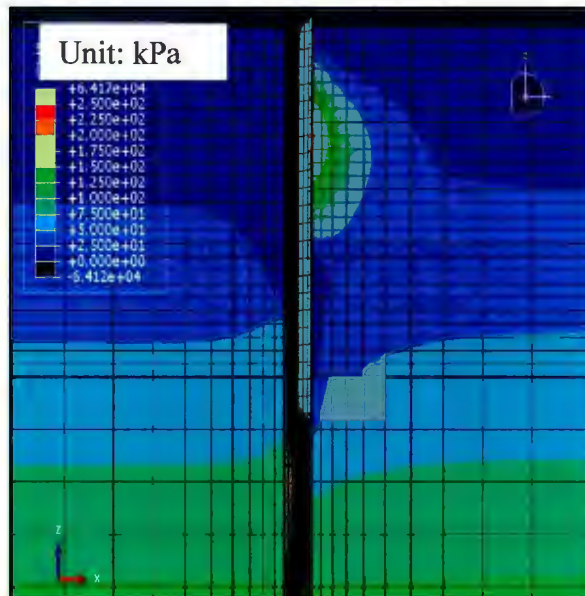


Figure 3-19: Mean effective stress at the end of loading (P=266.9 kN)

3.3.4.11 Plastic Strain

Figure 3-20 shows the magnitude of plastic shear strain at 266.9 kN lateral load. For clarity, only the zone where high plastic strain is developed near the top of the pile is shown. The plastic strain is developed both in front and back of the pile. In the front of the pile, the plastic strain is developed because of loading while in the back of the pile it is developed by unloading in the lateral direction. As mentioned in Section 3.3.2, the mobilized friction angle (ϕ') and dilation angle (ψ) are varied in the present analysis as a function of plastic strain (PEMAG). The zone near the top of the pile where the plastic shear strain (PEMAG) is greater than 4.5% the friction angle is almost at the critical state condition. On the other hand, the elements far from the pile or at deeper depth are at a higher friction angle, and dilation angle as the plastic shear strain is less. In other words, the values of ϕ' and ψ are not the same in all soil elements but dependent upon plastic strain. The reduction of friction angle from the peak value is mainly occurred in a zone of soil near the pile where significant plastic strain is developed. Further study is required to find a representative value of ϕ' if someone wants to follow API (2000) recommendations.



Figure 3-20: Magnitude of plastic strain at the end of loading (P=266.9 kN)

3.4 Finite Element Modeling of Rollins et al. (2005) Full-Scale Test

In this section, FE simulation of another full-scale test conducted by Rollins et al. (2005) is presented. Rollins et al. (2005) conducted a series of full-scale tests at the National Geotechnical Experiment Site (NGES) on Treasure Island in San Francisco Bay, Calif. The 3x3 pile group was driven into loose to medium dense sand to perform a lateral pile load test. A pile load test was also conducted on a single pile to evaluate group effects. In the present study, FE modeling is performed only for the single pile load test. During the preparation of the test site, about 1.2 m of soil was excavated first. Cone penetration and Standard penetration tests were conducted for soil characterization. The interpreted soil profile and geotechnical properties are shown in Fig. 3-21. As shown in the figure, the soil profile consists of mainly in the sand and silty sand.

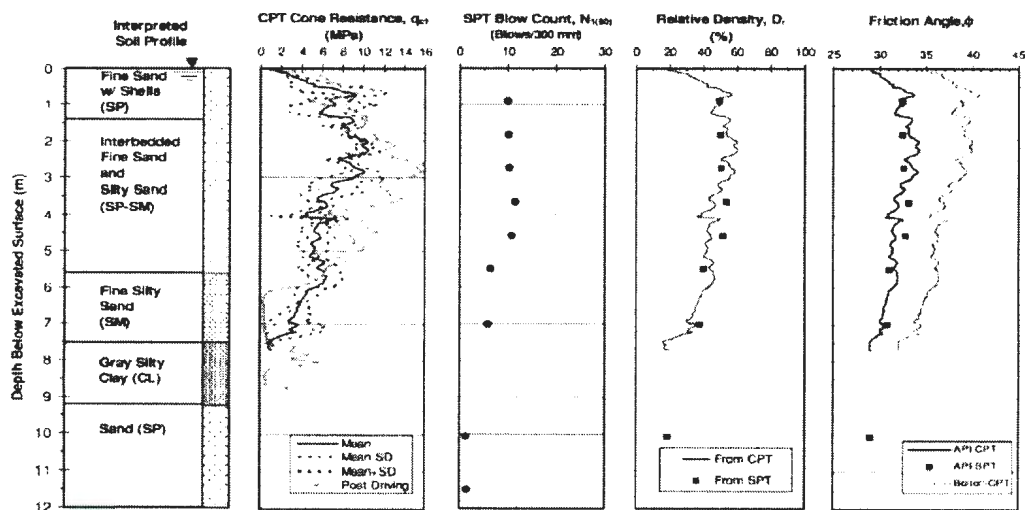


Figure 3-21: Soil profile (after Rollins et al. 2005)

An open ended steel pipe pile of 0.324 m outer diameter and 9.5 mm wall thickness was driven to a depth of approximately 11.5 m below the excavated ground surface. The lateral load test was performed in a displacement controlled approach. A maximum displacement of 38 mm was applied on the top of the pile at 0.69 m above the ground surface. The load was measured by the load cell. Strain gauges were attached along the length of the pile to measure bending moments. The data was analyzed, and the response of the pile was reported for four lateral load cases of 24 kN, 45.6 kN, 67.6 kN and 89 kN.

Similar to the previous case, the three-dimensional FE analysis is performed using ABAQUS FE software. The finite element model is shown in Fig. 3-22. A soil domain of 20 m diameter and 15m height is modeled. A steel pipe pile of 324 mm diameter and 11.5m length is located at the center of the soil domain. Four layers of loose to medium dense sand and a thin layer of clay between 7.5 to 9.25m depth are considered in this study. The boundary conditions used in this case are the same as the boundary conditions used to simulate Cox et al. (1974) pile load tests described in Section 3.3.

Mesh sensitivity analysis is also performed. After several trial analyses with different mesh sizes, the optimum mesh shown in Fig. 3-22 is selected. Fine mesh is used for the upper 10 m of soil, and coarse mesh is used for 10 to 15 m soil depth as it does not have a significant effect on the load-displacement behaviour.

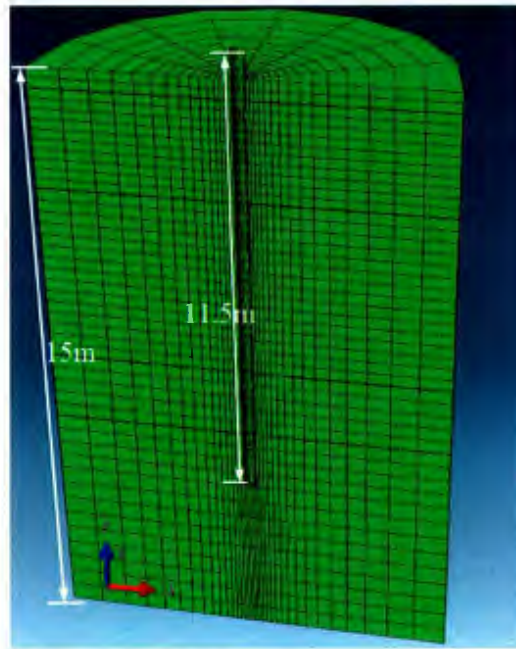


Figure 3-22: Finite element model

3.4.1 Modeling of Pile and Soil

The pile is modeled as linear elastic material with a modulus of elasticity (E_p) of 207×10^6 kN/m² and Poisson's ratio (ν_p) of 0.3. The interface friction coefficient μ equal to 0.4 is used. A detailed discussion on estimation of μ is given in Section 3.3.1.

The sand is modeled using the modified form of Mohr-Coulomb soil model as described in Section 3.3.2. The values of ϕ' and ψ are varied with plastic shear strain (PEMAG) similar to Fig. 3.2. In FE analyses, the soil profile is divided into 5 layers. The geotechnical parameters used in numerical analyses are shown in Table 3-2. These parameters are estimated from the information provided by Rollins et al. (2005) from the site investigation as shown in Fig. 3-21. The thin clay layer is modeled in undrained

condition with $c_u=19.2$ kPa as reported by Rollins et al. (2005). Note that this layer does not have a significant effect on lateral response of the pile.

Table 3-2: Geometry and mechanical properties used in finite element analysis for Rollins et al. (2005)

| | |
|---|-------------------------------------|
| Pile: | |
| Length of the pile (L) | 11.5 m |
| Diameter of the pile (D) | 324 mm |
| Thickness of the pile (t) | 9.5 mm |
| Modulus of elasticity of pile (E_p) | 207×10^6 kN/m ² |
| Poisson's ratio (ν_p) | 0.3 |
| Soil (sand) | |
| Poisson's ratio, ν_s | 0.3 |
| Submerged unit weight of soil, γ' | 10.3 kN/m ³ |
| Upper sandy soil (0 to 0.5 m depth) | |
| Reference modulus of Elasticity | 170,000 kN/m ² |
| Angle of internal friction, ϕ'_p | |
| Dilation angle, ψ_m | 39° |
| 2 nd layer sandy soil(0.5 to 3.0m depth) | 9° |
| Reference modulus of Elasticity | |
| Angle of internal friction, ϕ'_p | 120,000 kN/m ² |
| Dilation angle, ψ_m | 39° |
| 3 rd layer sandy soil (3.0 to 7.5 m depth) | 9° |
| Reference modulus of Elasticity | |
| Angle of internal friction, ϕ'_p | 60,000 kN/m ² |
| Dilation angle, ψ_m | 36° |
| 4 th layer clayey soil (7.5 to 9.25 m depth) | 6° |

| | |
|--|---------------------------|
| Cohesion, c_u | |
| Submerged unit weight of soil, γ' | 19.2 kPa |
| bottom layer sandy soil (9.25 to 15.0 m depth) | 9.5 kPa |
| Reference modulus of Elasticity | 120,000 kN/m ² |
| Angle of internal friction, ϕ'_p | 33° |
| Dilation angle, ψ_m | 3° |

The elastic modulus is varied with mean effective stress as Eq. 3-1. Variation of elastic modulus, dilation and friction angle is incorporated through user subroutine USDFLD.

3.4.2 Numerical Results

In the following section, FE results are compared with full-scale test data. Rollins et al. (2005) also conducted LPILE analyses based on API (2000) code. Instead on repeating the same analyses their LPILE results, based on API recommendations, are also compared.

3.4.2.1 Lateral Load vs. Displacement Curve

Figure 3-23 shows the pile head displacement obtained from the present three-dimensional FE analyses and full-scale test data (Rollins et al., 2005). As shown in this figure, the present FE results matched reasonably well with the pile load test results. The LPILE analysis with API code computes significantly higher displacements for a given lateral load than FE and full-scale test results.

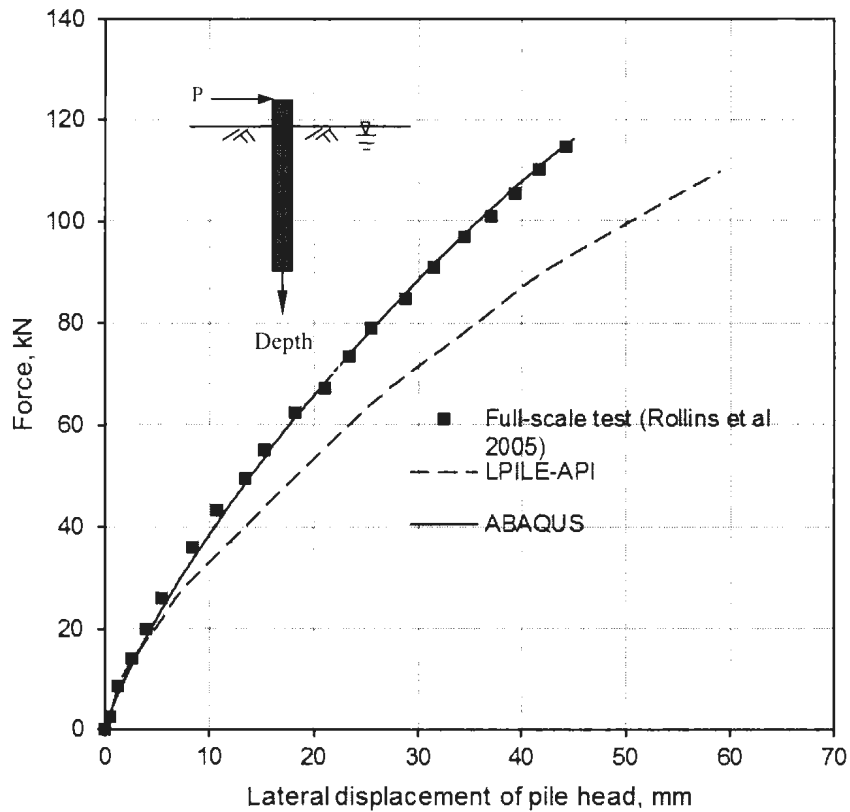


Figure 3-23: Comparison of load displacement between numerical predictions and full-scale test result

3.4.2.2 Bending moment versus depth

The variation of bending moment with depth is shown in Figure 3-24. Again the computed bending moment matched reasonably well with pile load test results for the four load cases reported.

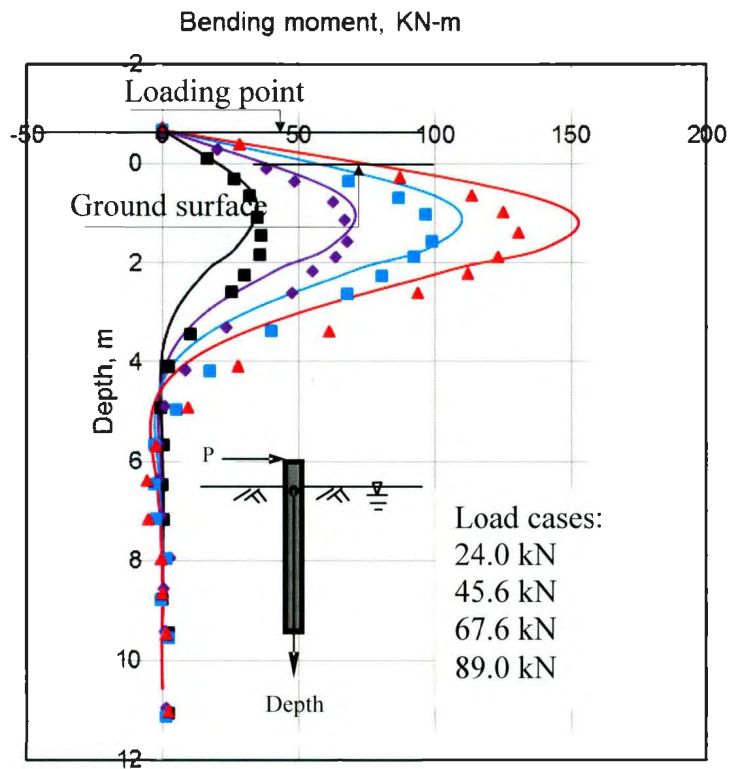


Figure 3-24: Variation of bending moment with depth (solid lines for FE analysis, and data points for full-scale test)

3.4.2.3 Maximum bending moment versus lateral load

The variation of maximum bending moment with lateral load is shown in Figure 3-25. The maximum bending moment obtained from the present FE analyses also compares well with the measured values. Although at higher lateral load, the computed bending moment is slightly higher than measured values. One of the reasons might be the selection of soil parameters.

Computed bending moments using LPILE based on API recommendations are also shown in this figure. The computed bending moment is significantly higher than the measured values.

It is to be noted here that Rollins et al. (2005) adjusted the friction angle based on Bolton's (1986) method in order to match the test results with the LPILE analyses. However, in the present study, it is shown that the finite element modeling can simulate the field tests using fundamental soil properties.

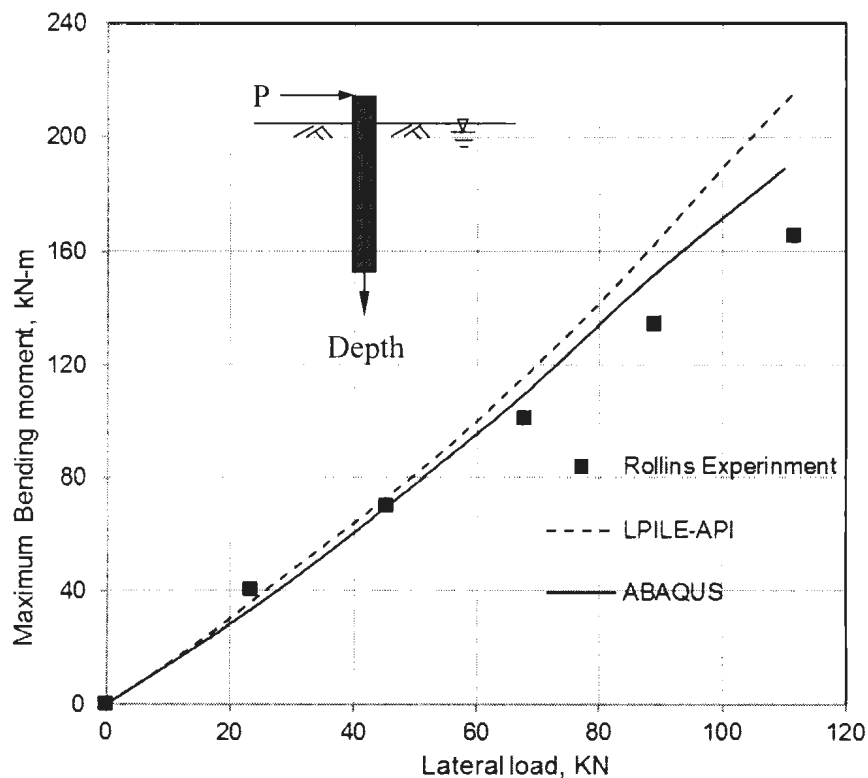


Figure 3-25: Comparison of maximum Bending moment and Lateral load

3.4.2.4 Displacement profile

Figure 3-26 shows the computed lateral displacement of the pile with depth for the four load cases from finite element analysis. For comparison with field data, the displacement of the pile at the point of lateral load application obtained in the full-scale test is also shown in this figure by solid circles which match very well with the present FE analysis.

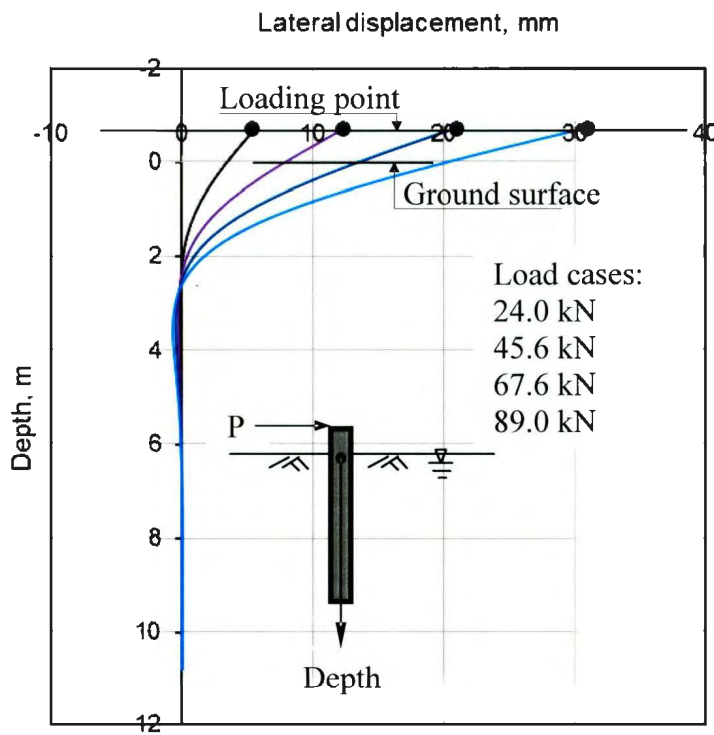


Figure 3-26: Lateral displacement of pile (solid lines: FE analysis and solid circles: measured at pile top in pile load test)

Finally, the variation of soil pressure, shear force in the pile, p - y curves, shear and mean effective stresses, and plastic shear strain are very similar to Figs. 3-13 to 3-20. Therefore, those figures are not shown in this thesis.

3.5 Discussion and Conclusions

The p - y curve based software packages, such as LPILE, are widely used in engineering practice to calculate the load-displacement behaviour of laterally loaded piles. Although this method is very simple, it has a number of limitations. The soil resistance is modeled as discontinuous nonlinear springs defining the properties empirically. Moreover, the pile/soil interface behaviour cannot be modeled in the p - y curve method. In this chapter of this thesis, three-dimensional finite element analyses are presented for a laterally loaded flexible pile in sand. Analyses are performed using a modified form of Mohr-Coulomb soil model, where the variation of the mobilized angle of internal friction and dilation angle with plastic shear strain is considered. The nonlinear variation of elastic modulus with mean effective stress is also considered in the present FE analyses. Numerical analyses are also performed by using the commercially available LPILE software. The geotechnical parameters required in the FE analysis can be easily obtained from the conventional laboratory shear strength tests. The variation of mobilized friction angle and dilation angle with plastic shear strain can be obtained from triaxial test data. On the other hand, the post-peak softening behaviour cannot be incorporated in the p - y curve method. Therefore, a constant representative value of ϕ' between the peak and critical state is required to be selected. The initial modulus of subgrade reaction (k) is also related to ϕ' and relative density as shown in Fig. 3-4. Note that k is not a fundamental

soil property. Consider a pile foundation in dense sand having the peak and critical state friction angles of 41° and 31° . For successful prediction of the response of a laterally loaded pile using the p - y curve method a representative value of ϕ' between 41° and 31° is needed. API (1987) recommended an empirical equation for estimating the representative value of ϕ' as a function of relative density. However, the computation with this recommended value of ϕ' over predicts the maximum bending moment and lateral displacement (Rollins et al. 2005). The limitations of the p - y curve method could be overcome by using FE modeling as presented in this paper. The response of the pile is calculated using the fundamental soil properties such as friction angle, dilatancy and stiffness. It is also shown that the FE model can successfully simulate the full-scale test results.

Chapter 4

NUMERICAL MODELING OF PULLOUT CAPACITY OF SUCTION CAISSON IN SAND UNDER OBLIQUE LOAD

4.1 General

Suction piles are widely used in mooring system for deep water oil and gas development projects. In this chapter, three-dimensional finite element analyses are performed to estimate the pullout capacity of a suction pile subjected to oblique loading. The numerical modeling is performed using ABAQUS finite element software. The effects of two key variables, loading angle and mooring line position, are investigated. The finite element results are compared with centrifuge test results available in the literature.

4.2 Introduction

A suction pile (also known as suction caisson) is a large cylinder, usually made of steel, with an open bottom and a closed top that is installed in the ground mainly by suction applied by pumping water out of the caisson interior. Suction piles have been widely used in offshore industries ranging from anchors for floating facilities to offshore foundations. Geometrically the suction piles are larger in diameter than typical piles used. Figure 4-1 shows some of the suction piles used for various projects in the world. Suction piles could be installed both in clay and sand sea beds, although the mechanism during

installation is different. Housby and Byrne (2005a, b) present the design procedure for installation of suction piles in sand, clay and other geomaterials.

Suction piles are widely used in mooring systems for deep water oil and gas development projects, where the pullout capacity is one of the main requirements. The piles are normally pulled by a chain connected to a pad eye on the side of the pile. The inclined pull-out capacity of suction pile depends on both horizontal and vertical load capacities.

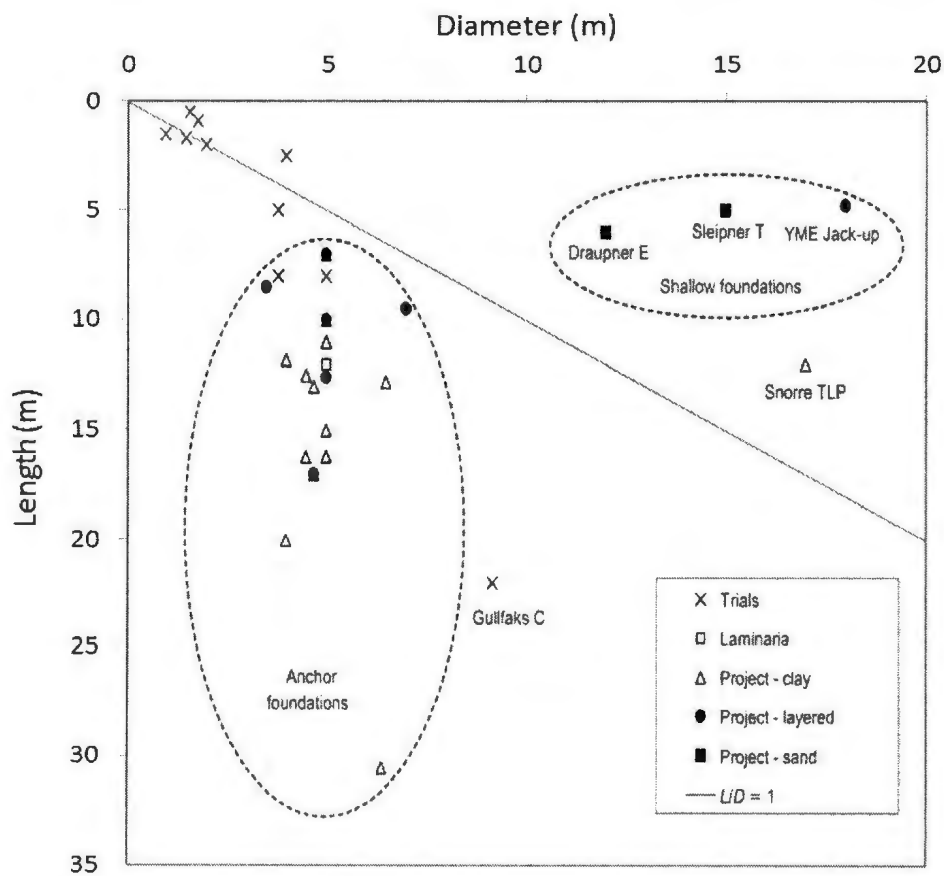


Figure 4-1: Suction piles used in various projects (Byrne 2005b)

The inclined load capacity of typical pile foundations has been studied by several researchers. Yoshimi (1964) studied the behavior of rigid vertical and battered piles in a cohesionless soil subjected to inclined loading. Broms (1965) also analyzed the Yoshimi (1964) experiments and proposed an equation for the pull out resistance. Poulos and Davis (1980), based on the experiments of Yoshimi (1964) and analysis of Broms(1965), proposed a simplified theoretical method to predict the ultimate resistance of a vertical pile under oblique loading. Finite element analysis of a single pile under lateral and oblique pulling has also been conducted by some researchers. Erbrich (1994) conducted a series of finite element analyses to estimate the capacity of suction caissons used as foundations for fixed offshore steel platforms. As the aspect ratio (L/D) is different, the response of a suction caisson is expected to be different from typical pile foundation.

Bye et al. (1995) presented the analyses of the Europe 16/11E and sleipner T foundation in dense sand. Sukumarn et al. (1999) and Sukumaran and McCarron (1999) showed the application of the finite element method to estimate the capacity of suction pile foundations installed in soft clays and subjected to axial and lateral loads under undrained conditions. Handayanu et al. (1999 and 2000) used a quasi-three-dimensional finite element model to study the response of suction caissons subjected to vertical uplift and inclined loads. Deng and Carter (2000) presented finite element analyses using axisymmetric elements and proposed a simplified relationship for estimating inclined pullout capacity of a suction caisson in the sand in drained conditions. Zdravkovic et al. (2001) conducted finite element analyses to study effects of load inclination, caisson aspect ratio, soil adhesion, and soil anisotropy on behavior of suction piles in clay. Cho

and Bang (2002) examined the application of the failure envelop developed by Bransby and Randolph (1999) from the observation in clay for estimating inclined load capacity of a suction caisson in sand. Bang et al. (2011) conducted a series of centrifuge tests to estimate the pullout capacity of a suction caisson installed in sand.

This chapter presents three-dimensional finite element analysis of a steel suction pile embedded in sand subjected to oblique loading at different load inclination and mooring positions. A total of 25 cases is analyzed to evaluate the pull-out capacity of a suction pile. The finite element results are compared with centrifuge test results. The effects of loading angle and mooring positions on the ultimate pullout capacity, lateral displacement and soil reactions on suction piles are discussed.

4.3 Problem Definition

Finite element (FE) analyses are performed to calculate the pullout capacity of suction piles. A suction pile of diameter D and length L installed in sand is loaded at different mooring positions and loading angles. The notations used in this study are shown in Figure 4-2. The load is applied at five pad-eye locations as shown by solid circles on the left.

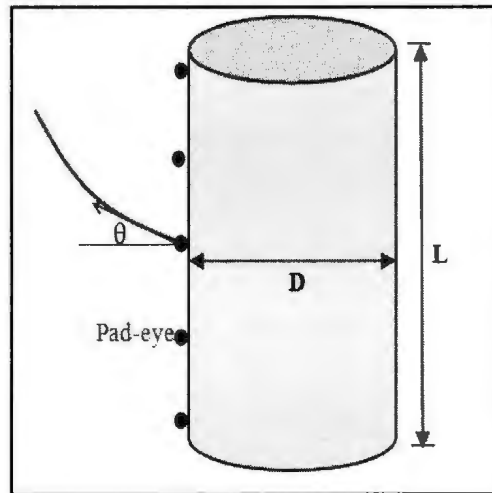


Figure 4-2: Problem definition

4.4 Numerical Modeling

In this study, numerical analyses are carried out using finite element software ABAQUS/standard 6.10-EF-1. A cuboid soil domain of 40 m length, 20 m width and 20 m height as shown in Figure 4-3 is modeled. The size of the soil domain is sufficiently large compared to the size of the pile and therefore, boundary effects are not expected on calculated load, displacement and deformation mechanism. The vertical plane of symmetry of the soil domain is restrained from any displacement perpendicular to it while the other three vertical sides of the soil domain are restrained against lateral displacement using roller supports at the nodes. The bottom boundary is restrained from any vertical displacement, and the top boundary is free to displace.

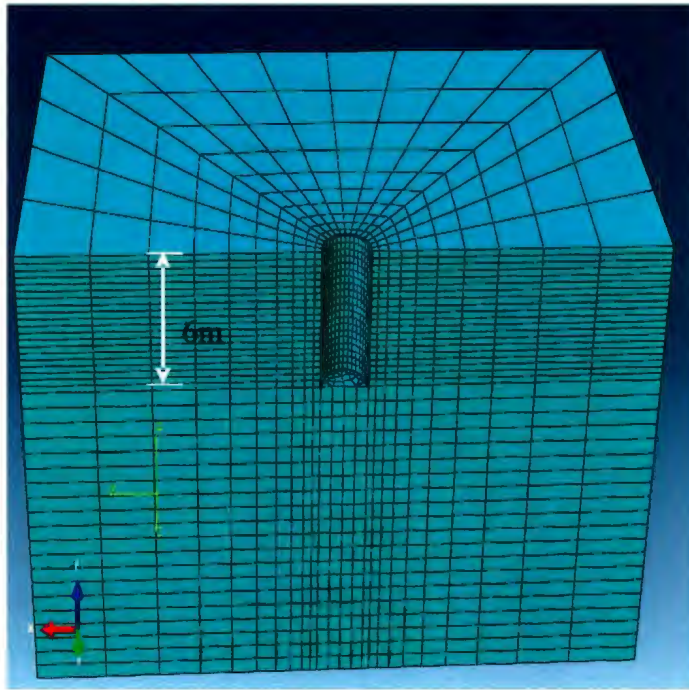


Figure 4-3: Finite element model using in analysis

The finite element mesh used in this study is shown in Figure 4-3. The elements used are the solid homogeneous C3D8R element, which is an 8-noded linear brick, multi-material and reduced integration with hourglass control.

The numerical analysis consists of two major steps: gravity and loading step. In gravity step, the soil domain is loaded up to the in-situ stress condition, and in the loading step, lateral, oblique (upward) or vertical displacements are applied on the nodes at the desired depth (pad-eye location) on the left side of the outer surface of the caisson as shown in Figs. 4-2 and 4-3.

4.4.1 Modeling of Caisson

A steel suction caisson of 6 m length and 3 m diameter with 100 mm wall thickness is modeled in this study. The caisson is modeled as an elastic material with a modulus of elasticity (E_p) of 208×10^6 kN/m² and Poisson's ratio (ν_p) of 0.3.

4.4.2 Soil Modeling

It is assumed that the excess pore water pressure in sand fully dissipates during the application of pulling force and drained behaviour of sand governs the response of the caisson. Rate of pulling has a significant effect on pullout capacity. A rapid pullout test causes undrained condition that gives a far in excess capacity of any design interest (El-Gharbawy et al. 1998). A partially drained behaviour might better represents some field loading conditions. As the drained condition is simulated, the results presented in the following sections are applicable to the cases of sustained loading on the caisson.

The sand is modeled by the Mohr-Coulomb model available in ABAQUS FE software using the following soil parameters: angle of internal friction, $\phi' = 39^\circ$; dilation angle, $\psi = 9^\circ$; modulus of elasticity, $E_s = 60,000$ kPa; and Poisson's ratio, $\nu_p = 0.3$. The submerged unit weight of soil is 8.2 kN/m³. The geometry and mechanical properties used in the analysis are shown in Table 4-1. Note that the geometry and soil parameters mentioned above and in Table 4-1 are very similar to Bang et al. (2011) as the numerical results presented in this study are verified using their test results.

Table 4-1: Geometry and mechanical properties used in the analysis

| | |
|--|----------------------------------|
| Pile: | |
| Length of the pile (H) | 6 m |
| Diameter of the pile (D) | 3 m |
| Wall thickness of the pile (t) | 100 mm |
| Modulus of elasticity of pile (E_p) | $208 \times 10^6 \text{ kN/m}^2$ |
| Poisson's ratio (ν_p) | 0.3 |
| Soil (sand): | |
| Modulus of elasticity, E_s | $60,000 \text{ kN/m}^2$ |
| Poisson's ratio, ν_s | 0.3 |
| Submerged unit weight of soil, γ' | 8.2 kN/m^3 |
| Angle of internal friction, ϕ'_p | 39° |
| Dilation angle, ψ | 9° |

The soil/pile interaction has been modeled using Coulomb friction model, which defines the friction coefficient (μ) as $\mu = \tan(\phi_\mu)$, where ϕ_μ is the pile/soil interface friction angle.

The value of ϕ_μ is assumed to be equal to $0.7\phi'$ in this analysis.

4.4.3 Mesh Sensitivity Analysis

The size of the mesh has a significant effect on finite element modeling. Often a finer mesh yields more accurate results, but computational time is higher. For successful modeling of load-displacement behaviour of piles under oblique load, denser mesh should be used near the pile. As shown in Figure 4-4, smaller soil elements are used near the pile and the size of the elements are increased with radial distance from the center of the pile. Also, a denser mesh is used in the top 6 m of soil where the caisson is located. Below 6 m depth, a coarser mesh is used which does not have a significant effect on the calculation.

After several trial analyses with different mesh size, the optimum mesh is selected. Figure 4-4 shows the lateral load versus lateral displacement of the pile for three different types of mesh. In the coarse mesh, a total of 5,380 elements, in the medium dense mesh 7,300 elements and in the fine mesh 11,140 elements are used. The distribution of mesh size is shown in Figure 4-3. As shown in Figure 4-4, the number of elements has a considerable effect on force-displacement behavior. The analyses presented in the following sections are conducted using a medium mesh with 7,300 elements.

4.4.4 Centrifuge Modeling

Bang et al. (2011) conducted a series of centrifuge model tests of a suction pile embedded in sand to evaluate its pullout capacity. The effects of load inclination angle and the point of mooring line attachment are studied. The tests were conducted at 100g using a

geotechnical centrifuge. The test condition and geotechnical properties of sand are similar to those described in Sections 4.4.1 and 4.4.2.

4.5 Numerical Results

Numerical modeling is carried out for a single pile applying the load at five mooring positions: 5%, 25%, 50%, 75% and 95% distance from top of the pile. At each mooring position, the load is also applied at five different angles of inclination with the horizontal axes: 0°, 22.5°, 45°, 67.5° and 90°. That means a total of 25 (=5×5) numerical modeling is conducted to show the effects of inclination angle and mooring position on pull-out capacity.

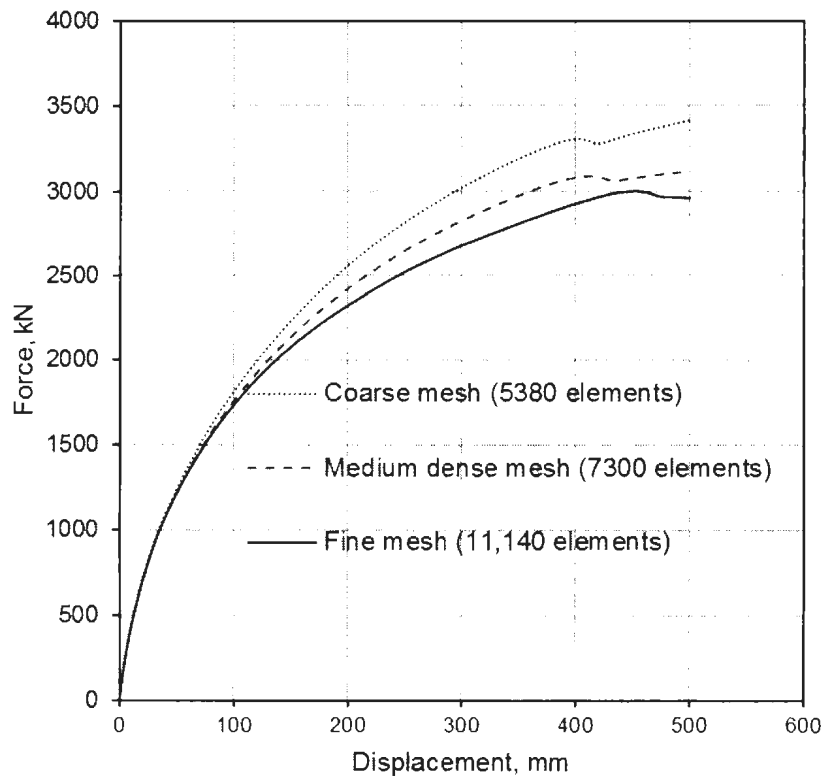


Figure 4-4: Mesh sensitivity analysis

4.5.1 Load-Displacement curves

The variation of total (inclined) load with total displacement of the suction caisson for five different mooring positions is shown in Figure 4-5 to Figure 4-9. The total load is calculated from the vertical and horizontal nodal force components at the point of loading. As shown in these figures, for example Fig. 4-5, that the load is increased with an increase in displacement. For higher values of load inclination angle θ , the load displacement curves become almost horizontal at large displacement. However, for lower values of θ the load is continuously increasing with displacement. It is expected that at a very large displacement, significant rotation of the caisson will be occurred, and the ultimate load could be obtained. However, in ABAQUS/Standard such a large deformation could not be applied because of significant mesh distortion. Therefore, in this study the load corresponding to the displacement of 10% pile diameter (i.e. $0.1 \times 3 = 0.3$ m) is considered as pullout capacity of the pile. The pull-out capacity is shown by the vertical arrows in Figure 4-5. The author understands that the pullout capacity for lower values of θ is slightly lower than ultimate pullout capacity, which is the limitation of this study.

Bang et al. (2011) did not report the load-displacement curves, and therefore, direct comparison of FE and centrifuge results could not be performed. Note that stretching of the cable significantly affects load-displacement curve as shown in Fig. 2.10. However, the load-displacement curves shown in Fig. 4.5 are very similar to the numerical results of Deng and Carter (2000).

Bang et al. (2011) reported the pullout capacity from their centrifuge tests. The pullout capacity is the peak force during loading which is expected to be occurred at a very large displacement for lower values of θ and could not be reached in the present FE analysis using ABAQUS/Standard. The range of their pullout capacity is shown by the arrows on the right vertical axis. The numerical prediction in the present analyses reasonably matches with the centrifuge test results.

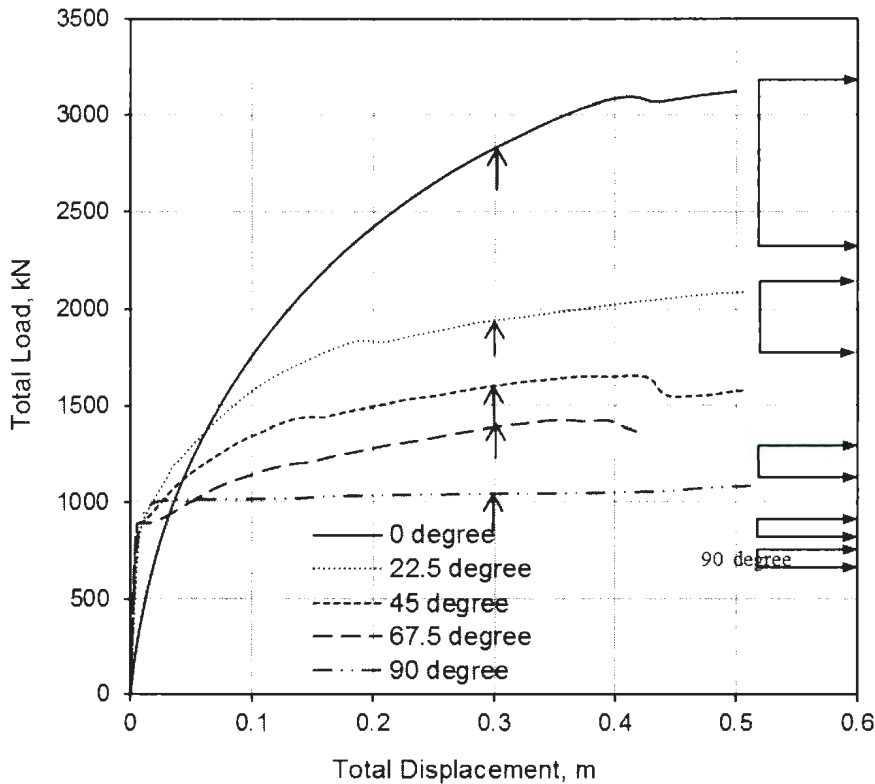


Figure 4-5 : Load-displacement curves for 5% mooring position (right arrows represent the range of centrifuge test results)

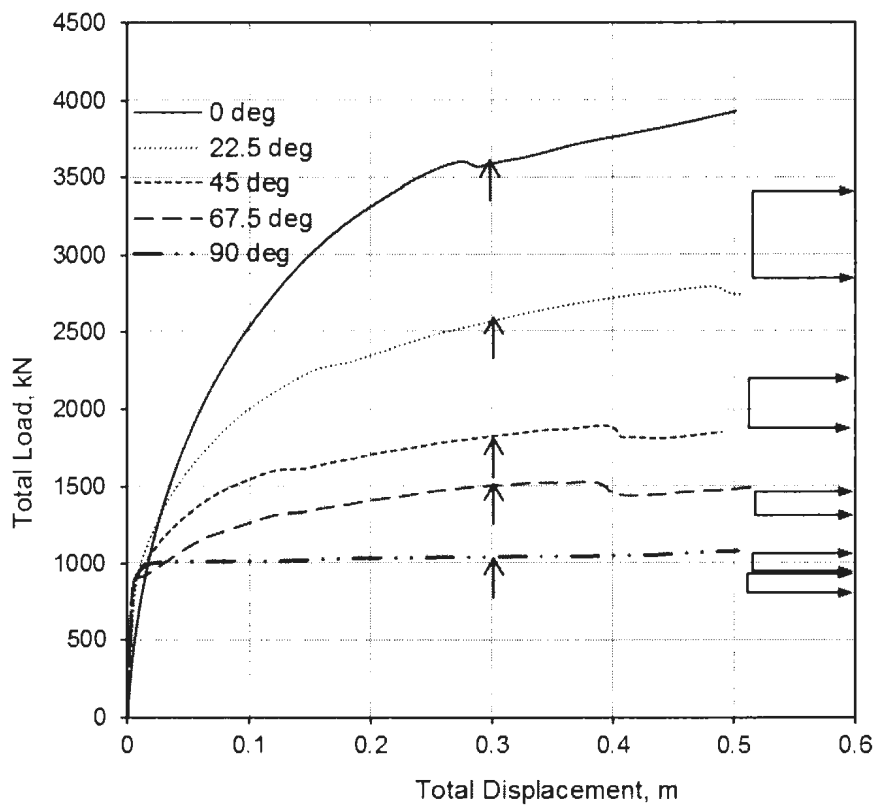


Figure 4-6 : Load-displacement curves for 25% mooring position

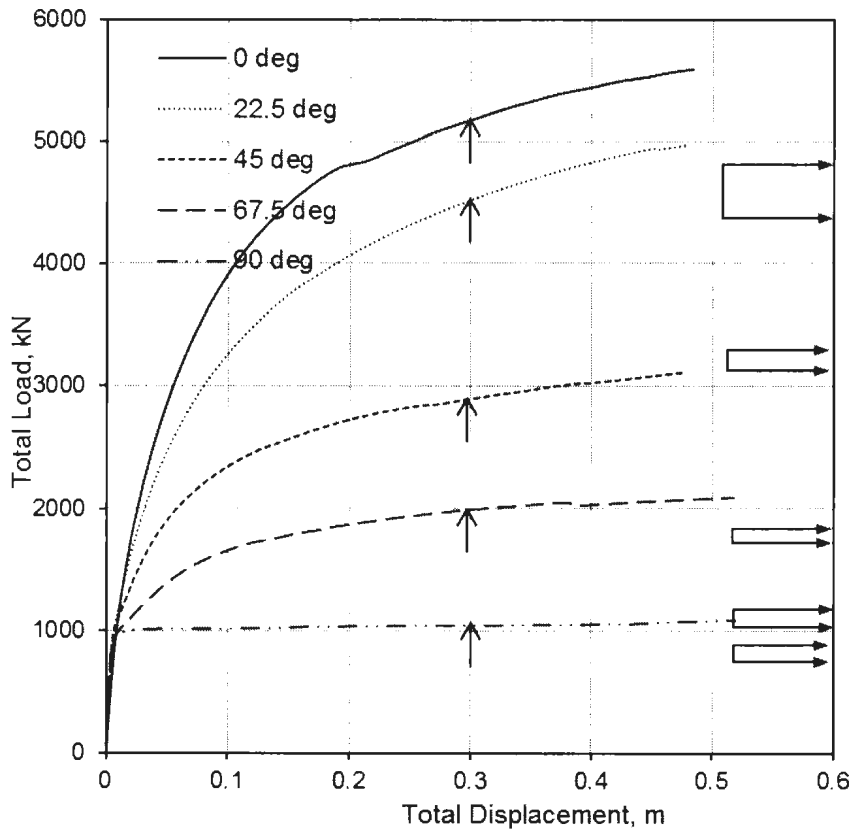


Figure 4-7: Load-displacement curves for 50% mooring position

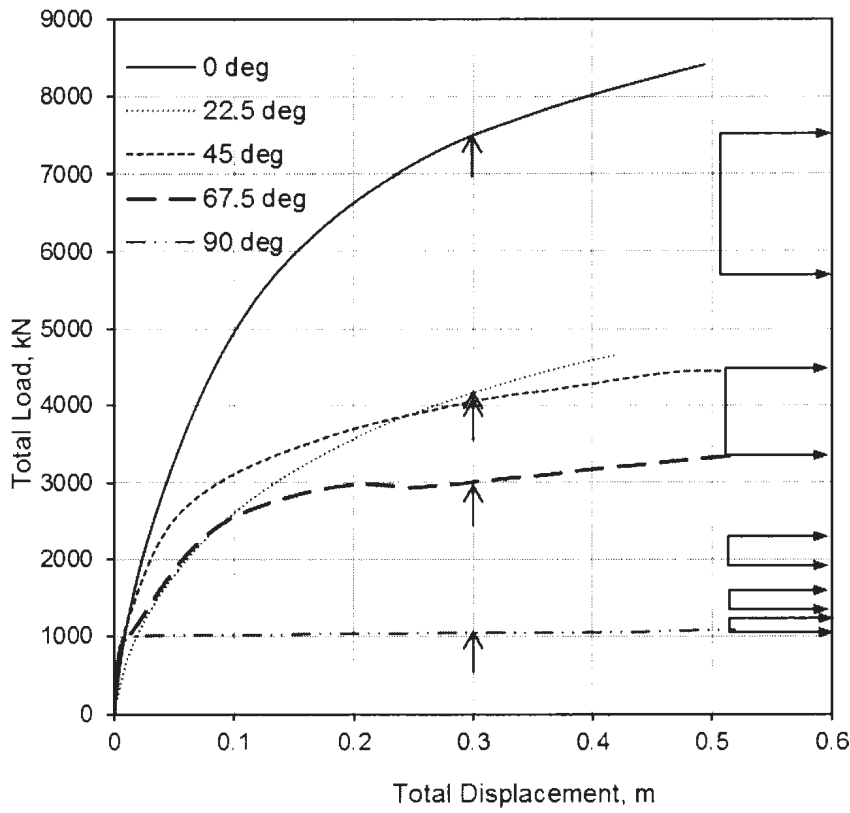


Figure 4-8: Load-displacement curves for 75% mooring position

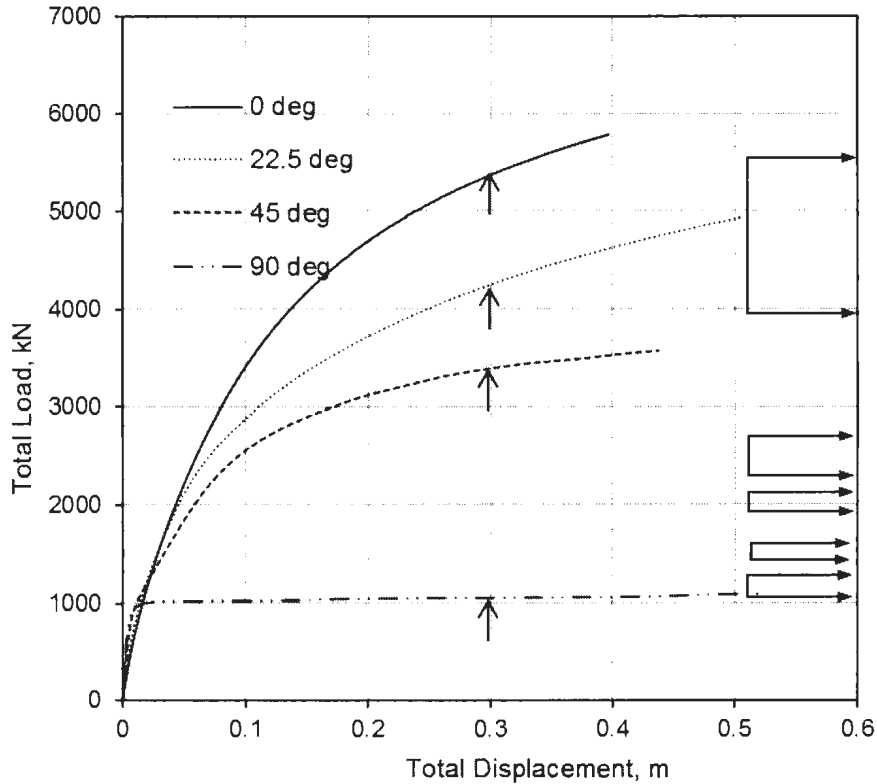


Figure 4-9: Load-displacement curves for 95% mooring position

4.5.2 Effects of Depth and Angle of Pulling

Figure 4-10 shows the variation of the lateral load with lateral displacement ($\theta=0$) for five different mooring positions. Again, the pullout capacity obtained in centrifuge tests is shown on the right vertical axis using horizontal arrows. The pullout capacity (vertical arrows) in the present finite element analysis compares well with centrifuge test results. The pullout capacity increases as the depth of mooring position increases. The maximum pullout capacity is obtained for 75% mooring position. After that, for example, at 95% mooring position, the pullout capacity decreases. This is because of displacement and

rotation of the pile under mooring force, which will be further discussed in the following sections. The computed pullout capacity is very similar to experimental results (e.g. Bang et al., 2011; Kim et al., 2010; Kim et al., 2005).

As mentioned before, a total of 25 finite element analyses are presented in this paper. The pullout capacity for various mooring position obtained from FE analysis is plotted in Figure 4-11. As shown in this figure that the pullout capacity is maximum when the padeye location is at 75% depth from the top of the caisson. Figure 4-12 shows the centrifuge test results reported by Bang et al. (2011). The pullout capacity obtained from the present FE analysis is comparable with the centrifuge test results. Bang et al. (2011) also developed an analytical solution to calculate the pullout capacity. Figure 4-13 shows the comparison between analytical solution and centrifuge test results for three different load inclination angles. Comparing these three figures (4-11 to 4-13) it can be concluded that the present finite element model can simulate the pullout capacity of suction caisson in sand.

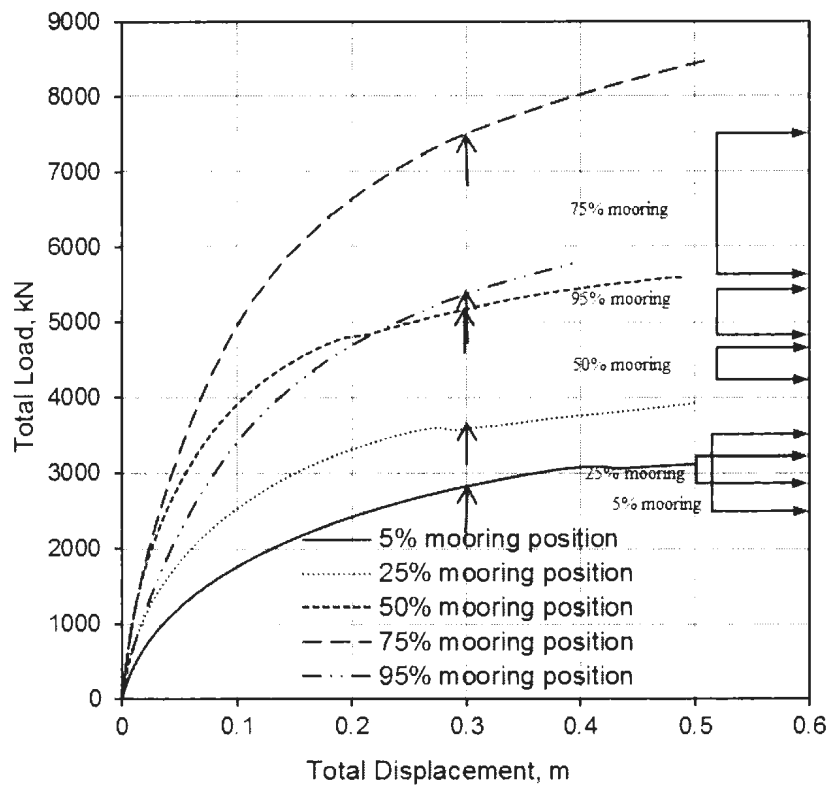


Figure 4-10: Lateral load vs. lateral displacement for different mooring positions

(Right arrows represent the range of centrifuge results)

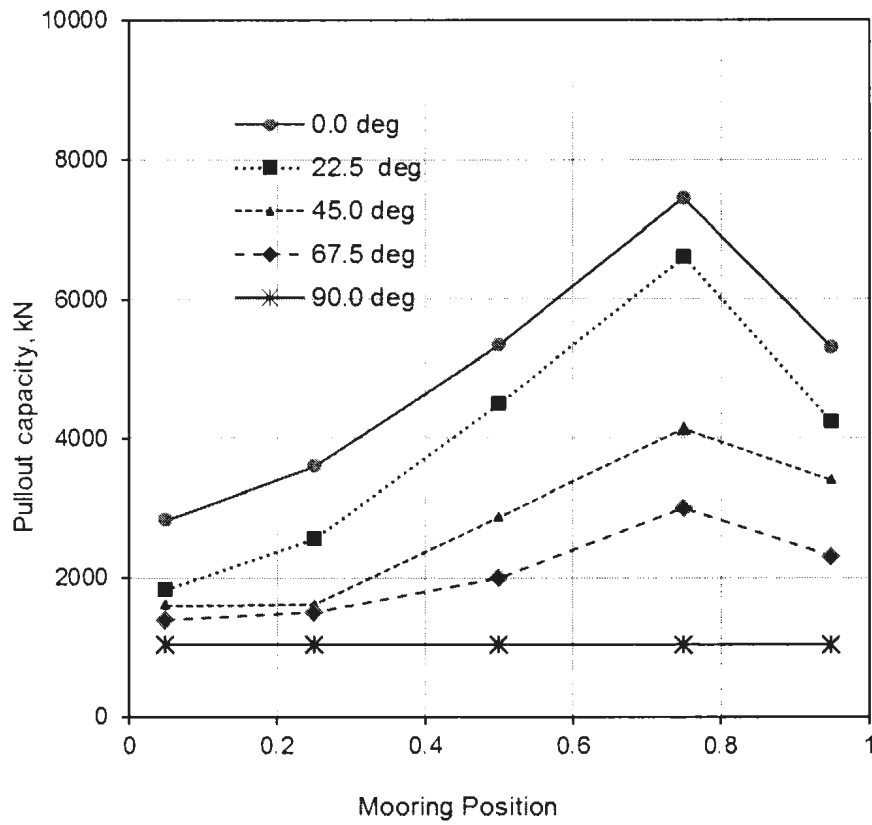


Figure 4-11: Pullout capacity for different loading angle and mooring position from FE analysis

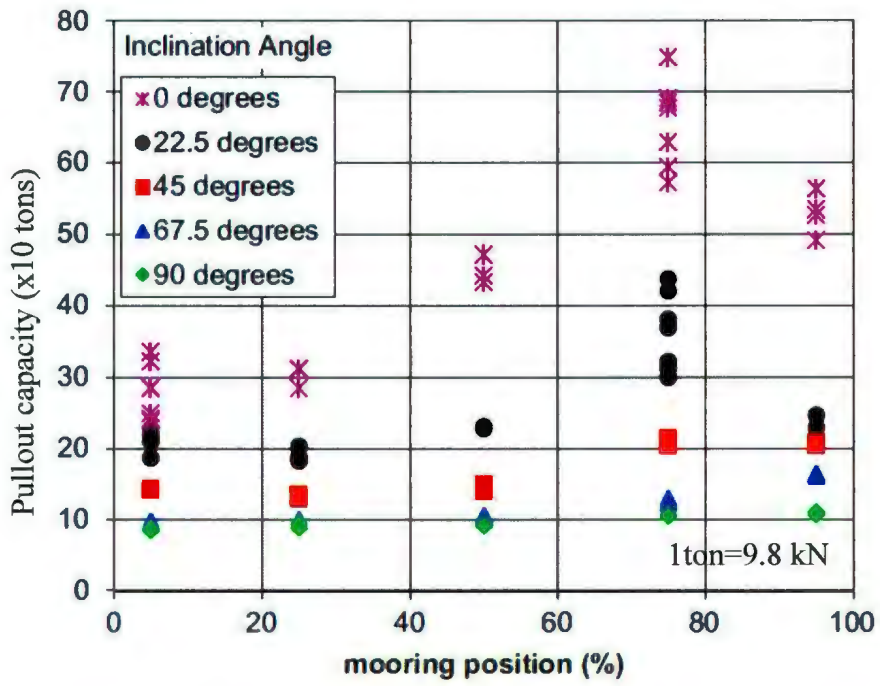


Figure 4-12: Pullout capacity for different loading angle and mooring position from centrifuge test (Bang et al. 2011)

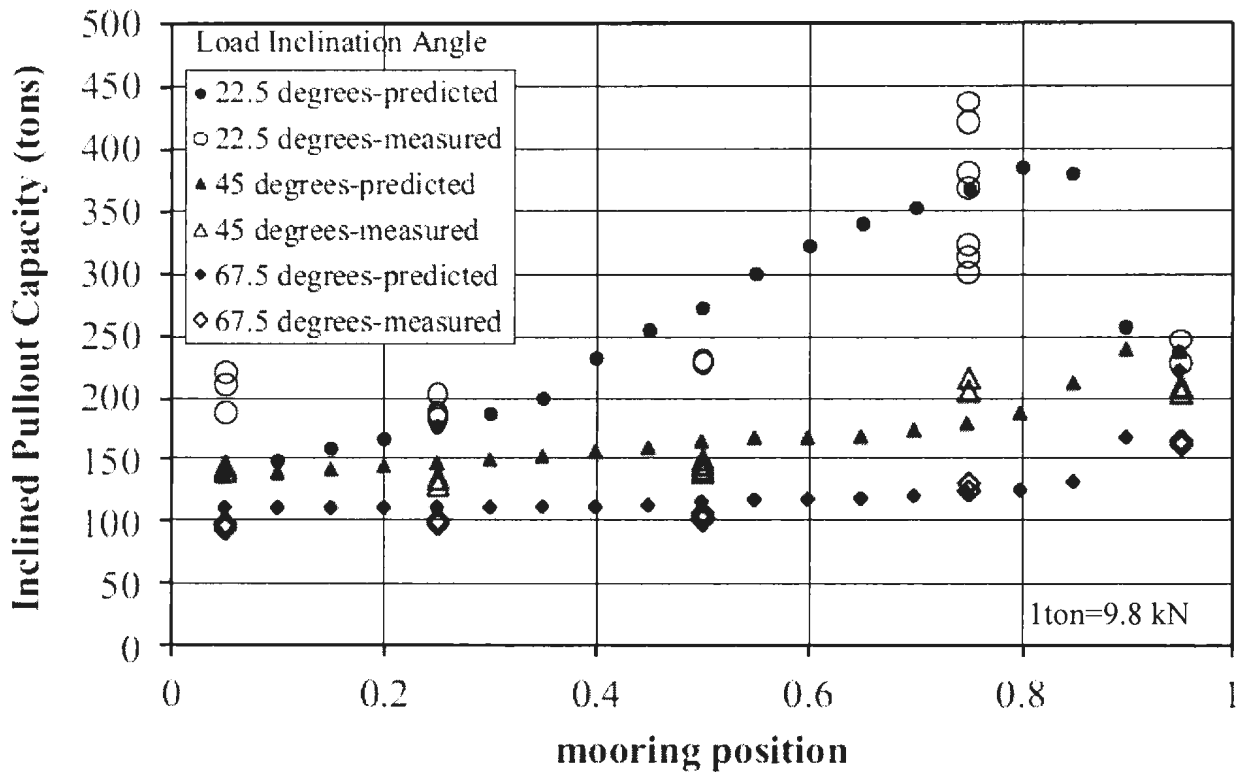


Figure 4-13: Comparison between centrifuge test results and analytical solution (Bang et al. 2011)

Figure 4-14 shows the variation of pullout capacity with mooring line inclination angle. As shown in this figure that the pullout capacity decreases with increase in inclination angle. For lower value of θ , for example $\theta=0$ (lateral loading), the pullout capacity significantly depends on mooring position and is maximum for 75%. However for uplift ($\theta=90^\circ$) the pullout capacity is almost independent of mooring position. The pattern shown in Fig. 4-14 is very similar to the centrifuge test results by Kim et al. (2010).

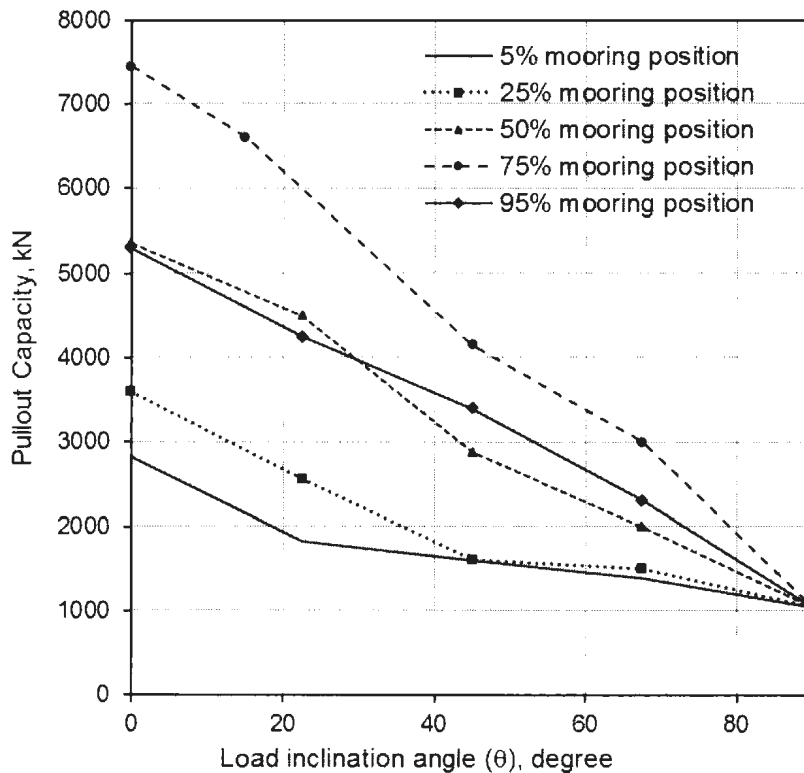


Figure 4-14: Pullout capacity for different loading angle and mooring position

4.5.3 Plastic Strain and Displacement Vector Diagram

Figure 4-15 and Fig. 4-16 show the plastic strain and displacement contour for two cases. For 5% mooring position, the plastic strain mainly developed on the left side of the caisson. The bottom of the failed soil wedge on the left extends almost linearly to the bottom of the caisson. On the other hand the shape of the plastic zone on the left side of the caisson for 75% mooring position (Fig. 4-16) is different from the shape shown in Fig. 4-15. Similarly, the magnitude of deformation is also different for these two cases.

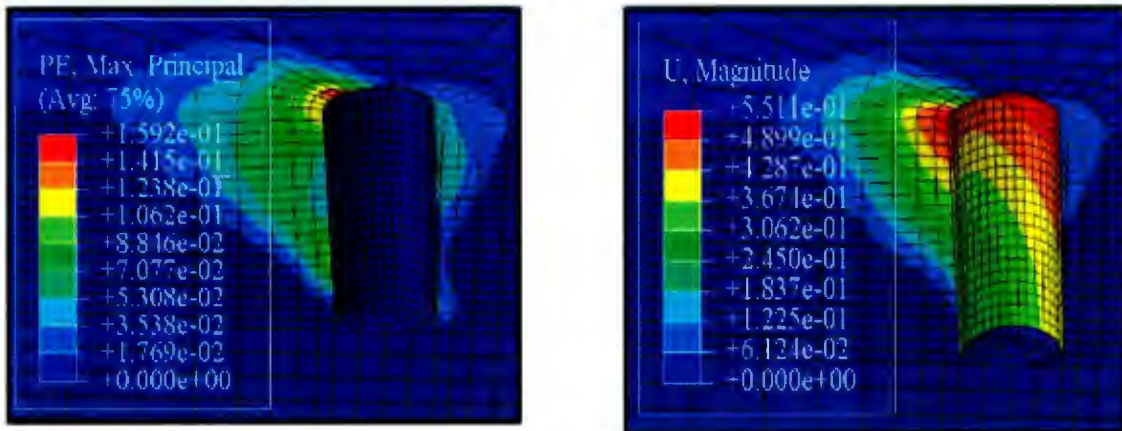


Figure 4-15: Maximum principle plastic strain and displacement vector diagram for 5% mooring position and 0.5m displacement at 22.5° angle.

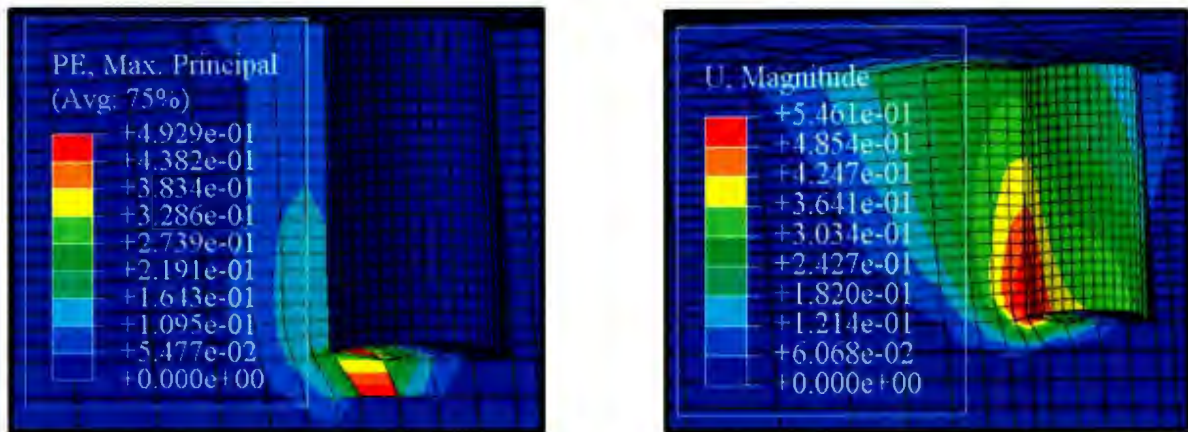


Figure 4-16: Maximum principle plastic strain and displacement vector diagram for 75% mooring position and 0.5m displacement at 15° angle.

Figure 4-17 shows the vertical displacement and displacement vectors for 5%, 50% and 95% mooring position at 0.3m displacement of the caisson loaded at 22.5° to the horizontal. As shown in this figure that a large volume of soil is displaced at 95%

mooring position. This pattern is very similar to the experimental observation reported by Allersma et al. (2000) as shown in Fig. 4-18.

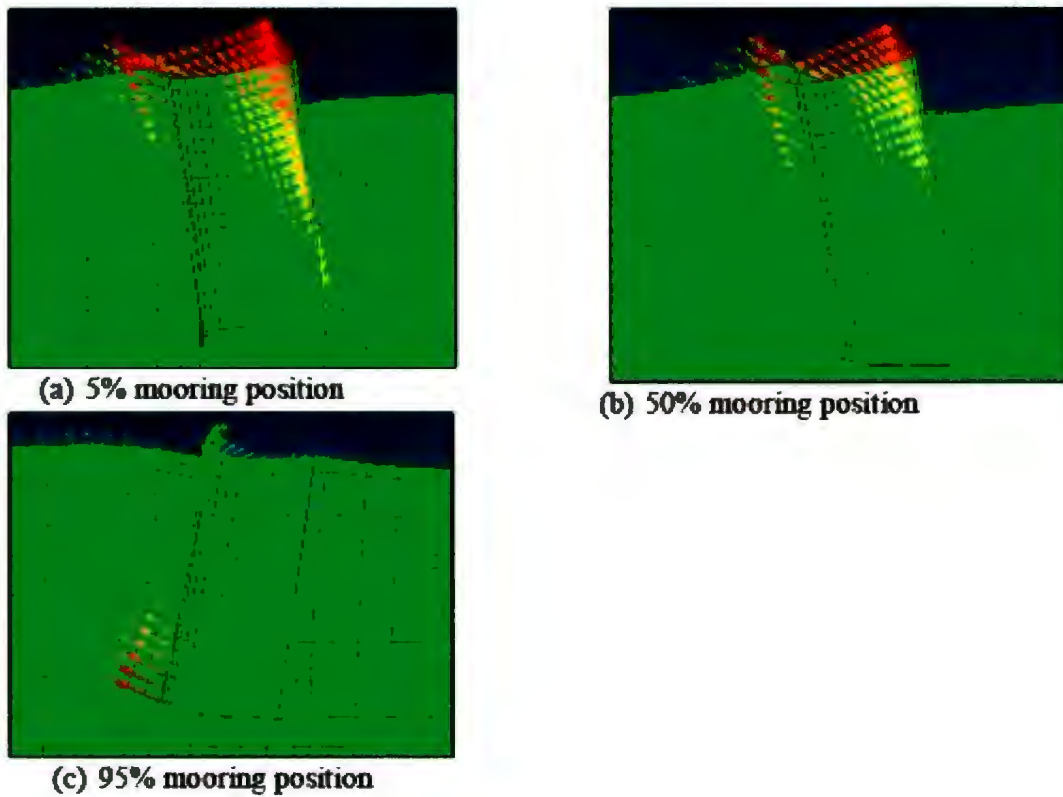


Figure 4-17: Vertical displacement vector for 0.3m displacement at 22.5 degree with horizontal

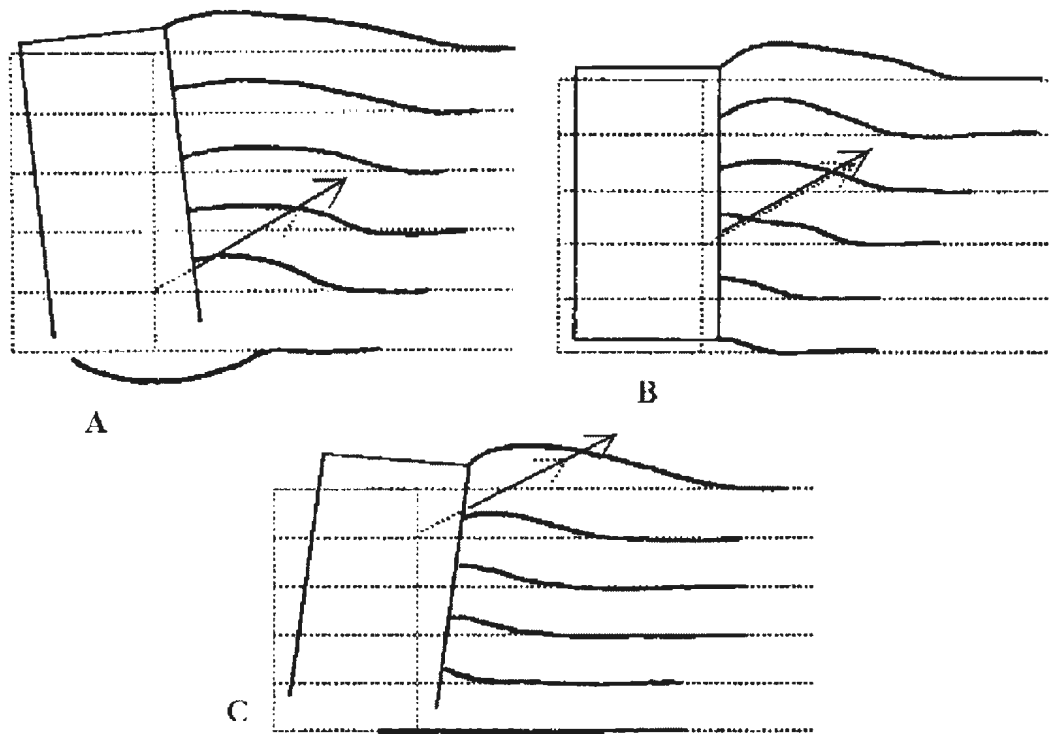


Figure 4-18: Vertical displacement and failure mechanism observed in centrifuge test (Allersma et al. 2000)

4.5.4 Lateral Displacement

Figure 4-19 shows the lateral displacement along the centerline of the caisson with depth for different loading angles at 5% mooring position at 0.3 m displacement. The lateral displacement is obtained from the displacement of the center nodes of the caisson. As shown in this figure, the lateral displacement is almost linear. That means the displacement pattern of a suction caisson is very similar to a short pile and rotates almost as a rigid body. The degree of rotation and the center of rotation are dependent upon the angle of loading. The rotation has a significant effect on pullout capacity. As expected, the rotation of the caisson is less for higher load inclination angle (e.g. 67°).

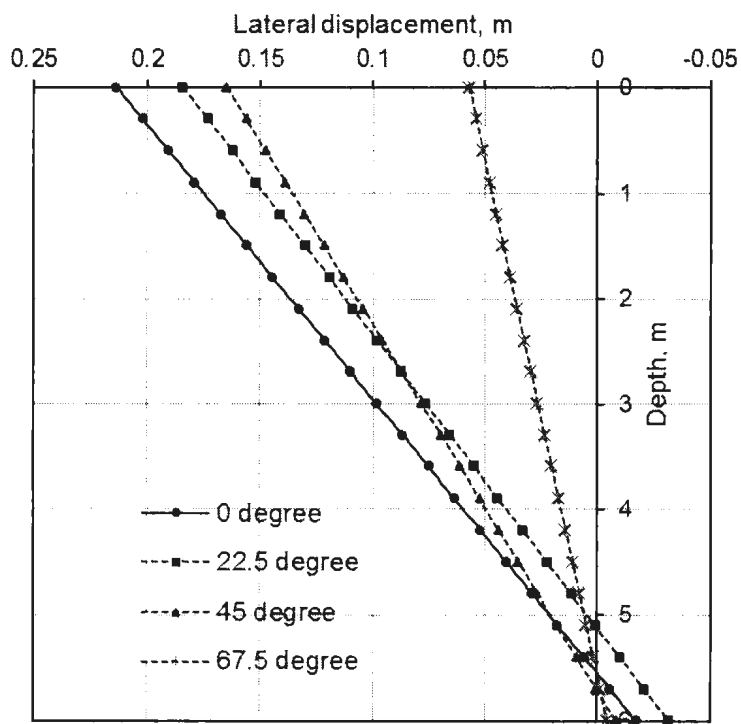


Figure 4-19: Lateral displacement for different loading angle at 5% mooring position

Figure 4-20 shows the variation of lateral displacement with depth for different mooring positions under lateral loading for 0.3 m lateral displacement. The suction caisson is rotated toward the left when the mooring position is less than 50% while it rotates toward the right when it is at 95%. The minimum rotation occurs for the 75% mooring position and that result higher pullout capacity. The pattern of rotation is very similar to Kim et al. (2010).

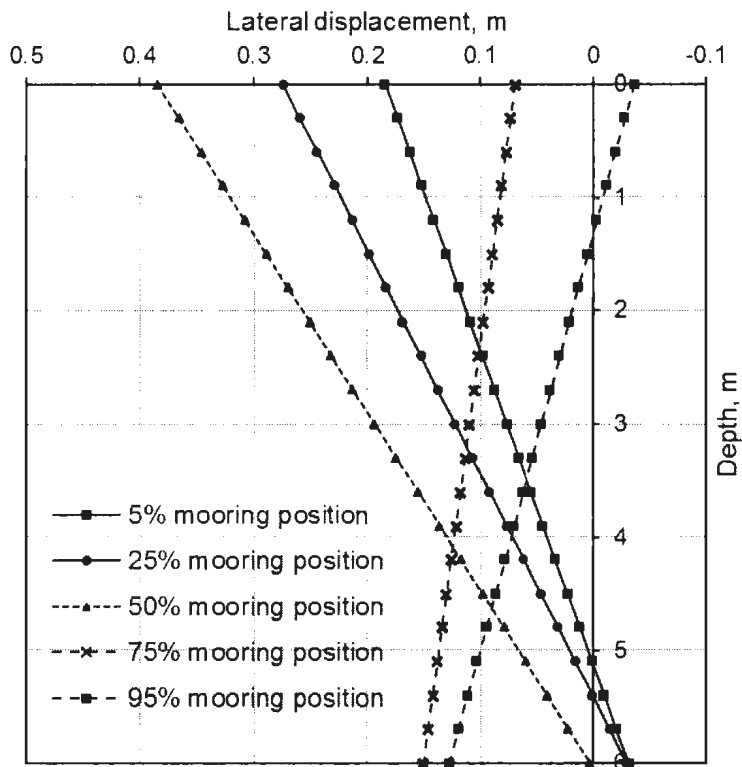


Figure 4-20: Lateral displacement for different mooring positions

4.5.5 Rotation vs. Mooring Position

Figure 4-21 shows the rotations of the pile with respect to the central axis of the pile at 0.3 m displacement at various mooring positions and load inclination angles. As shown in this figure that the direction of rotation is changed from +ve (leftward) to -ve (rightward) at mooring position of about 0.75. The rotation of the caisson is almost zero at this mooring position. The pattern of rotation is very similar to the measured values in centrifuge test (Kim et al., 2010). It is to be noted here that rotation presented in Fig. 4-21 is for displacement of 0.3 m. On the other hand Kim et al. (2010) presented the rotation of the caisson at failure which could not be achieved in the present FE analysis for lower

value of θ using ABAQUS/Standard because of mesh distortion. Therefore, the rotation shown in this figure is lower than the measured values in centrifuge for low value of θ , although the pullout capacity is comparable as shown before.

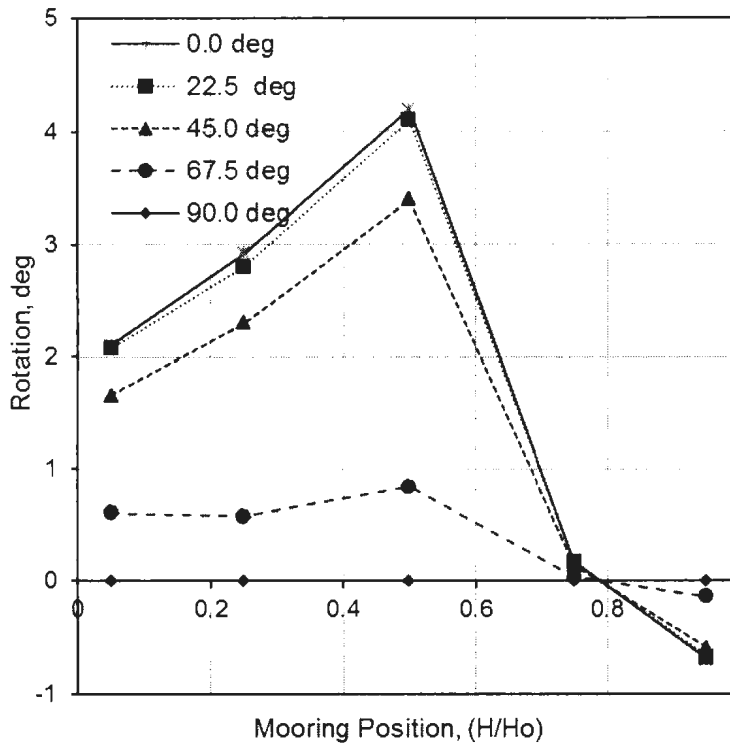


Figure 4-21: Soil reaction for different mooring positions

4.5.6 Mobilized Soil Reaction

Figure 4-22 shows the variation of mobilized soil reaction (load per unit length of the pile) with depth at 0.3 m displacement for different loading angle at 5% mooring position. In the finite element analysis, the soil reaction is obtained from the sum of the lateral components of nodal force at a particular depth dividing by the vertical distance between two node sets at the point of interest. As noted, with increases in loading angle

the soil reaction decreases because of less lateral deformation and interaction between the horizontal and vertical movement.

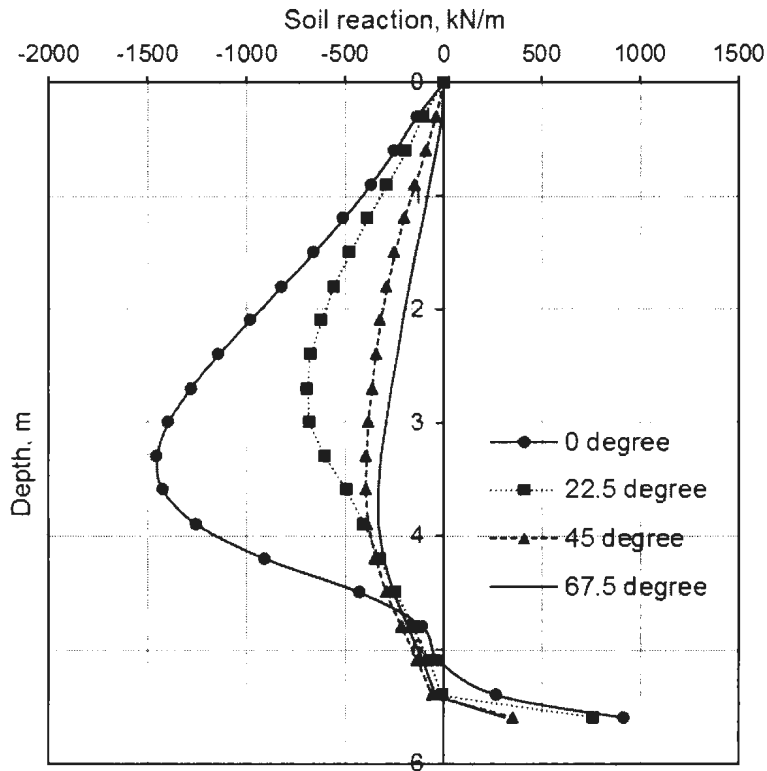


Figure 4-22: Soil reaction for different loading angle at 5% mooring position

The effect of mooring position on mobilized soil reaction is shown in Figure 4-23, where the mobilized soil reaction is dependent on mooring position. For a mooring position less than 50%, the pattern of mobilized soil reaction curve is similar while after 50% mooring position it is different, which is because of the rotation of the pile.

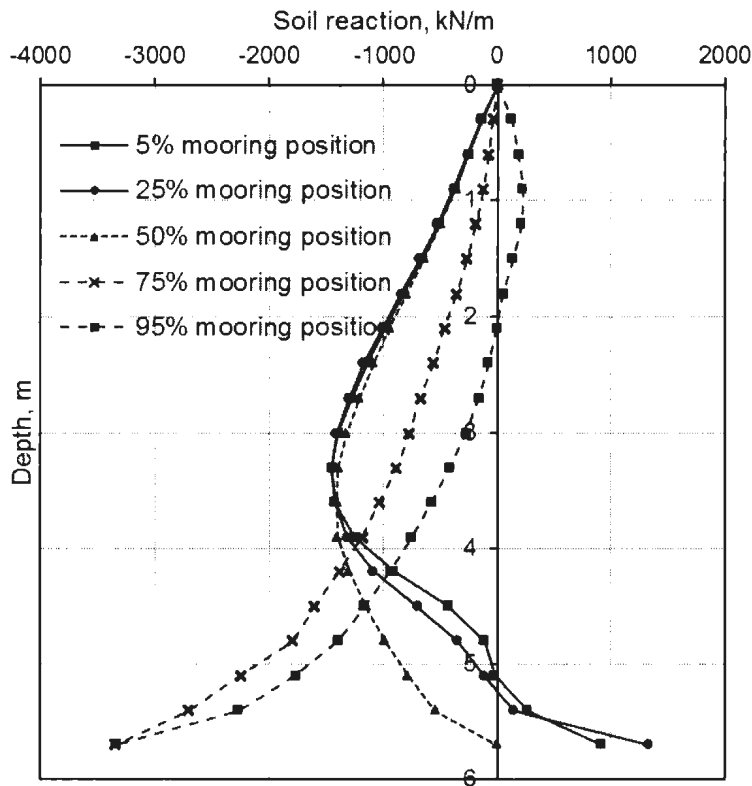


Figure 4-23: Soil reaction for different mooring positions

4.6 Conclusion and discussions

A total of 25 finite element analyses is conducted to evaluate the pullout capacity of a suction pile. The effects of two key variables examined in this study are: loading angle and mooring position. Finite element results have been compared with centrifuge test results. It is shown that the pullout capacity of suction piles increases as the mooring position moves towards the pile tip, and the 75% mooring line attachment gives the maximum pullout capacity for the cases presented in this paper. Pullout capacity also decreases with an increase in loading angle. The shape of the soil failure wedge is

dependent on mooring position and loading angle which has a significant effect on pullout capacity.

Chapter 5

CONCLUSIONS AND FUTURE RECOMMENDATIONS

5.1 Conclusions

Steel piles are commonly used in onshore and offshore environments. Depending upon loading conditions, these piles are subjected to not only axial downward load but also lateral and inclined upward load. Proper estimation of lateral and pullout capacities of these piles is required for successful design. In this thesis, finite element analyses have been performed to model the response of two types of steel piles in the sand: (i) long steel pipe piles under pure lateral load, and (ii) suction piles in sand under oblique upward load. The FE analyses have been performed using ABAQUS FE software.

In chapter 3, the analyses of a long steel pipe pile in the sand are presented. The variation of dilation angle and friction angle of sand has been incorporated in the soil constitutive model to capture the post-peak softening behaviour of sand as observed in laboratory tests. The increase in elastic modulus with mean effective stress is also incorporated in the analyses. To validate the model, the FE results have been compared with two well documented full-scale test results available in the literature. Both of these full-scale tests were conducted in sand deposits. The numerical analyses have also been performed using LPILE-5.0 software which is widely used in the design of pile foundations under lateral load. The present FE analyses show that the FE technique can better simulate the response of the pile. The variation of pile displacement, bending moment, shear force,

and lateral soil pressure matched well with the full-scale test results. Based on FE analyses, the p - y curve which is typically used in simplified method of design is also developed. The p - y curves obtained from the present FE analysed matched better with full-scale test results. The lateral pressure in front of the pipe pile is far from uniform, especially below 1.0 m for the case analysed here.

In the conventional design practice based on the p - y curve method, a constant representative value of ϕ' between the peak and critical state is required to be selected. The initial modulus of subgrade reaction, which is not a fundamental soil property, is obtained from ϕ' and relative density. API (1987) recommended an empirical equation for estimating the representative value of ϕ' as a function of relative density. However, the computation with this recommended value of ϕ' over predicts the maximum bending moment and lateral displacement (Rollins et al. 2005). Such limitations of the p - y curve method are overcome using FE modeling presented in this study. The input parameters required in FE analyses are fundamental soil properties such as friction angle, dilatancy and stiffness.

The analysis in Chapter 4 consists of a series of finite element analysis of a suction pile in sand under oblique loading to estimate the pullout capacity. In this case, the FE results are compared with a series of centrifuge test results. A total of 25 cases are simulated to evaluate the pullout capacity of a suction pile under various loading condition. The sand is modeled by the Mohr-Coulomb model available in ABAQUS FE software. It is shown that the pullout capacity of suction piles increases as the mooring position moves towards the pile tip, and the 75% mooring line attachment gives the maximum pullout capacity

for the cases presented in this paper. Pullout capacity also decreases with the increase in loading angle. The shape of the soil failure wedge is dependent on mooring position and loading angle which has a significant effect on pullout capacity.

5.2 Recommendations for Future Work

In the present study, the response of long steel pipe piles and suction piles is simulated using commercially available ABAQUS FE software. A number of important features have been simulated in this study which cannot be performed using the conventional p - y curve method. However, there are some limitations of this study which might be addressed in future research.

- The effects of post-peak softening should be incorporated in the analyses of suction piles. Because of significant mesh distortion finite element simulation using ABAQUS/Standard could not be continued until the ultimate resistance, especially for lower inclination angle. Advanced FE techniques for large deformation behaviour might be used for this.
- Laboratory test should be conducted to develop the relationship between friction angle and dilation angle with plastic shear strain. The variation not only in triaxial conditions but also in other stress combination needs to be identified.
- The analyses presented here are only for three piles: two long piles and one suction pile. Parametric study with different pile size should be performed.

- Only single pile under lateral load is modeled in the presented study. FE analyses of group piles under different loading conditions also need to be performed.
- The effects of cyclic loading need to be considered to simulate more realistic conditions in offshore environments.
- The author understands the effects of installation on pile capacity. However, it is difficult to model as it depends upon construction process. It could be considered in future studies.

Bibliography

American Petroleum Institute (API) (1987). "Recommended practice for planning, designing and constructing fixed offshore platforms", API Recommended practice 2A (RP 2A), 17th Ed.

Albert, L.F., Holtz, R.D., and Magris, E., (1987). "The super pile system: A feasible alternate foundation for TLP in deep water", Proceedings of the 19th annual Offshore Technology Conference, Houston, Texas, OTC 5392, pp. 307-314.

Alizadeh, M. and Davisson, M.T., (1970). "Lateral load tests on piles-Arkansas river project", J.S.M.F.D., ASCE, vol. 96, SM 5, pp. 1583-1604.

Allersma, H.G.B., Brinkgreve, R.B.J., and Simon, T., Kirstein, A.A., (2000). "Centrifuge and numerical modeling of horizontally loaded suction piles", Int. Jour.Of Offshore and Polar Eng. Vol. 10(3), pp. 222-228.

API (2000). "Recommended practice for planning, designing and constructing fixed offshore platforms working stress design", RP2A-WSD 21st ed., American Petroleum Inst.

Ashour, M., and Norris, G., (2000). "Modeling lateral soil- pile response based on soil-pile interaction", J. of Geotechnical and Geoenvironmental Engineering", 126(5), pp. 420-428.

Aubeny, C.P., Han, S.W., and Murff, J.D., (2003a). "Inclined load capacity of suction caissons", *International Journal for Numerical and Analytical Methods in Geomechanics*, Vol. 27, pp. 1235-1254.

Aubeny, C.P., Han, S.W., and Murff, J.D., (2003b). "Refined model for inclined load capacity of suction caissons", *Proceedings of 22nd International Conference on Offshore Mechanics and Arctic Engineering*, Cancun, Mexico, OMAE2003-37502.

Bang, S., and Cho, Y., (1999). "Analytical performance study of suction piles in sand", *Proceedings of the ninth International Offshore and Polar Engineering Conference*, Brest, France.

Bang, S., Jones, K. D., Kim, K. O., Kim, Y.S. and Cho, Y., (2011). "Inclined loading capacity of suction piles in sand", *Journal of Ocean Engineering*, Vol. 38, pp. 951-924.

Barton, Y.O., (1980). "Laterally loaded model piles in sand, Centrifuge test and finite element analysis", PhD Thesis, University of Cambridge.

Baguelin, F., Frank, R. & Sa.d, Y. H., (1977). "Theoretical study of lateral reaction mechanism of piles", *Géotechnique* 27, No. 3, pp. 405-434.

Bolton, M., (1986). "The strength and dilatancy of sands", *Géotechnique*; 36(1), pp. 65–78.

Bouafia, A., and Bouguerra, A., (2006). "Single piles under lateral loads – centrifuge modeling of some particular aspects", *Proceedings of the 6th International Conference on Physical Modelling in Geotechnics*, v 1-2, pp. 915-920.

- Bouafia, A., (2007). "Single piles under horizontal loads in sand: determination of P–Y curves from the prebored pressuremeter test", *Geotech. Geol. Eng.*, Vol. 25, pp. 283–301.
- Broms, B., (1964a). "The Lateral resistance of piles in cohesive Soils", *J. Soil Mech. Found. Div.*, ASCE, 90, pp. 27-63.
- Broms, B., (1964b). "The lateral resistance of piles in cohesive soils", *J. Soil Mech. Found. Div.*, ASCE, 90, pp.123-156.
- Broms, B. B., (1965). "Piles in cohesionless soil subject to oblique pull", *Journal of the Soil Mechanics and Foundation Division, ASCE*, Vol. 91, pp. 199-205.
- Brown, D. A., (1985). "Behaviour of a large scale pile group subjected to cyclic lateral loading, Ph. D. Thesis", University of Texas at Austin.
- Brown, G.A., and Nacci, V.A., (1971). "Performance of hydrostatic anchors in granular soils", *Proceedings of the 3rd annual Offshore Technology Conference, Houston, Texas*, OTC 1472, pp. II 533-542.
- Brown DA, Shie C-F. (1991). "Some numerical experiments with a three dimensional finite element model of a laterally loaded pile", *Computers and Geotechnics*, 12, pp. 149–162.
- Bye, A., Erbrich, C., Rognlien, B., and Tjelta, T.I., (1995). "Geotechnical design of bucket foundations", *Proc. of Offshore Technology Conference*, OTC 7793.
- Byrne, B.W., (2000) "Investigations of suction caissons in dense sand", PhD Dissertation, Magdalen College, Oxford.

Byrne, B.W., and Houlsby, G.T., (2000). "Experimental investigation of the cyclic response of suction caissons in sand", 2000 Offshore Technology Conference, Houston, Texas, OTC 12194, pp. 787-795.

Byrne, B.W., and Houlsby, G.T., (2002a). "Experimental investigation of response of suction caissons to transient vertical loading", Journal of Geotechnical and Geoenvironmental Engineering, Vol. 128, No. 11, pp. 926-939.

Byrne, B.W., Houlsby, G.T., Martin, C., and Fish, P., (2002b). "Suction caisson foundation for offshore wind turbines", Wind Engineering, Vol. 26, No. 3, pp. 145-155.

Byung T.K., Nak-Kyung K., Woo J.L. and Young S.K., (2004) "Experimental load-transfer curves of laterally loaded piles in Nak-Dong river sand", Journal of Geotechnical and Geoenvironmental Engineering, Vol. 130, No. 04, pp. 416-425.

Cao, J., Phillips, R., and Popescu, R., (2001). "Physical and numerical modeling on suction caissons in clay", Proceedings of the 18th Canadian Congress of Applied Mechanics, Memorial University of Newfoundland, St. John's, Canada, pp. 217-218.

Cao, J., Phillips, R., Popescu, R., Al-Khafaji, Z., and Audibert, J.M.E., (2002a). "Penetration resistance of suction caissons in clay", Proceedings of the 12th International Offshore and Polar Engineering Conference, Kitakyushu, May 26-31, pp. 800-806.

Cao, J., Phillips, R., Audibert, J.M.E., and Al-Khafazi, Z., (2002b). "Numerical analysis of the behavior of suction caissons in clay", Proceedings of the 12th International Offshore and Polar Engineering Conference, Kitakyushu, Japan, May 26-31, pp. 795-799.

Cao, J., Phillips, R., Popescu, R., Audibert, J.M.E., and Al-Khafaji, Z., (2003). "Numerical analysis of the behavior of suction caissons in clay", *International Journal of Offshore and Polar Engineering*, Vol. 13, No. 2, pp. 154-159.

Cauble, D.F., (1996). "An experimental investigation of the behavior of a model suction caisson in a cohesive soil", PhD Dissertation, Massachusetts Institute of Technology.

Cho, Y. and Bang, S., (2002). "Inclined Loading Capacity of Suction Piles", *Proceedings of The Twelfth International Offshore and Polar Engineering Conference*, Kitakyushu, Japan, May 26–31, pp. 827-832.

Clukey, E.C., and Morrison, M.J., (1993). "A centrifuge and analytical study to evaluate suction caissons for TLP applications in the Gulf of Mexico", In *Design and performance of deep foundations: Piles and piers in soil and soft rock*, Edited by P.P. Nelson, T.D. Smith and E.C. Clukey, ASCE Geotechnical Special Publication No. 38, pp. 141-156.

Clukey, E.C., Aubeny, C.P., and Murff, J.D., (2003). "Comparison of analytical and centrifuge model tests for suction caisson subjected to combined loads", *Proceedings of 22nd International Conference on Offshore Mechanics and Arctic Engineering*, Cancun, Mexico, OMAE2003-37503.

Coffman, R.A., El-Sherbiny, R.M., Rauch, A.F., and Olson, R.E., (2004). "Measured horizontal capacity of suction caissons", *Proceedings of the annual Offshore Technology Conference*, Houston, Texas, OTC 16161.

Cox, W. R., Reese, L. C., and Grubbs, B. R., (1974). "Field testing of laterally loaded piles in sand", *Proc. 6th Annual Offshore Technology Conf.*, Houston, OTC2079.

Dilip, R. M., (2004). "A computational procedure for simulation of suction caisson behavior under axial and inclined loads", PhD Dissertation, The University of Texas at Austin.

Deng, W., and Carter, J.P., (2000a). "Inclined uplift capacity of suction caissons in sand," Offshore Technology Conference, Houston, Texas, OTC 12196, pp. 809-820.

Desai, C. S. & Appel, G. C., (1976). "3-D analysis of laterally loaded structures", Num. Meth. Geomech., Am. Soc. Civ. Engrs. Ed. Desai, C.S., 2, pp. 405-418.

Desai, C. S., (1982). "Numerical design-analysis for piles in sands", Geotech. Engrg. Div., ASCE, 100(6), pp. 613-635.

Det Norske Veritas, (1980). "Rules for the design, construction, and inspection of offshore structures", Appendix F: Foundations, Det Norske Veritas, Hovik, Norway.

Duhrkop, J., Grabe, J., Bienen, B., White, D.J., and Randolph, M.F., (2010) "Centrifuge experiments on laterally loaded piles with wings", Proc. Int. Conf. Phys. Model. Geotech., ICPMG.

Dyson, G.J., Herdsman, Randolph, M.F., (2001). "Monotonic lateral loading of piles in calcareous sand", Journal of Geotechnical and Geoenvironmental Engineering, v 127, n 4, pp. 346-352.

Dyvik, R., Anderson, K.H., Hansen, S.B., and Christophersen, H.P., (1993). "Field tests on anchors in clay. I: Description", Journal of Geotechnical Engineering, Vol. 119, No. 10, pp. 1515-1531.

Erbrich, C.T., (1994). "Modeling of a novel foundation for offshore structures", Proceedings of the 9th UK ABAQUS User's Conference, Oxford, England, pp. 235-251.

Fan, CC., and Long, J. H., (2005). "Assessment of existing methods for predicting soil response of laterally loaded piles in sand", Journal of Computer and Geotechnics, Vol. 32, Issue 4, pp. 274-289.

Goodman, L.J., Lee, C.N., and Walker, F.J., (1961). "The feasibility of vacuum anchorage in soil", Géotechnique, Vol. 1, No. 4, pp. 356-359.

Grundhoff, T., (1997). "Horizontal impact loads on large bored single piles in sand", Proceedings of the International Offshore and Polar Engineering Conference, v 1, pp. 753-760.

Grundoff, T., Latotzke, J., and Laue, J., (1998). "Investigation of vertical piles under horizontal impact", Centrifuge 98, Rotterdam: Balkema, pp. 569-574.

Handayanu, Swamidas, A.S.J., and Booten, M., (2000). "Ultimate strength of offshore tension foundations under vertical and inclined loads", Proceedings of ETCE/OMAE2000 Joint Conference, New Orleans, Louisiana, OMAE2000/OSU OFT-4032, pp. 95-100.

Hansen, Brinch J., (1961). "The ultimate resistance of rigid piles against transversal forces", Danish Geotechnical Institute (Geoteknisk Institute) Bull. Copenhagen, V 12, pp. 5-9.

Hardin, B.O. and Black, W.L., (1966). "Sand stiffness under various triaxial stresses", *Journal of the Soil Mechanics and Foundations Division, ASCE*, Vol. 92, No.SM2, pp. 27-42.

Handayanu, Swamidas, A.S.J., and Booton, M., (1999). "Behavior of tension foundation for offshore structures under extreme pull-out loads", *Proceedings of 18th International Conference on Offshore Mechanics and Arctic Engineering*, St. John's, Newfoundland, Canada, OMAE99/OFT-4204, pp. 635-641.

Handayanu, Swamidas, A.S.J., and Booton, M., (2000). "Ultimate strength of offshore tension foundations under vertical and inclined loads", *Proceedings of ETCE/OMAE2000 Joint Conference*, New Orleans, Louisiana, OMAE2000/OSU OFT-4032, pp. 95-100.

Helfrich, S.C., Brazill, R.L., and Richards, A.F., (1976). "Pullout characteristics of a suction anchor in sand", *Proceedings of the 8th annual Offshore Technology Conference*, Houston, Texas, OTC 2469, pp. 501-506.

Hesar, M., (1989). "Behaviour of pile-anchors subjected to monotonic and cyclic loading", PhD Thesis, University of Sunderland, UK.

Hogervorst, J.R., (1980). "Field trials with large diameter suction piles", *Proceedings of the 12th annual Offshore Technology Conference*, Houston, Texas, OTC 3817, pp. 217-224.

Houlsby, G.T. and Byrne, B.W., (2005a). "Calculation procedures for installation of suction caissons in sand", Proc ICE - Geotechnical Engineering, Vol. 158, No 3, pp. 135-144.

Houlsby, G.T. and Byrne, B.W., (2005b). "Calculation procedures for installation of suction caissons in clay and other soils", Proc ICE - Geotechnical Engineering, Vol. 158, No 2, pp. 75-82.

House, A.R., (2000). "The response of suction caissons to catenary loading", 4th ANZ Young Geotechnical Professional Conference, ACT, Australian Geomechanics Society, Vol. 35, No. 3, pp. 13-22.

Iftkharuzzaman, M. & Hawlader, B., (2012). "Finite Element Modeling of Offshore Mooring Pile", 65th Canadian Geotechnical Society Conference, Winnipeg, Manitoba, Canada.

Iftkharuzzaman, M. & Hawlader, B., (2012). "Numerical modeling of lateral response of long flexible piles in sand", Journal of the Southeast Asian Geotechnical Society.

Iftkharuzzaman, M. & Hawlader, B., (2012). "Numerical Modeling of Inclined Loading of Offshore Mooring Pile in Sand", Second International Conference on Géotechnique, Construction Materials & Environment, Kuala Lumpur, Malaysia, ISBN: 978-4-9905958-1-4 C3051.

Ismael N. F., (2007). "Lateral load tests on bored piles and pile group in sand", 7th Int. Symp. On Field Measurements in Geomechanics.

Janbu, N., (1963). "Soil compressibility as determined by oedometer and triaxial tests", Proc. Euro. Conf Oil Soil Mech. 111/1.1 FUUlld.Ic-llgrg., German Society for Soil Mechanics and Foundation Engineering, Wissbaden, Germany, Vol I, 1925.

Keaveny, J.M., Hansen, S.B., Madshus, C., and Dyvik, R., (1994). "Horizontal capacity of large-scale model anchors", Proceedings of the 13th International Conference on Soil Mechanics and Foundation Engineering, New Delhi, India, pp. 677-680.

Kim, Y.S., Kim, K.O., and Cho, Y., (2005). "Centrifuge Model Tests on Embedded Suction Anchors", Proc. Of the Fifteenth Int. Offshore and Polar Eng. Con. Sepi:, Korea.

Kim, Y., Kim, K., and Cho, Y., (2010). "Centrifuge model tests on suction pile pullout loading capacity in sand", Physical Modelling in Geotechnics, ICPMG, Vol. 2, pp. 787-792.

Kimura M, Adachi T, Kamei H, Zhang F., (1995). "3-D finite element analyses of the ultimate behaviour of laterally loaded cast-in-place concrete piles", In Proceedings of the Fifth International Symposium on Numerical Models in Geomechanics, NUMOG V, pp. 589-594.

Kim, Y., In-Shik, S., Kim, B., and Bang, I., (1998). "Model tests and analysis of laterally loaded piles in sand", Proceedings of the 1998 17th International Conference on Offshore Mechanics and Arctic Engineering, OMAE.

Kondner, R. L. (1963). "Hyperbolic stress-strain response: Cohesive soils", J. Soil Mech. Found. Div., 89(1), pp. 115-144.

Kubo, J., (1965). "Experimental study of the behaviour of laterally loaded piles", Proc. 6th Int. Conf. S.M. & F.E., Vol. 2, pp. 275-279.

Kulhawy, F. H., (1991). "Drilled shaft foundations, Chapter 14 in Foundation Engineering Handbook", 2nded, Hsai-Yang Fang Ed., Van Nostrand Reinhold, New York.

Lee, S.H., Cho, Y., Kim, K.O., Kim, Y.S., Lee, T.H., and Kwag, D.J., (2003). "Centrifuge model tests on embedded suction anchor loading capacities," Proceedings of The Thirteenth International Offshore and Polar Engineering Conference Honolulu, Hawaii, USA.

LPILE Plus 5.0 (2005). ENSOFT, INC., 3003 West, Howard Lane, Austin, Texas 78728.

Long, J. H., and Reese, L. C., (1984). "Testing and analysis of two offshore drilled shafts subjected to lateral loads", Laterally Loaded Deep Foundations: Analysis and Performance, Kansas City, MO, USA.

Long, J. H., and Reese, L. C., (1985). "Methods for predicting the behaviour of piles subjected to repetitive lateral loads", Proc., 2nd Shanghai Symp. On Marine Geotechnology and Nearshore Offshore Structures, Shanghai, China.

Mackereth, F.J.H., (1968). "A portable core sampler for lake deposits", Limnology and Oceanography, 3, pp. 181-191.

Madhav, M. R., Rao, N. S. V. K. & Madhavan, K., (1971). "Laterally loaded pile in elastoplastic soil. Soils Fdns", 11, No. 2, pp. 1-15.

Mahmoud, M., and Burley, E., (1994). "Lateral load capacity of single piles in sand", Proceedings of the Institution of Civil Engineers Geotechnical Engineering, Vol. 107, n 3, pp. 155-162.

Matlock, H., (1970). "Correlations for design of laterally loaded piles in soft clay", Proc. 2nd Offshore Tech. Conf., Houston, Texas, 1, pp. 577-594.

McVay, M., Zhang, L., Molnit, T., and Lai, P., (1998). "Centrifuge testing of large laterally loaded pile groups in sands", Journal of Geotechnical and Geoenvironment Engineering, Vol. 124, No. 10.

Mercier, R.S., (2003). "Experience with fixed and floating platforms for the oil and gas industry", PowerPoint Presentation on CD-ROM of the Workshop on Deep Water Offshore Wind Energy Systems, Washington, D.C.

Meyerhof, G. G., Sastry, V. V. R. N. and Yalcin, A. S. (1988). "Lateral resistance and deflection of flexible piles", Canadian Geotechnical Journal, 25(3), pp. 511-522.

Meyerhof, G. G., Mathurs, S. K., and Valsangkar, A. J., (1981). "Lateral resistance and deflection of rigid walls and piles in layered soils", Canadian Geotechnical Journal, 18, pp. 159-170.

McVay, M., Zhang, L., Molnit, T., and Lai, P., (1998). "Centrifuge testing of large laterally loaded pile groups in sands", J. Geotech. Geoenviron. Eng., 124(10), pp. 1016–1026.

- Murchison, J. M., and O'Neill, M. W., (1984). "Evaluation of p-y relationships in cohesionless soil", Analysis and design of pile foundations, ASCE, New York, pp. 174–191.
- Nobahar, A., Popescu, R., and Konuk, I., (2000). "Estimating progressive mobilization of soil strength", Proceedings of the 53rd Canadian Geotechnical Conference, Montreal.
- Norris, G. (1986). "Theoretically based BEF laterally loaded pile analysis", Numerical Methods in Offshore Piling 3rd Int. Conf., Navtes, pp. 361–386.
- Nunez, I.L., Phillips, R., Randolph, M.F., and Wesselink, B.D., (1987). "Modeling laterally loaded piles in calcareous sand", Cambridge University, Engineering Department, (Technical Report) CUED/D-Soils.
- Patra, N. and Pise, P., (2001). "Ultimate Lateral Resistance of Pile Groups in Sand", J. Geotech. Geoenviron. Eng., 127(6), pp. 481–487.
- Phillips, R., Clark, J.I., Paulin, M.J., Meaney, R., Millan, D.E.L., and Tu, K., (1994). "Canadian national centrifuge center with cold regions capabilities", Centrifuge 94, pp. 57-61.
- Poulos, H.G., (1971). "Behaviour of laterally loaded piles", I- Single piles, J. of the Soil Mechanics and Foundations, Div. 97(5), pp. 711-731.
- Poulos and Davis, (1980). "Pile foundation analysis and design", New York: John Wiley & Sons.
- Poulos, H.G., Chen, L.T., and Hull, T.S., (1995). "Model tests on single piles subjected to lateral soil movement", Soils and Foundations, Vol. 35, No. 4, pp. 85-92.

Prakash, S., and Kumar, S., (1996). "Nonlinear lateral pile deflection prediction in sands", *Journal of Geotechnical Engineering*, Vol. 122, No.2.

Randolph, M. F., (1981). "The response of flexible piles to lateral loading", *Géotechnique*. Vol. 31, No. 2, pp. 247-259.

Randolph, M.F., O'Neill, M.P., and Stewart, D.P., (1998). "Performance of suction anchors in fine-grained calcareous soils", 1998 Offshore Technology Conference, Houston, Texas, OTC 8831, pp. 521-529.

Reese, L. C. & Matlock, H., (1956). "Non-dimensional solutions for laterally loaded piles with soil modulus assumed proportional to depth", *Proc. 8th Texas Conf. on Soil Mech. Foundation. Engineering*, Austin, Texas, pp. 1-41.

Reese, L. C., Cox, W. R., and Koop, F. D., (1974). "Analysis of laterally loaded piles in sand", *Proc. 5th Annual Offshore Technology Conf.*, Houston, OTC2080.

Reese, L.C.; Allen, J.D.; Hargrove, J.Q., (1981). "Laterally loaded piles in layered soils", *Proceedings of the International Conference on Soil Mechanics and Foundation Engineering*, Stockholm, Sweden.

Reese, J. C. & Van Impe, W. F., (2001). "Single piles and pile groups under lateral loadings", A. A. Balkema, Rotterdam.

Rollins, K. M., Lane, J. D., and Gerber, T. M., (2005). "Measured and computed lateral response of a pile group in sand", *J. Geotech. Geoenviron. Eng.*, 131(1), pp. 103-114.

Ruesta, P. F., and Townsend, F. C., (1997). "Evaluation of laterally loaded pile group at Roosevelt Bridge", *J. Geotech. Geoenviron. Eng.*, 123(12), pp. 1153-1161.

Salgado, R. (2008). "The engineering of foundations", The McGraw-Hill Companies, Inc.

Scott, R. F., (1980). "Analysis of centrifuge pile tests: Simulation of pile driving", Research Rep. OSAPR Project 13, American Petroleum Institute, Washington, DC.

Sparrevik, P., (2001). "Suction pile technology and installation in deep waters", Proceedings of OTRC 2001 International Conference Honoring Professor Wayne A. Dunlap", Geotechnical, Geological, and Geophysical Properties of Deepwater Sediments, Houston, pp. 182-197.

Steensen-Bach, J.O., (1992). "Recent model tests with suction piles in clay and sand", Proceedings of the 24th annual Offshore Technology Conference, Houston, Texas, OTC 6844, pp. II 323-330.

Scott, R.F., (1979a). "Cyclic lateral loading of piles, analysis of centrifuge tests", Research Program for API-OSASAPR Project 13. California Institute of Technology.

Scott, R.F., (1979b). "Cyclic model pile tests in a centrifuge", Proc. 11th Offshore Technology Conference, pp. 1159-1168.

Scott, J. B., Ross, W. B., Bruce, L. K., and Dongdong, C., (2005). "Behavior of pile foundations in laterally spreading ground during centrifuge tests", Journal of Geotechnical and Geoenvironment Engineering, Vol. 131, No. 11.

Sukumaran, B., McCarron, W.O., Jeanjean, P., and Abouseeda, H., (1999a). "Efficient finite element techniques for limit analysis of suction caissons under lateral loads", Computers and Geotechnics, Vol. 24, pp. 89-107.

Sukumaran, B., and McCarron, W.O., (1999b). "Total and effective stress analysis of suction caissons for Gulf of Mexico conditions", In Analysis, Design, Construction and Testing of Deep Foundations, Edited by J.M. Roesset, Proceedings of the OTRC'99 Conference, Geotechnical special publication No. 88, pp. 247-260.

Taiebat, H.A., and Carter, J.P., (2001). "A semi-analytical finite element method for three-dimensional consolidation analysis", Computers and Geotechnics, Vol. 28, pp. 55-78.

Terashi, M., Kitazume, M. and Kawabata, K., (1989). "Centrifuge modeling of a laterally loaded pile", Proc. 12th Int. Conf. Soil Mech. And Found. Eng., Rio de Janeiro, Vol. 2, pp. 991-994.

Trochanis AM, Bielak J, Christiano P., (1991). "Three-dimensional nonlinear study of piles. Journal of Geotechnical Engineering", 117(3), pp. 429-447.

Wakai A, Gose S, Ugai K., (1999). "3-d Elasto-plastic finite element analysis of pile foundations subjected to lateral loading", Soil and Foundations, 39(1), pp. 97-111.

Wang, M.C., Nacci, V.A., and Demars, K.R., (1975). "Behavior of underwater suction anchor in soil", Ocean Engineering, Vol. 3, pp. 47-62.

Wang, M.C., Demars, K.R., and Nacci, V.A., (1977). "Breakout capacity of model suction anchors in soil", Canadian Geotechnical Journal, Vol. 14, pp. 246-257.

Wang, M.C., Demars, K.R., and Nacci, V.A., (1978). "Applications of suction anchors in offshore technology", Proceedings of the 10th annual Offshore Technology Conference, Houston, Texas, OTC 3203, pp. 1311-1320.

Wagner, A.A., (1953). "Lateral load tests on pile for design information", Symp. on Lateral Load Test on Piles. ASTM, STP 154, pp. 59-72.

Weaver, T. W., Ashford, S. A., and Rollins, K. M., (2005). "Response of 0.6 m cast-in-steel-shell pile in liquefied soil under lateral loading", Journal of Geotechnical and Geoenvironmental Engineering, Vol. 131, No. 1.

Wesselink, B. D., Murff, J. D., Randolph, M. F., Nunez, I. L., and Hyden, A. M., (1988). "Analysis of centrifuge model test data from laterally loaded piles in calcareous sand", Engineering for calcareous sediments, Vol. 1, Balkema, Rotterdam, The Netherlands, pp. 261-270.

Yan, L. & Byrne, P. M., (1992). "Lateral pile response to monotonic pile head loading", Can. Geotech. J. 29, pp. 955-970.

Yang, Z., and Jeremic, B., (2002). "Numerical analysis of pile behavior under lateral loads in layered elastic-plastic soils", Int. J. for Numerical and Analytical Methods in Geomechanics, 26, pp. 385-1406.

Yimsiri, S., (2001). "Pre-failure deformation characteristics of soils: anisotropy and soil fabric", Ph.D. Dissertation, University of Cambridge, Cambridge, England.

Yoshimi, Y., (1964). "Piles in cohesionless soil subject to oblique pull", Journal of the Soil Mechanics and Foundation Division, ASCE, Vol. 90, pp. 11-24.

Zdravkovic, L., Potts, D.M., and Jardine, R.J., (2001). "A parametric study of the pull-out capacity of bucket foundations in soft clay", Géotechnique, Vol. 51, No. 1, pp. 55-67.

Appendix-A

Finite Element Modeling of Steel Pile Foundation in Sand Under Lateral Load, 65th
Canadian Geotechnical Society Conference, September 30 - October 3, Winnipeg,
Manitoba 8p

Finite Element Modelling of Steel Pile Foundation in Sand Under Lateral Load



Md. Iftexharuzzaman & Bipul Hawlader
Memorial University of Newfoundland
Faculty of Engineering and Applied Science, St. John's, Canada

ABSTRACT

This paper presents finite element analysis of a pile foundation in sand subjected to lateral load. Three-dimensional finite element analyses are performed for pure lateral load applied at the top of a free-head steel pile. The commercially available software package ABAQUS/Standard is used in numerical analysis. The sand around the pile is modeled using the built-in Mohr-Coulomb soil constitutive model in ABAQUS. Numerical analysis is also performed by using another software LPILE, which is based on p - y curve. The finite element and LPILE results are compared with a full-scale test results. It is shown that the finite element method model better the pile-soil response under lateral load.

RÉSUMÉ

Ce document présente l'analyse par éléments finis d'une fondation sur pieux dans le sable soumis à une charge latérale. Tridimensionnelles analyse par éléments finis sont exécutées pour une charge latérale pur appliquée à la partie supérieure d'un pieu en acier sans tête. Le logiciel disponible dans le commerce ABAQUS / Standard est utilisé dans l'analyse numérique. Le sable autour du pieu est modélisée en utilisant le modèle intégré dans le sol de Mohr-Coulomb constitutive dans ABAQUS. Analyse numérique est également réalisée en utilisant un autre logiciel LPILE, qui est basé sur la courbe p - y . L'élément fini et les résultats sont comparés avec LPILE un résultat d'essai à grande échelle. Il est montré que le modèle éléments finis méthode meilleure est la réponse du pieu-sol sous charge latérale.

1 INTRODUCTION

Lateral resistance and deflection of pile foundation are key design considerations in many civil engineering structures both in onshore and offshore environment. Wind, wave, earthquake and ground movement might create significant lateral load on pile foundations.

Hansen (1961) proposed a method for estimating the ultimate lateral load resistance of vertical piles based on earth pressure theory. Broms (1964 a,b) also proposed methods for calculating ultimate lateral resistance based on earth pressure theory simplifying the analyses for purely cohesionless and purely cohesive soils for short rigid and long flexible piles. Meyerhof et al. (1981, 1988) also proposed methods to estimate ultimate lateral resistance and groundline displacement at working load for rigid and flexible piles.

Lateral deflection of pile head is one of the main requirements in the current design practice, especially in limit state design. Two approaches are available in the literature for modeling lateral load deflection behaviour of the piles. In the first approach the response of soil under lateral load is modelled by using nonlinear independent springs in the form of p - y curve, where p is the soil-pile reaction (i.e. the force per unit length of the pile) and y is the lateral deflection of the pile. Reese et al. (1974) proposed a method to define the p - y curves for static and cyclic loading. A modified version of Reese et al. (1974) is employed by the American Petroleum Institute (API 2000) in its manual for recommended practice. Both of these models have been implemented in the commercially available software LPILE Plus 5.0 (2005). Ashour and Norris (2000) showed that their strain wedge (SW) model is capable of evaluating some additional effects such as

bending stiffness of the pile, pile shape, pile head fixity and depth of embedment on p - y curves. The second approach is based on continuum modeling of pile and soil. Poulos (1971) presented finite element analysis of a single pile situated in an ideal elastic soil mass. Finite element analyses of single piles under lateral load have also been conducted by other researchers (Brown and Shie 1991, Kimura et al. 1995, Wakai et al. 1999, Yang and Jeremic 2006). Brown and Shie (1991) performed three-dimensional finite element analysis by modeling the soil using von Mises and extended Drucker-Prager constitutive model. Trochanis et al. (1991) examined the effects of nonlinearity of the soil and separation or slippage between the soil and the pile surfaces. In addition, there are some full-scale test results (e.g. Cox et al. 1974, Rollins et al. 2005, Ruesta and Townsend 1997) and centrifuge test results (e.g. McVay et al. 1998) available in the literatures which are used in previous studies for model verification.

The purpose of this paper is to present a series of three-dimensional finite element analysis of a steel pipe pile in sand under lateral load. The finite element results are compared with LPILE analysis, and also with a full-scale test results. The limitations of p - y curve method are discussed based on lateral response of the pile.

2 FINITE ELEMENT MODELLING

The numerical analyses presented in this paper are carried out using the finite element software ABAQUS/Standard 6.10-EF-1. The modeling is done in Lagrangian framework. A soil domain of 15 m diameter and 30 m height as shown in Fig. 1 is modeled. The pile is located at the center of the soil domain. The size of the

soil domain is sufficiently large and therefore boundary effects are not expected on predicted lateral load, displacement and deformation mechanisms. The bottom of the soil domain is restrained from any vertical movement, while the curved vertical faces are restrained from any lateral movement using roller supports. The symmetric vertical xz plane is restrained from any movement in the y -direction. No displacement boundary condition is applied on the top, and therefore the soil can move freely.

Two layers of soil are considered in this study: the upper 6 m is medium dense sand and the lower 24 m is dense sand. The sand is assumed to behave as an anisotropic material available in ABAQUS FE software is used for modeling the behaviour of sand. Pile is modeled as an elastic material. The Coulomb friction model is used for the frictional interface between the outer surfaces of the pile and sand. In this method, the friction coefficient (μ) is defined as $\mu = \tan(\phi_\mu)$, where ϕ_μ is the pile/soil interface friction angle. The value of ϕ_μ is assumed to be equal to $0.7\phi'$ in this analysis. Considering the boundary conditions, geometry and loading conditions, the advantage of symmetry is used and only the half of the model under lateral load is analyzed.

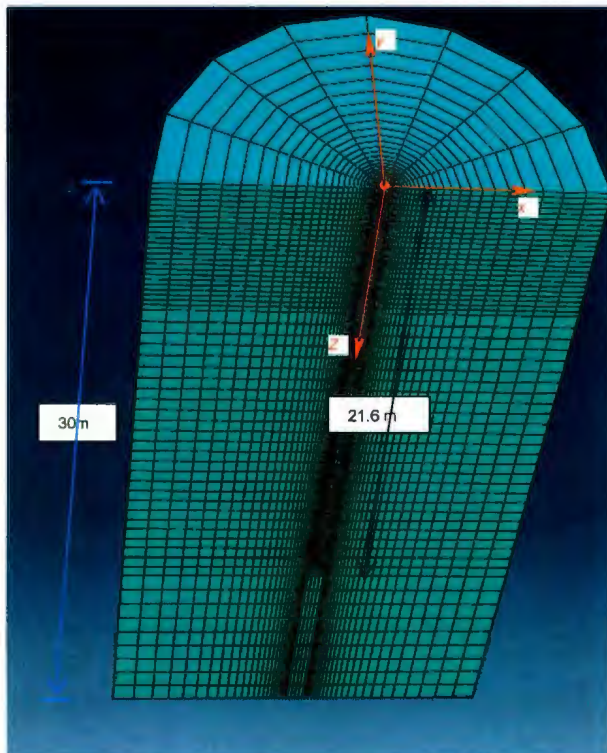


Figure 1 Finite Element Model with medium dense mesh

Both soil and pile are modeled using the solid homogeneous C3D8R element, which is an 8-noded linear brick, multi-material and reduced integration with hourglass control.

The numerical analysis consists of mainly two major steps: gravity step and loading step. In gravity step the soil domain is reached to the in-situ stress condition. In

loading step the lateral displacement in the x -direction is applied on the nodes at the top of the pile.

2.1 Modelling of Pile

A free-head steel pipe pile of 610 mm (24") outer diameter with 9.53 mm (3/8") wall thickness is modeled in this study. The embedded length of the pile is 21.6 m. The lateral load is applied at 0.3 m above the ground surface. The pile is modeled as linear elastic material with modulus of elasticity (E_p) of 208×10^6 kN/m² and Poisson's ratio (ν_p) of 0.3.

2.2 Soil Modelling

The built-in Mohr-Coulomb constitutive model in ABAQUS is used for modeling the soil. The top layer of soil (0–6 m) is medium dense sand which is modeled using the following soil parameters: angle of internal friction, $\phi' = 35^\circ$; dilation angle, $\psi = 5^\circ$; modulus of elasticity, $E_s = 60,000$ kPa; and Poisson's ratio, $\nu_s = 0.3$. The soil layer below 6 m is dense sand. The soil properties used for this layer are: $\phi' = 39^\circ$, $\psi = 9^\circ$, $E_s = 60,000$ kPa, and $\nu_s = 0.3$. The location of the groundwater table is at the ground surface. Submerged unit weight of 10.4 kN/m³ is used for both soil layers. Geometry and mechanical properties used in the analysis are shown in Table 1.

Table 1. Geometry and mechanical properties used in the analysis

| | |
|--|-------------------------------------|
| Pile: | |
| Length of the pile (L) | 21.6 m |
| Diameter of the pile (D) | 610 mm (24") |
| Thickness of the pile (t) | 9.53 mm (3/8") |
| Modulus of elasticity of pile (E_p) | 208×10^6 kN/m ² |
| Poisson's ratio (ν_p) | 0.3 |
| Soil (sand) | |
| Modulus of elasticity, E_s | 60,000 kN/m ² |
| Poisson's ratio, ν_s | 0.3 |
| Submerged unit weight of soil, γ' | 10.4 kN/m ³ |
| Initial modulus of subgrade reaction (k) | 20000 kN/m ³ |
| Upper soil (0 to 6 m depth) | |
| Angle of internal friction, ϕ'_p | 35° |
| Dilation angle, | 5° |
| Lower soil (6 to 30 m depth) | |
| Angle of internal friction, ϕ'_p | 39° |
| Dilation angle, ψ | 9° |

2.3 Mesh Sensitivity Analysis

The size of the mesh has a significant effect on finite element modeling. Often finer mesh yields more accurate results but computational time is higher. For successful modeling of load-displacement behaviour of piles under lateral load the top five to ten diameters depth should be properly modeled. Therefore, fine mesh is used for the upper 6 m soil and medium mesh is used for 6–21 m. For the soil layer below the pile (>21 m depth) coarse mesh is

used, as it does not have significant effects on load-displacement behaviour.

After several trial analyses with different mesh size, the optimum mesh is selected. Figure 2 shows the load-displacement behaviour of the pile for different types of mesh. In the coarse mesh, a total of 12,021 elements, in the medium dense mesh 18,027 elements and in the fine mesh 24,096 elements are used. The distribution of mesh size is shown in Fig. 1. As shown in Fig. 2 that the number of elements has negligible effect on force-displacement behaviour after medium dense mesh. Therefore, the analyses presented in the following sections are conducted using medium dense mesh with 18,027 elements.

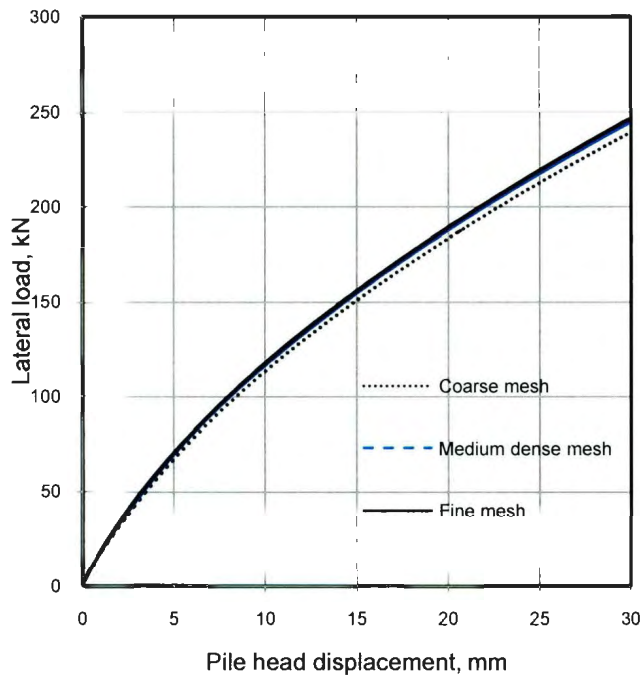


Figure 2 Mesh Sensitivity Analysis

3 LPILE ANALYSIS

Lateral loading analyses for single piles are also conducted for static loading using LPILE Plus 5.0 (2005) software. LPILE uses the finite difference method and the pile is modeled as a beam with lateral stiffness based on elastic modulus and moment of inertia of the pile. The nonlinear p - y curves are defined by using the method proposed by Reese et al. (1974). In this method the ultimate soil resistance per unit length of the pile can be calculated by using the angle of internal friction of the soil (ϕ'). The initial straight-line portion of the p - y curve is defined by using the modulus of subgrade reaction (k). The typical value of k for different values of ϕ' and relative density is shown in Fig. 3 as recommended by the American Petroleum Institute (API, 2000). The value of k of 20,000 kN/m^3 is used in this study.

4 NUMERICAL RESULTS

In this study the finite element results are verified using the full-scale test results reported by Cox et al. (1974). The comparison is done only for single pile under static load. Cox et al. (1974) reported the results of a suit of full-scale lateral load tests in sand at Mustang Island. Test on single pile were conducted using a pipe pile of 610mm diameter and 9.53 mm wall thickness. A 9.75m length of the test pile near the ground surface was instrumented to obtain the response of the pile under lateral load. Lateral load was applied using a hydraulic jack at 0.3m above the ground surface. Data was collected for lateral load increments of 11.1kN up to 66.6kN and then in increments of 5.56kN to a maximum lateral load of 266.9kN.

Two boreholes were drilled near the test site. Field tests and laboratory tests on collected samples from these boreholes were conducted for soil characterization (Cox et al. 1974). The soil parameters used in the present study (Table 1) are based on this soil investigation report.

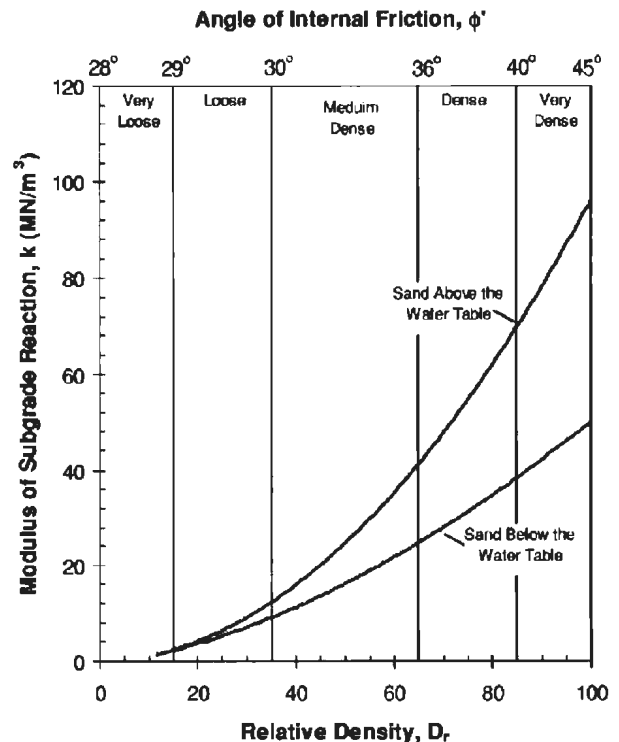


Figure 3 Lateral Modulus of subgrade reaction (API 2000)

4.1 Load-deflection curves

Figure 4 shows the variation of lateral load with lateral displacement of the pile at the ground surface. The data obtained from full-scale test (Cox et al. 1974) is also shown in this figure. As shown, there is a very good agreement between the full-scale test results and present finite element analysis. For comparison, the prediction using LPILE is also shown in this figure.

In finite element analysis lateral displacement is applied at the top of the pile (0.3 m above the ground surface). The lateral load is calculated by adding

horizontal component of nodal forces on all the nodes at this level. The lateral displacement at the ground level is calculated by averaging the lateral displacement of all the nodes of the pile at ground level.

In LPILE the lateral load is applied on the top of the pile in 11 increments. The pile is divided into 100 small divisions. The lateral displacement at the ground surface is obtained from the displacement of the element at this level.

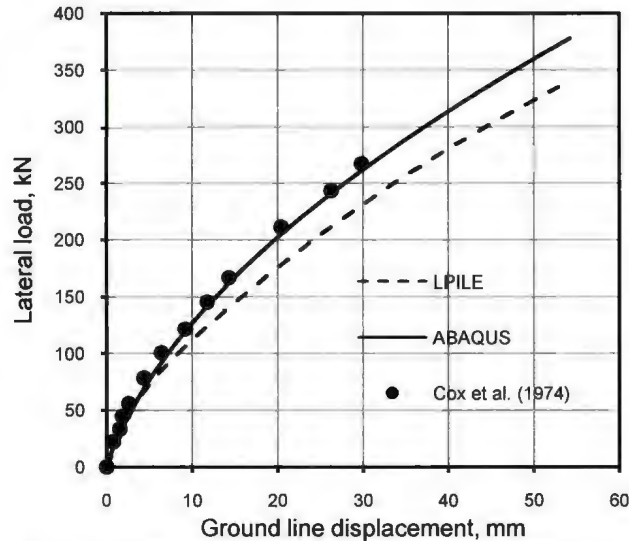


Figure 4 Comparison between numerical prediction and full-scale test result

4.2 Bending moment with depth

Figures 5 to 8 shows the variation of bending moment with depth for the upper 6 m length of the pile. In the following figures the depth in vertical axis represents the distance from the top of the pile. Although the pile is 21 m length the variation of bending moment only for upper 6 m is shown because the maximum bending moment and its variation mainly occur in this zone. A total of 11 lateral load cases (33.4kN, 55.6kN, 77.8kN, 77.8kN, 101.1kN, 122.3kN, 144.6kN, 166.8kN, 189kN, 211.3kN, 211.3kN, 244.6kN, and 266.9kN) are considered in this study. In finite element analyses the bending moment is obtained from the axial stresses in the pile. However, in LPILE it can be easily obtained as the pile is modeled as a beam. As shown in Figs. 5-8, for a given lateral load the FE modeling gives lower bending moment than that of from LPILE. For lower values of lateral load (e.g. 33.4 kN) the calculated bending moment using either finite element or LPILE is higher than the measured values. One of the reasons for this could be the selection of appropriate value of elastic properties for the soil at that level. However, the finite element results are closer to the measured data points than LPILE results. The maximum bending moment using LPILE is 10 to 20 percent higher than that of using ABAQUS.

The depth at which the maximum bending moment occurs in finite element analysis is less than LPILE analysis. For example, the maximum bending moment for 266.9 kN is at 2.5 m while it is at 3.0 m in LPILE analysis.

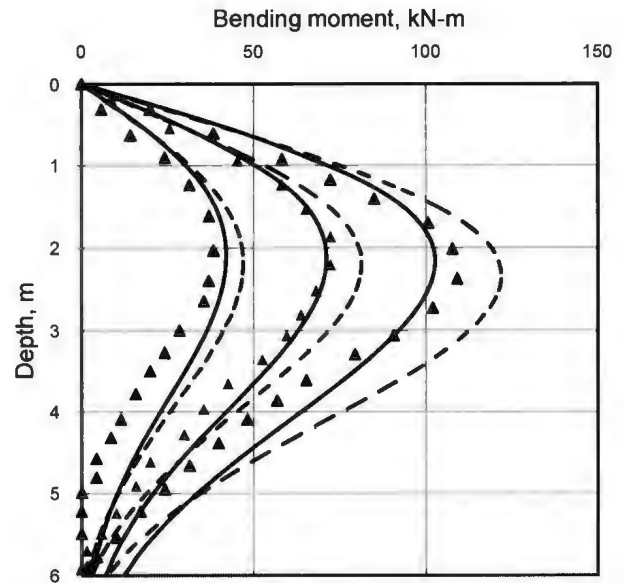


Figure 5: Bending moment vs. Depth (Load cases:33.4kN, 55.6 kN and 77.8 kN; solid lines for FE analysis, dashed line for LPILE and data points for full scale test)

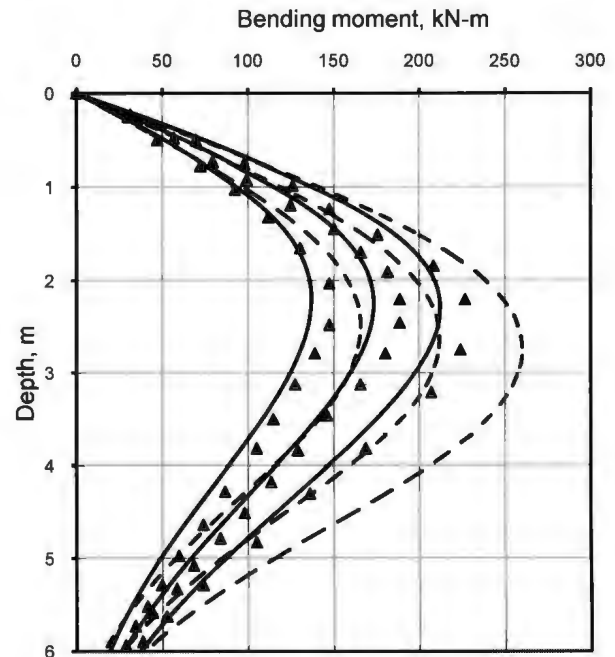


Figure 6 Bending moment vs. Depth (Load cases: 101.1kN, 122.3 kN and 144.6 kN; solid lines for FE analysis, dashed line for LPILE and data points for full scale test)

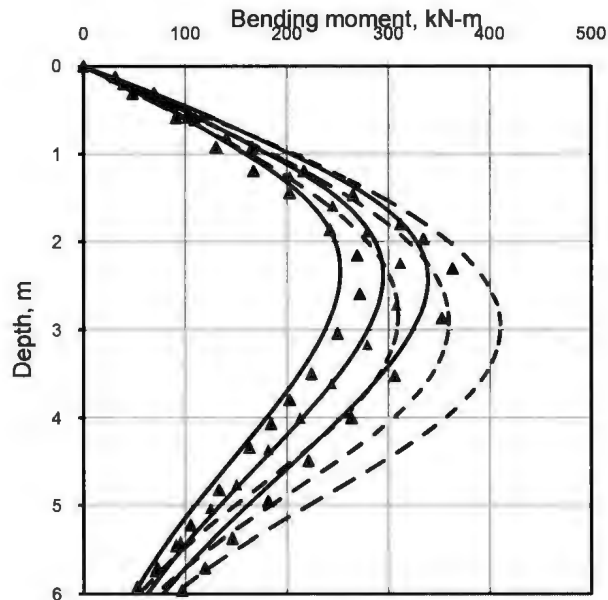


Figure 7 Bending moment vs. Depth (Load cases: 166.8 kN, 189 kN and 211.3 kN; solid lines for FE analysis, dashed line for LPILE and data points for full scale test)

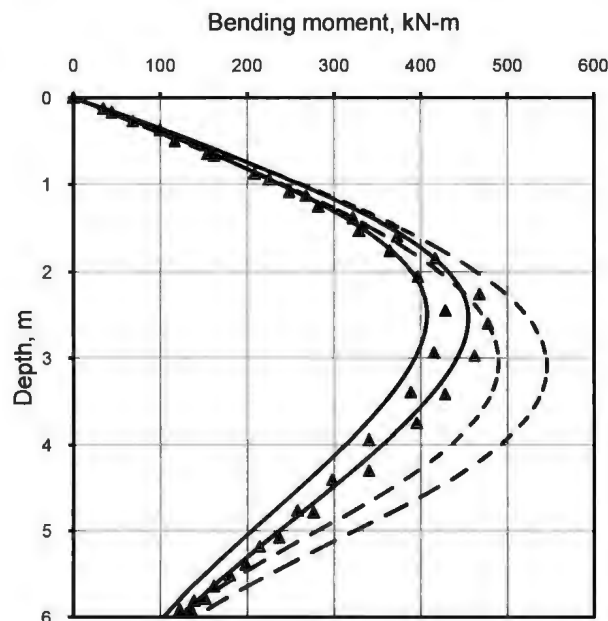


Figure 8 Bending moment vs. Depth (Load cases: 244.6 kN and 266.9 kN; solid lines for FE analysis, dashed line for LPILE and data points for full scale test)

It is to be noted here that the pile is in elastic condition even at highest lateral load. The maximum bending moment for 266.9 kN of lateral load is 550 kN-m. This gives the maximum tensile/compressive stress of 175 MPa, which is less than yield strength of steel. That means, the analyses conducted in this study using elastic behaviour of the pile is valid even for highest lateral load.

4.3 Maximum bending moment

Figure 9 shows the variation of the maximum bending moment with lateral load. The maximum bending moment increases with increase in lateral load. At low values of lateral load, both finite element and LPILE compare well with measured values. However, at larger load the predicted maximum bending moment using LPILE is higher than the values obtained from finite element analysis and full-scale test data.

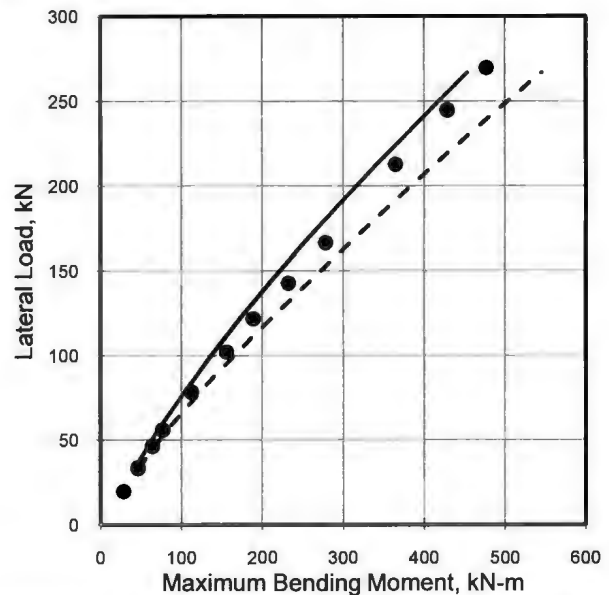


Figure 9 Comparison of Maximum moment vs. Lateral load in ABAQUS, LPILE and Cox et al. (1974) (Solid line is ABAQUS and dotted line is LPILE).

4.4 Lateral displacement

Figure 10 shows the variation of lateral displacement of the pile with depth for 11 load cases. The FE results are compared with the lateral displacement obtained from LPILE which are also shown in this figure. As shown the lateral displacement obtained from FE and LPILE are very similar at low values of lateral load. However, at higher lateral load LPILE calculated higher pile head displacement. For example, for 266.9 kN lateral load, the FE calculated 35 mm and LPILE calculated 41 mm of pile head displacement. It is also to be noted here that the lateral displacement of the pile below 4.5 m is not very significant.

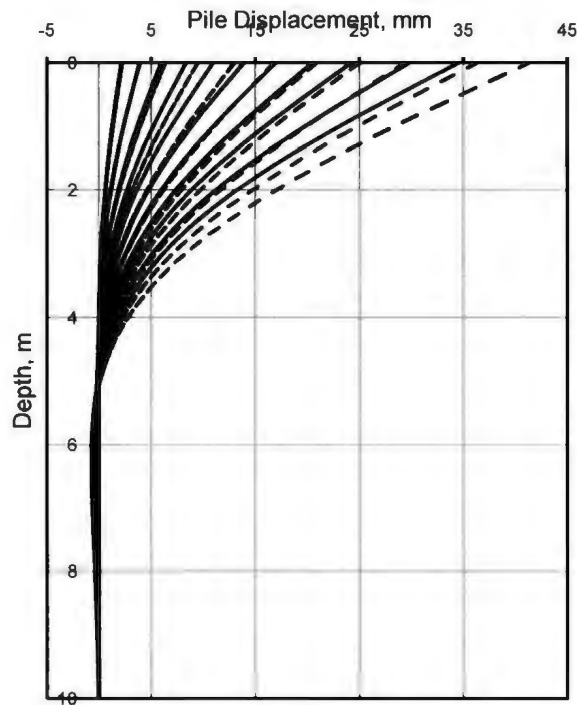


Figure 10: Lateral displacement of pile (Load cases:33.4kN, 55.6kN, 77.8kN, 77.8kN, 101.1kN, 122.3kN, 144.6kN, 166.8kN, 189kN, 211.3kN, 244.6kN and 266.9kN; solid lines for FE analysis, dashed line for LPILE)

4.5 Soil reaction

Lateral soil reaction (force per metre length of pile) is plotted in Fig. 11. For clarity the calculated results for 5 load cases are shown in this figure. In finite element analysis, the x-component (lateral) of nodal force is calculated first for all the nodes at a given depth. Dividing the sum of the nodal force in the x-direction by the vertical distance between two sets of nodes in the pile, the lateral soil reaction is obtained. In LPILE analysis the soil reaction can be easily obtained from the data file as it models the soil as discrete springs. As shown in this figure that calculated soil reaction from both LPILE and FE is very similar up to the depth of 1.2 m. However, below 1.2 m the soil reaction obtained from FE analysis is higher than the reaction obtained from LPILE. Moreover, after reaching to the maximum value of soil reaction, it decreases quickly with depth in finite element analysis. In both analyses the maximum soil pressure was obtained at greater depth for larger value of lateral loads. Finite element also calculated lower negative soil reaction below approximately 5 m depth.

It is to be noted here that Ramadan (2011) conducted some centrifuge tests for estimating load capacity of piles in sand. The soil pressure diagram shown in Fig. 11 is very similar to his test results.

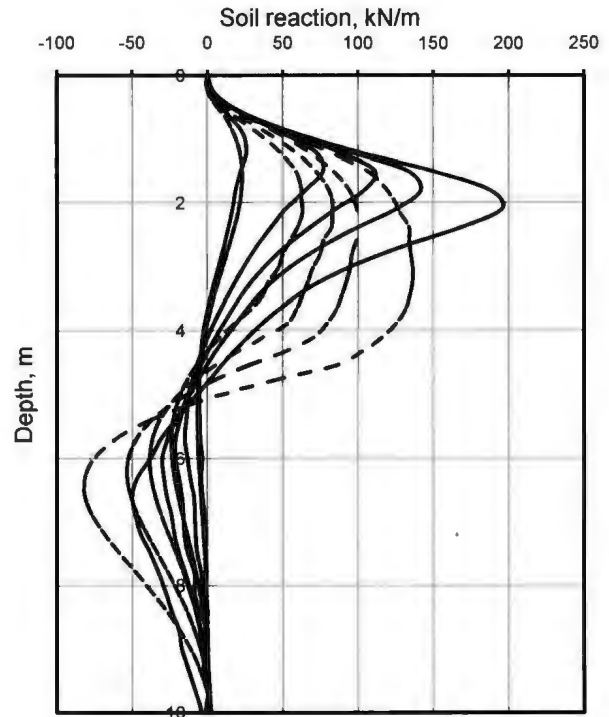


Figure 11 Soil reaction on pile (Load cases:33.4 kN, 100.1 kN, 144.6 kN, 189 kN and 266.9 kN; solid lines for FE analysis, dashed line for LPILE)

4.6 Shear force in the pile

Figure 12 shows the variation of shear force in the pile with depth for five lateral loads. In finite element analysis the shear force is obtained by subtracting the sum of the x-component of nodal force above the point of interest from the lateral load applied at pile head. As shown in Fig. 11 that the calculated soil reaction in finite element is higher near the ground surface. Therefore, the shear force is decreased quickly in finite element analysis near the ground surface as shown in Fig. 12. The maximum negative shear force from LPILE analyses is higher than that obtained from finite element analyses. Below the depth of 9 m the shear force is negligible in both analyses.

4.7 p - y curves

In the current practice the modeling of a laterally loaded pile is generally performed as a beam on elastic foundation which is represented by discrete springs. The soil springs are defined by using nonlinear p - y curves. The p - y curves for four depths are shown in Fig. 13. In LPILE the p - y curve for a given depth can be easily obtained from the data file. In finite element analysis the soil is modeled as a continuum, not as discrete springs. The value of p at a given depth and lateral displacement is obtained from nodal forces and nodal displacement at that level, respectively. In this study the model proposed by Reese et al. (1974) for static lateral loading is used in LPILE analysis. The p - y curve in Reese et al. (1974) consists of four segments: (i) initial linear segment, which is mainly govern by k value, (ii) parabolic segment

between the initial linear segment and lateral displacement of $D/60$, (iii) linear segment between lateral displacements of $D/60$ and $3D/80$, and (iv) constant soil resistance segment after lateral displacement of $3D/80$. Calculated $p-y$ curves obtained from LPILE and FE are

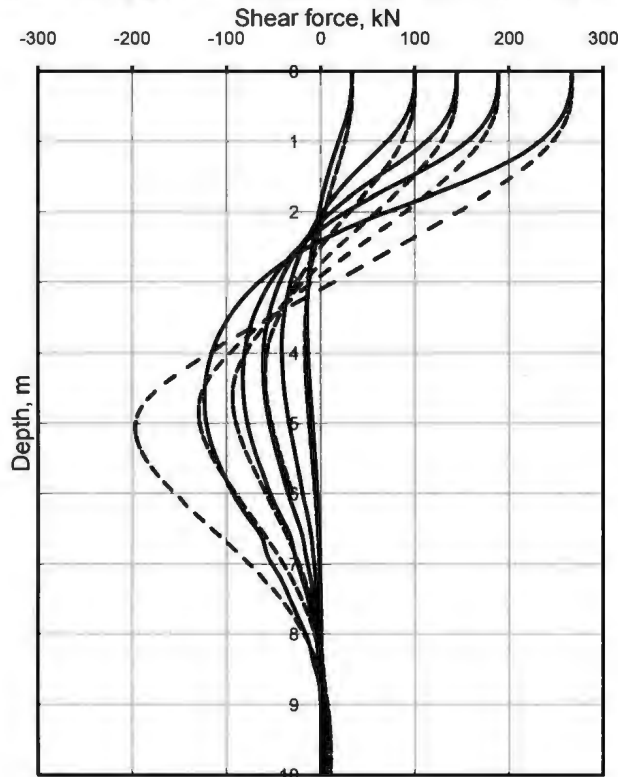


Figure 12 Shear force in the pile (Load cases: 33.4 kN, 100.1 kN, 144.6 kN, 189 kN and 266.9 kN; solid lines for FE analysis, dashed line for LPILE)

also compared with measured data in the full-scale test (Cox et al. 1974). As shown in this figure, the $p-y$ curves obtained from finite element analyses match better with the measure values. However, at lower depths and higher lateral displacements, the $p-y$ curves obtained even from the finite element analyses do not match well with the measured values. One of the reasons could be the limitations of the Mohr-Coulomb constitutive model used in the present analysis. Advanced constitutive model for sand might give better results. Unfortunately, in most of the commercially available software, such as in ABAQUS, the advanced soil constitutive models are not implemented.

5 CONCLUSIONS

Most of the designers prefer $p-y$ curve method to calculate the deflection of a pile under lateral load. Based on the $p-y$ curve method the software package LPILE is developed in finite difference approach that is widely used in the industry for modeling lateral soil-pile response. The interaction between soil layers and pile/soil interface behaviour cannot be modeled using the $p-y$ curve method.

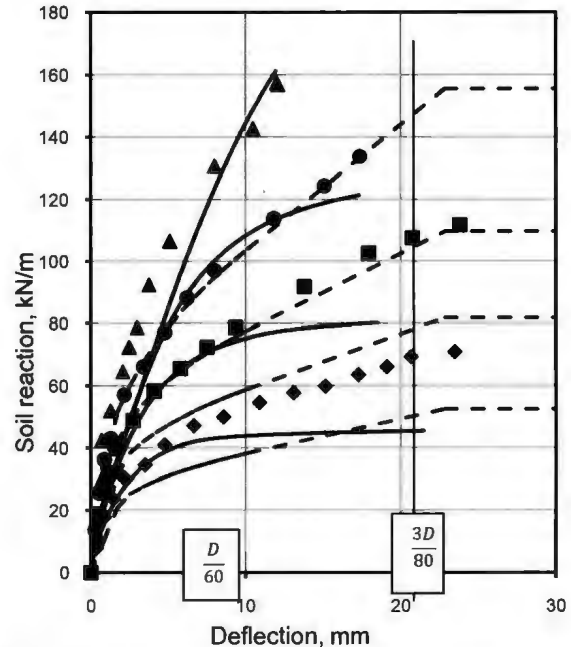


Figure 13 Comparison of $p-y$ curves (depths: 0.61m, 0.91m, 1.22m and 1.83m; solid lines for FE analysis, dashed line for LPILE and data points for full scale test)

The present study shows that some of the limitations of $p-y$ curve method could be overcome by using continuum finite element analysis. Although the load-deflection behaviour could be matched by using appropriate input parameters in LPILE, the finite element analysis gives better results not only for the load-deflection behaviour but also for other responses such as bending moment profile and soil reaction.

While this paper shows some advantages of finite element modeling, the Mohr-Coulomb constitutive model may not be the appropriate model for analysis of soil-pile response under lateral load. Moreover, constant modulus of elasticity and dilation angle are used in this study. The modulus of elasticity of sand generally varies with mean effective stress. Also, the dilation angle decreases with increase in plastic shear strain. The prediction might be better if these effects are considered in the analysis.

6 ACKNOWLEDGEMENTS

The work presented in this paper has been funded by MITACS, PRAC and NSERC Discovery grant.

7 REFERENCES

- API 2000. Recommended practice for planning, designing and constructing fixed offshore platforms working stress design, RP2A-WSD 21st ed., American Petroleum Inst.
- Ashour, M., and Norris, G., 2000. Modelling lateral soil-pile response based on soil-pile interaction, J. of Geotechnical and Geoenvironmental Engineering, 126(5):420-428.

- Broms, B., 1964a. The Lateral resistance of piles in cohesive Soils, *J. Soil Mech. Found. Div., ASCE*, 90: 27-63.
- Broms, B., 1964b. The lateral resistance of piles in cohesive soils, *J. Soil Mech. Found. Div., ASCE*, 90: 123-156.
- Brown DA, Shie C-F. 1991. Some numerical experiments with a three dimensional finite element model of a laterally loaded pile. *Computers and Geotechnics*, 12:149-162.
- Cox, W. R., Reese, L. C., and Grubbs, B. R., 1974. Field testing of laterally loaded piles in sand, *Proc. 6th Annual Offshore Technology Conf., Houston, OTC2079*.
- Hansen, Brinch J. 1961. The ultimate resistance of rigid piles against transversal forces. *Danish Geotechnical Institute (Geoteknisk Institut) Bull. Copenhagen*, 12:5-9.
- Kimura M, Adachi T, Kamei H, Zhang F. 1995. 3-D finite element analyses of the ultimate behaviour of laterally loaded cast-in-place concrete piles. In *Proceedings of the Fifth International Symposium on Numerical Models in Geomechanics, NUMOG V:589-594*.
- LPILE Plus 5.0 2005. ENSOFT, INC., 3003 West, Howard Lane, Austin, Texas 78728.
- Meyerhof, G. G., Sastry, V. V. R. N. and Yalcin, A. S. 1988. Lateral resistance and deflection of flexible piles. *Canadian Geotechnical Journal*, 25(3): 511-522.
- Meyerhof, G. G., Mathurs, S. K., and Valsankara, A. J. 1981. Lateral resistance and deflection of rigid walls and piles in layered soils. *Canadian Geotechnical Journal*, 18:159-170.
- McVay, M., Zhang, L., Molnit, T., and Lai, P. 1998. Centrifuge testing of large laterally loaded pile groups in sands, *J. Geotech. Geoenviron. Eng.*, 124(10): 1016-1026.
- Poulos, H.G., 1971. Behaviour of laterally loaded piles: I- Single piles, *J. of the Soil Mechanics and Foundations, Div. 97(5): 711-731*.
- Ramadan, Mohamed 2011. Physical and numerical modeling of offshore piles under mooring force, PhD thesis, Memorial University of Newfoundland, Canada, p. 269.
- Reese, L. C. and Van Impe, W.F. 2001. *Single piles and pile group under lateral loading*, A.A. Balkeme, Brookfield, VT, 463p.
- Reese, L. C., Cox, W. R., and Koop, F. D. 1974. Analysis of laterally loaded piles in sand, *Proc. 5th Annual Offshore Technology Conf., Houston, OTC2080*.
- Rollins, K. M., Lane, J. D., and Gerber, T. M., 2005. Measured and computed lateral response of a pile group in sand, *J. Geotech. Geoenviron. Eng.*, 131(1):103-114.
- Ruesta, P. F., and Townsend, F. C. 1997. Evaluation of laterally loaded pile group at Roosevelt Bridge, *J. Geotech. Geoenviron. Eng.*, 123(12): 1153-1161.
- Trochanis AM, Bielak J, Christiano P. 1991. Three-dimensional nonlinear study of piles. *Journal of Geotechnical Engineering*, 117(3):429-447.
- Wakai A, Gose S, Ugai K. 1999. 3-d Elasto-plastic finite element analysis of pile foundations subjected to lateral loading. *Soil and Foundations*, 39(1):97-111.
- Yang, Z., and Jeremic, B., 2002. Numerical analysis of pile behavior under lateral loads in layered elastic-plastic soils, *Int. J. for Numerical and Analytical Methods in Geomechanics*, 26:1385-1406.

